Experimental Investigation of Tribological, Metallurgical and Mechanical Behavior of AZ31-Mg Reinforced Composite through Powder Metallurgy Process

Betelhem T/ Haymanot H/Maryam

A Thesis Submitted to

The Department of Mechanical Engineering,

School of Mechanical, Chemical and Materials Engineering

Presented in Partial Fulfillment of the Requirement for the Degree of Master's in Manufacturing Engineering

Office of Graduate Studies

Adama Science and Technology University

June, 2022

Adama, Ethiopia

Experimental Investigation of Tribological, Metallurgical and Mechanical Behavior of AZ31-Mg Reinforced Composite through Powder Metallurgy Process

Betelhem T/ Haymanot H/ Maryam

Advisor: Dr. Devendra Kumar Sinha (Assistant Professor)

A Thesis Submitted to

The Department of Mechanical Engineering

School Of Mechanical, Chemical and Materials Engineering

Presented in Partial Fulfillment of the Requirement for the Degree of Master's in Manufacturing Engineering

Office of Graduate Studies

Adama Science and Technology University

June, 2022

Adama, Ethiopia

Approval Sheet

I, the advisor of the thesis entitled "Tribological, Metallurgical and Mechanical Behavior of AZ31-Mg Reinforced Composite through Powder Metallurgy Process" and developed by Ms. Betelhem T/ haymanot, hereby certify that the recommendation and suggestions made by the board of examiners are appropriately incorporated into the final version of the thesis.

______________________	______________________	______________
Major Advisor	Signature	Date

Approval of Board of Examiners

We, the undersigned, members of the Board of Examiners of the thesis by Ms. Betelhem T/ haymanot have read and evaluated the thesis entitled “Tribological, Metallurgical and Mechanical Behavior of AZ31-Mg Reinforced Composite through Powder Metallurgy Process” and examined the candidate during the open defense. This is, therefore, to certify that the thesis is accepted for Partial Fulfillment of the Requirement for the Degree of Master of Science in Manufacturing Engineering.

______________________	________________	________________
Chairperson	Signature	Date
______________________	________________	________________
Internal Examiner	Signature	Date
______________________	________________	________________
External Examiner	Signature	Date

Finally, approval and acceptance of the thesis are contingent upon the submission of its final copy to the Office of Postgraduate Studies (OPGS) through the Department Graduate Council (DGC) and School Graduate Committee (SGC).

______________________	________________	________________
Department Head	Signature	Date
______________________	________________	________________
School Dean	Signature	Date
______________________	________________	________________
Office of Postgraduate Studies, Dean	Signature	Date

Declaration

I hereby declare that this Master thesis proposal entitled "Tribological, Metallurgical and Mechanical Behavior of AZ31-Mg Reinforced Composite through Powder Metallurgy Process" is my original work. That is, it has not been submitted for the award of any academic degree, diploma, or certificate in any other university. All sources of materials that are used for this thesis have been duly acknowledged through citation.

____________________	____________________	____________
Name of student	Signature	Date

Recommendation of Advisors

I, the advisor(s) of this thesis, hereby certify that I have read the revised version of the thesis entitled "Tribological, Metallurgical and Mechanical Behavior of AZ31-Mg Reinforced Composite through Powder Metallurgy Process" prepared under my guidance by Ms. Betelhem T/ haymanot submitted in partial fulfillment of the requirements for the degree of Mater's of Science in Manufacturing Engineering. Therefore, I recommend the submission of the revised version of the thesis to the department following the applicable procedures.

___________________________ ________________________ ________________

Major Advisor Signature Date

ACKNOWLEDGEMENT

I sincerely would like to offer great gratitude to my advisor Dr. Devendra Kumar Sinha for his continuous follow-up during this paperwork. And also, his hard-working habit makes me to be more motivated and ambitious for further work. Therefore, I want to thank him a lot. Moreover, I want to thank Mr. Samuel Kefyalew (Ph.D. candidate) for his guidance and advice at any time when I needed the most. And, I would like to offer my sincere gratitude for the department of material science engineering in ASTU for providing the access to use the powder metallurgy utilities. At last, all people who lends me their hands during this paperwork has to take great respect. Thank you all!

TABLE OF CONTENTS

LIST OF TABLES

LIST OF FIGURES

LIST OF ACRONYMS AND ABBREVIATIONS

BM	Base Metal
CP	Compaction Pressure
DoE	Design of Experiment
GRA	Grey Relational Analysis
GRC	Grey Relational Coefficient
GRG	Grey Relational Grade
HEM/M	High Energy Mixer/ Miller Machine
Mg alloy	Magnesium Alloy
MMCs	Metal Matrix Composites
MMMCs	Mg Alloy Metal Matrix Composites
Mpt	Melting Point
MT	Milling Time
PM	Powder Metallurgy
Rt.	Reinforcement
S.Temp.	Sintering Temperature
SEM	Scanning Electron Microscope
UTM	Universal Testing Machine
VHT	Vickers Hardness Test
VHV	Vickers Hardness Value
XRD	X-ray Diffraction
PoD	Pin on Disc

Abstract

Nowadays, two important plans, namely lightweight materials and effective manufacturing process usage, takes a priority in sector of automotive and aerospace manufacturing industries during part production. For instance, 86% of their energy consumption is caused by having loads i.e. their weight and passengers for a passenger car. The objective of this research is to experimentally investigate the metallurgical, mechanical, and tribological behavior of MoS_2*, SiC and* ZrO_2 *reinforced AZ31 Magnesium metal matrix composite fabricated via powder metallurgy process. The experiment was designed using* L_9 *orthogonal array for four-factor at three levels. Accordingly, the reinforcement composition (5, 10, 15 vol. %), milling time (2, 4, 6 hrs.), compaction pressure (50, 60, 70MPa), and sintering temperature (400,425,450*^oc*) were considered as the factors with their levels. The density, porosity, hardness, and compression behavior were examined for the developed samples. The Taguchi-based grey relational analysis has been implemented to optimize the process parameters for obtaining better properties of manufactured samples. As a result, the optimum value was obtained as* $A_1B_1C_3D_2$ *using Grey relational grade. The results from the confirmation test revealed an improvement of 2.04 g/cm*^{3}*, 0.13, 131.89 HV, and 110.35 MPa for exp'tal density, porosity, hardness, and compression strength respectively relative to optimal level values. The uniform nature of particle distribution was observed through SEM micrograph under investigation during microscopy of the optimal sample. The average particle size of the optimal sample was also obtained around 809.14 nm. There was no* $Mg_{17}Al_{12}$ *phase detected in the XRD pattern. The wear test was carried out on the optimal sample using Pin on Disc apparatus. The improvement of the wear resistance performance at 10vol. % and 5vol. % SiC were revealed around 12.9% and 25.8%. Commonly, abrasive and mild types of wear were dominant as observed in SEM micrographs at various magnifications. The fracture mechanisms of the optimal sample resulting from the compression test were studied under SEM micrographs and it revealed that both ductile and brittle fractures occurred. Finally, the optimal sample of MMMCs has provided desirable mechanical and tribological properties to the desired areas of applications.*

Keywords: *Powder Metallurgy, Tribology, wear morphology, fractography, metal matrix composite.*

CHAPTER ONE: INTRODUCTION

1.1 Background of the study

Composite materials are the most promising material that will have power in the future due to their low density and advanced mechanical property. In composite materials, metal matrix composites are applicable after more than a quarter of a century of active research that comprises a metal as a matrix and other materials as dispersed phases such as ceramic or metals. Accordingly, MMCs provide a significant contribution to industrial and engineering areas. Figure 1.1 shows that the investigation of demands on MMCs over the year was approved. And, it can predict the increment towards the demands in the upcoming years. The MMCs can be grouped by the types of the metal matrix such as aluminum, magnesium, titanium as well as copper matrix composites, and others.

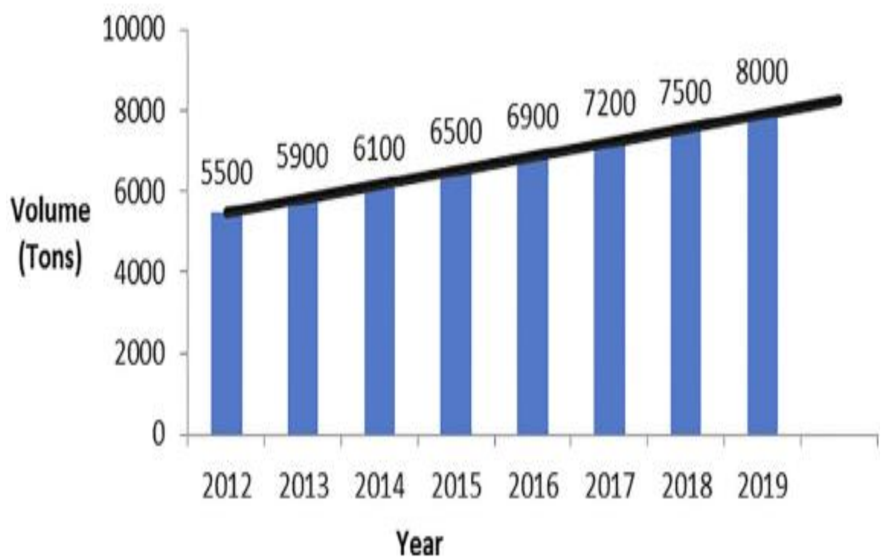

Figure 1.1 Global demands for metal matrix composites (Malaki *et al*., 2019).

From the matrix materials, Mg only occurs in a combined form with other elements that have a high reactive property when it is prepared as a free element artificially. Mg is less dense than aluminum but it lacks strength even though it categorizes as light in weight material. Its stiffness-to-weight ratio is very high; comparatively, one kilogram of magnesium has a stiffness property equal to 3.96 kg of aluminum and 4.62 kg of steel (Paul and Georges, 2011).

1.1.1 Magnesium metal matrix composites

In magnesium metal matrix composites, Mg alloys are the primary ones used to combine the features of lightness and strength in one when it is used as a matrix in composites. Comparatively, they have a relatively low Young's modulus and low specific gravity than aluminum and steel common alloys i.e. 42 GPa and 1.74 g/cm^3 respectively (Mallick, 2020). Due to the property of Mg alloys, they are widely exposed to use as the lightest structural material for lightweight applications (Tjong, 2013). AZ31 magnesium alloy is one of the most popular ones among other types of magnesium alloy in different areas of applications.

Industrially, several types of alloys have been produced from those, AZ31 is one of the most popular Mg alloys with aluminum. As Paul and Georges (2011) reviewed that the 3% Al, by weight, content permit to overcome the ductility problem at high working temperature likewise it stands for strengthening a matrix by solid solution. Therefore, it suggests to utilize in manufacturing wrought products such as sheets and plates, as well as extruded bars and shapes. And also, AZ31 Mg alloy is usually used for light weight or specific gravity properties such as aircraft industry to produce flat parts with ribs like brackets (Dziubińska *et al*., 2015). AZ31 Mg alloy also has the ability to resist corrosion better than AZ91 (Cheng *et al*., 2009).

Mg alloys can also be improved further for enhancing their property as desired in the application areas. Abbas *et al*. (2021) reviewed that Mg alloys have a limitation on the thermal conductivity and capability of performing well between hot and cold temperatures in automotive areas. However, Improvements in tribological characteristics, dimensional stability, damping capacity, and elevated temperature creep properties can be circumvented by the proper selection in type, size elastic modulus, and volume fraction of the reinforcement materials in general harder and stiffer ceramic particles reinforcements. Mostly, ceramics were used as the reinforcement materials in metal matrix composites to enhance the mechanical properties of the materials, especially in hardness, strength, wear resistance, corrosion resistance, and other properties of the materials. From those, SiC, ZrO_2, and other types of ceramics are used to improve the property of the matrix materials. The properties improvement was also observed in other researchers' results (Kavimani *et al.*, 2019; Mazaheri *et al.*, 2020). The reinforcement of the dry lubricant materials is also used to enhance the uniform distribution of the particles over the matrix. The dry lubricants were significant due to working as a lubricant between the particles and that make the particles easily disperse without interlocking with each other. This was approved by other studies on the composites (Madeshwaran *et al*, 2018; Narayanasamy & Selvakumar, 2017).

Magnesium alloy has strength and limitations as per the application areas of the manufactured product. Mostly, their demand is significantly high due to having the property of high strength-to-weight ratios. And, they have also the character of exceptional machinability as well as their cost is comparatively low. For instance, it took advantage of aluminum in the way of having low latent heat, so more casting can be produced per unit time, Better surface quality and dimensionality, smaller draft angle, and ability to fabricate curved surfaces. Moreover, they have high specific strength (14% higher than aluminum). Nevertheless, Mg alloy has a limitation due to its ability to inhibit corrosion, creep at high temperatures, and also blaze (Makar & Kruger, 1993; Ddodson, 2013).

1.1.2 Manufacturing methods of magnesium metal matrix composites

For Mg metal matrix, some methods are used to manufacture particulate reinforced magnesium metal matrix composites (MMCs) including powder metallurgy, squeeze casting, gas pressure infiltration, stir casting, and disintegrated melt deposition (Z. Ren *et al.*, 2010). From those, Powder metallurgy is a solid-state fabrication technique of composite material that is used to add value to the engineering process for the fabrication of MMCs parts. Its process comprises powder preparation, compaction, and sintering of the pressed part as the general stage for producing the desired materials which are used to enhance the mechanical, metallurgical, and other properties of the products. Indeed, it depends on the process parameter used to follow for providing the desired property such as compaction pressure, sintering temperature, sintering time, type and rate of reinforcement, size of the matrix and reinforcing elements, etc. (Naveen *et al.*, 2020).

In the Powder metallurgy process, the stage has generally been stated during producing the material using the powder metallurgy process as shown in figure 1.2. First, the material is prepared in form of fine powder which causes a high cost in the preparation of powders. And, mixing of the two or more materials, i.e. metal or non-metal, to obtain a fairly dispersed (homogeneous) mixture is followed. In addition, the milling process reveals size reduction of the material particles based on the time duration for milling the materials. The mixture is then introduced into a mold cavity or die and then compacted to find a weak cohesive mass which is called a green compact. This makes the particles or powders of the milled material (i.e. matrix and reinforcements) to have the desired shape using the die profile. Thereafter, the green compact is then subjected to very high temperature and pressure below the melting temperature of materials for a specific period to obtain a hardened mass. This process provides high strength property for the produced samples due to developing bonds between the particles.

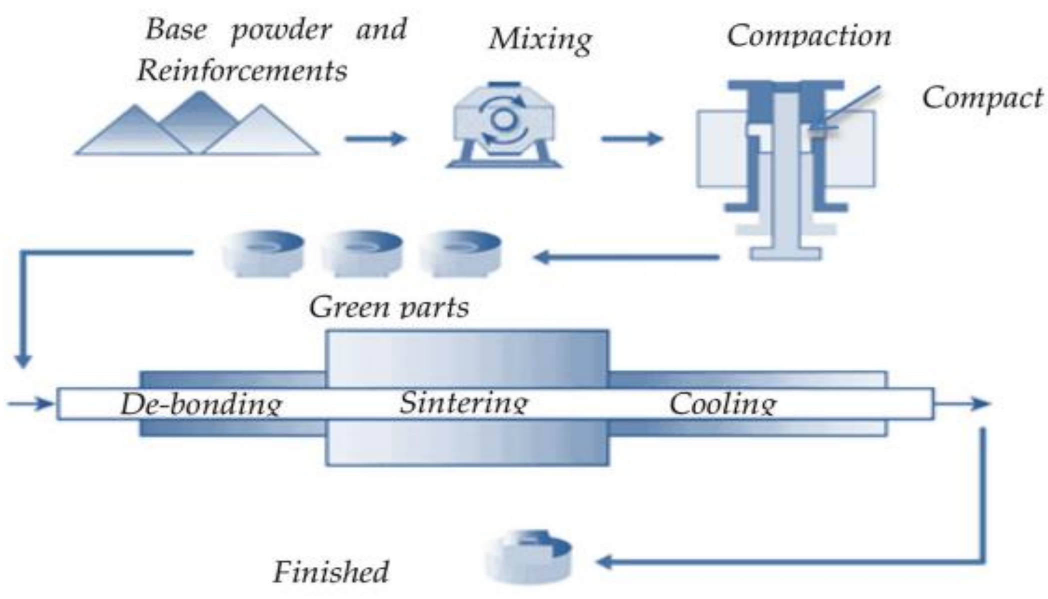

Figure 1.2 Principles of the powder metallurgy process (Prashantha & Xavior, 2018).

1.1.3 Application areas of magnesium metal matrix composites

Currently, The Mg alloy MMCs have a broad area of application towards mass saving application i.e. less fuel consumption, and also the requirement of higher strength and stiffness. In addition, Mg alloys are the popular lightest structural alloys among the others (Trang *et al.*, 2018). In structural applications, Mg and its composites are used in Transfer case, radiator support, instrument penal beam, and steering components in the automotive category. It is also utilized in the aerospace industry in different parts, and that makes it to be a promising material for the future aviation industry. Namely, The Boeing 727 aero planes contain 12 parts, including control surfaces, wheels, engine gearbox, structural items, door frames, and edge flaps are made of magnesium alloys (Abbas *et al.*, 2021). Soviet air crafty industries, including the TU-95MS plane and TU-134, are using magnesium alloys up to 780Kg at different locations (Luo, 2013).

1.2 Statement of the problem

The high interest in obtaining novel and advanced engineering materials with effective modern technology has not been an option in the field of the automotive and aerospace sectors that leads to the advancement of MMCs. As a general rule for passenger cars, 86% of their energy consumption is the cause of having loads i.e. their weight and passengers (Hooftman *et al*., 2018). In the present condition of global warming due to the increase of co_2, the legislation on the limitation of emission has activated the acts to engage with magnesium alloy and its composites.

According to current market demand, lightweight materials with optimum property and performance are still required. Indeed, aluminum and its alloy are widely used in automotive and aerospace applications to satisfy the interest. But, further enhancement in strength to weight ratio, refined microstructure, corrosive, and wear resistivity are still in need. The manufacturing methods have also their role in order to meet the goal. Powder metallurgy is preferable for manufacturing metal matrix composites due to high raw material utilization and requires less amount energy based on different researchers' investigations. Therefore, this research aims to the development of metal matrix composites composed of MoS_2, SiC, and ZrO_2 as a reinforcement and AZ31-Mg as a matrix using powder metallurgy manufacturing process to overcome the existing limitations of low strength to weight ratio with poor mechanical and tribological properties.

1.3 Research questions

1. What are the main process parameters of the powder metallurgy process? How the experimental procedure will be designed?
2. How the samples can be produced?
3. How to determine the property of the samples?
4. How to decide the average, better and acceptable properties of the sample?

1.4 Objectives of the study

1.4.1 General objective

The general objective of this research is to experimentally investigate the tribological, metallurgical and mechanical behavior of AZ31-Mg alloy reinforced with MoS_2, SiC and ZrO_2 particles through powder metallurgy process.

1.4.2 Specific objectives

The specific objectives are as follows:

- To determine the density, porosity, hardness, and compressive strength of the developed material.
- To optimize the process parameters and model mathematically the output characteristics.
- To determine the density, porosity, hardness, and compressive strength of the optimum sample including fractography.
- To determine the particle size distribution and phase of the substance.
- To determine the wear characteristics of the developed material including its morphology.

1.5 Significance of the study

The Mg alloy-based composite has played a great role in the automotive and aerospace industries. This research provides a novel metal matrix composite used to provide a new solution. The significance of this study will be to overcome the limitation of the materials such as strength to weight ratios, less corrosive resistance, wear resistance in harsh environments, low creep resistance at high temperatures, and other mechanical properties. And, it investigates further on obtaining fine grain powder composite used to support fuel consumption economy, simple and low-cost production i.e. quality-based approach.

1.6 Scope of the study

This research is mainly focused on the fabricating the samples of MMMCs with randomly combined levels of input parameters as per design of experiment, and testing the material mechanical and physical properties i.e. density, porosity, hardness and compression strength. In addition, the optimization process is carried out based on the testing results using Taguchi based GRA tool which used to obtain optimal levels. The sample, that is manufactured using the optimal level input combination, are used to test the tribological behavior i.e. wear resistance and characterize the sample i.e. particle size distribution, fractography and wear morphology.

1.7 organization of the thesis

This study is constructed and classified with detailed plans for achieving the specific task as described in the chapters. In chapter one, the research focused on the introduction including the background of the study, problem statement, research questions, objectives, significance, and limitations. And, Chapter two focuses on reviewing the kinds of literature based on the importance of the study, and the methods and designs to indicate problems raised in previous research. In chapter three, the materials and methods are briefly described from conducting an experiment using PM after sample preparation to the testing procedures in order to investigate the effect of input process parameters (namely ratio of matrix and reinforcement, milling time, compaction pressure, sintering temperature) on mechanical properties particularly on hardness, compression as well as density and porosity properties on the fabricated sample of MMCs. It deals with finding the optimum combination of process parameters using the Taguchi-based GRA multi-objective optimization method. And, it focuses on testing the wear resistance, mechanical as well as metallurgical (microstructure) properties of the optimized samples. The results, which are obtained from different tests, are interpreted and discussed briefly what the results mean in addition to the limitations and importance of the study as well as prediction to future work under chapter four. In chapter five, the results are discussed comparatively to the shreds of evidence in the review part to conclude and summarize the findings.

1.8 Limitations for the study

In this study, the constraints faced during the manufacturing of the samples are listed below;

- ❖ The availability of materials and the willingness of lab organizations to work together.
- ❖ The availability and efficiency of machines and facilities used for conducting the test and experiment
- ❖ And also, the machine installation for the specific operation and skilled man requirement.

CHAPTER TWO: LITERATURE REVIEW

2.1 Introduction

In a composite material, Metal matrix composites are accepted after more than a quarter of a century of active research. MMCs comprise a metal as a matrix and other material as a dispersed phase. In this chapter, the literatures was taken to review about reinforcing materials, manufacturing method i.e. powder metallurgy, stir casting and others, process parameters of manufacturing method, properties of MMMCs, and data analysis methods.

2.1.1 Reinforcing materials and magnesium metal matrix composites

Lightweight materials utilization is one of the important strategies preferred by automotive manufacturing to improve efficiency. Therefore, Magnesium based MMC is one of the preferable MMCs to meet the demand requirements. Karuppusamy *et al.* (2021) studied that MMCs composed of AZ91 Mg-MMCs as matrix and tungsten carbide as reinforcement were investigated with 1.5 and 3.0 wt.% of reinforcement. And the mechanical properties were improved after the sample was tested in the solution of 420 ^{o}C and artificially aged at 175 ^{o}C. Even though WC addition had obtained better compressive strength, it had shown a reduction in tensile strength based on Characterization. This shows the common and desired average property for the compressive and tensile properties were not attained for better acceptability of the product. As a result, the piston made from AZ91 alloy resisted a load of 10 KN during quasi-static load testing. In addition, the strength of the pistons was exceeded approximately 30% and 70% when WC used as reinforcement. Therefore, it assures that Mg-MMCs provide an opportunity to utilize pistons with 35% reduced weight in application areas.

Sun *et al.* (2021) examined a novel fine-grained AZ31 magnesium alloy reinforced with sub-micron vanadium particles fabricated by powder metallurgy. It was found that vanadium particles could accelerate the pile-up of dislocations and the refinement of Mg crystallite sizes during the milling process. Additionally, the AZ31-2.5 wt. % vanadium particle composite exhibited competitive mechanical properties. Results proved that, compared to the cast AZ31 Mg alloy, the micro hardness, yield strength, ultimate tensile strength, and elongation of AZ31-2.5 wt. % vanadium particle composite increased by 102%, 128%, 59% and 10%, respectively. This has shown how the reinforcement alters the mechanical property.

Sukriti *et al.* (2021) investigated the mechanical and corrosion behavior of Al-based composites reinforced with 3, 6, and 9 wt% of hybrid reinforcements i.e. SiC, graphite, and ZrO_2 fabricated via a stir casting process. Due to the addition of hard ceramic reinforcement, the density was increased slightly with the wt.% of hybrid reinforcement, and the porosity was affected by the fabrication procedure of composites. The mechanical properties such as hardness, tensile strength, and impact strength of pure aluminum were improved. As a result, 3 wt% of micro/nano hybrid aluminum composite showed the least void content (1.7%) in the composite and optimum mechanical properties along with minimum corrosion rate, and its micro-hardness increased by 27.5% (42.6 VHN) in comparison to that of the unreinforced Al (33.3 VHN).

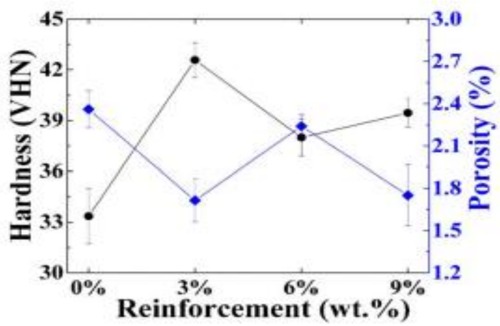

Figure 2.1 Variation in micro hardness relative to hybrid reinforcement (Sukriti *et al.*, 2021).

And relative to pure Al, the Impact strength of the composite increased by 27.2% for 6 wt.% hybrid reinforcement (247.1 J) and then started decreasing, whereas the tensile strength of the composite increased by 8% for 9 wt.% hybrid reinforcement (124.0 MPa). However, the flexural strength of the pure Al was reduced with the addition of hard reinforcing particles, and the fracture behavior of the composite was changed from ductile to the mixed mode of fracture (dominated by the ductile nature) when wt.% of hybrid reinforcement increases.

Table 2.1 Mechanical properties of micro or nano reinforced hybrid Aluminum composites. (Sukriti *et al.*, 2021).

Hybrid reinforcement (wt. %)	Tensile strength (MPa)	Ductility (%)	Hardness (VHN)	Flexural strength (MPa)	Impact strength (J)
0% SGZr	115.1	43.3	33.3	177.4	195.0
3% SGZr	109.0	28.1	42.6	141.2	242.1
6% SGZr	91.7	29.8	38.0	160.8	248.0
9% SGZr	124.0	39.1	39.5	146.5	242.1

Kumar *et al.* (2021) investigated the micro structure and mechanical properties of AZ31D Mg alloy reinforced with 1, 2, 3, and 4 wt. % of SiC using the stir casting process. The addition of SiC reinforcement notably reduced the grain size of the AZ31D Mg matrix (i.e. linear relation b/n the grain size and SiC particulate) as a reason for having better interfacial bonding among the base metal and reinforcement and dense dislocation as TEM micrographs indicated. Due to the reinforcement of SiC particles distributed in the alloy matrix, the composite's hardness, compressive and tensile strength was increased. As a result, the AZ31D composite with 4% SiC reinforcement had shown the highest compressive strength i.e. 380.20 MPa, and also the hardness improved to 29%. Finally, the homogeneous dispersion of refined SiC particles over the matrix material and effective load transfer between the reinforcement and matrix alloy provided better results upon the improving properties of AZ31D composite.

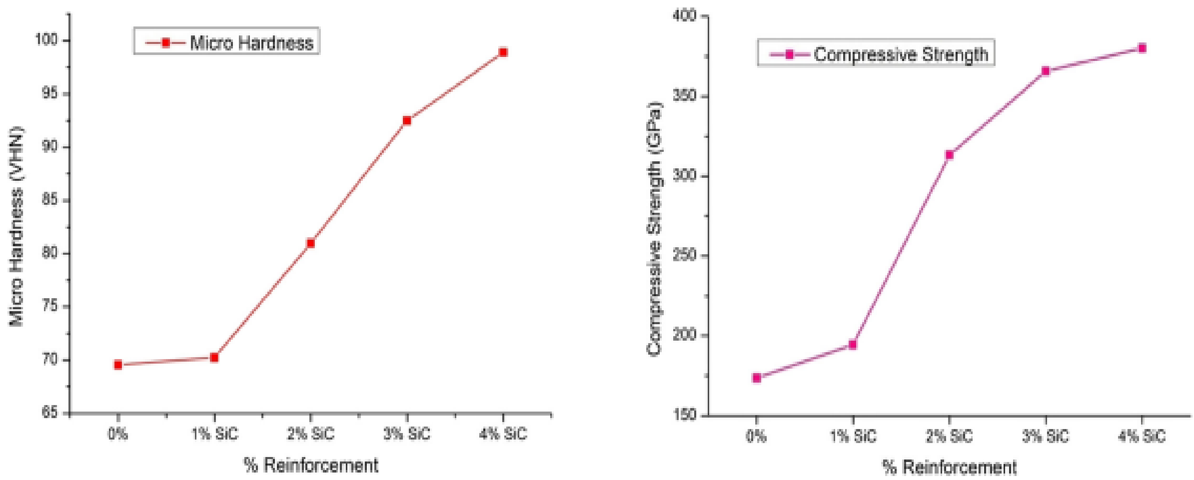

Figure 2.2 Micro hardness and Compressive strength vs. reinforcement percentages (Kumar *et al.*, 2021)

Qiao *et al.* (2021) investigated the mechanical, microstructural, corrosion, and tribological properties of AZ31/ZrO_2 nano composite fabricated by friction stir processing. With the addition of ZrO_2 particles, The average grain size was refined from 10 µm of Base metal (BM) to 3.2 µm i.e. with a grain size range of 0.1–14 µm. The micro hardness of FSP-ZrO_2 composites was also increased from 71 HV (BM) to 99 HV, the ultimate tensile strength (UTS) from 273 MPa (BM) to 427 MPa, yield strength (YS) from 137 MPa (BM) to 217 MPa. The electrochemical corrosion behavior of three samples in simulated body fluid (SBF) solution revealed a reduction in the corrosion rate but the corrosion resistance was increased for the composites. The main factors affecting the corrosion performance were the grain size and ZrO_2 particles.

Venkatesh & Deoghare (2021) studied the mechanical behavior of Aluminum matrix reinforced with kaoline metal matrix composite fabricated through powder metallurgy technique. Composite samples were fabricated by using the powder metallurgy technique with reinforcement percentages of 5%wt, 10%wt, 15%wt, and 20% wt. The hardness of the composite was increased from 77 VHN to 187 VHN with increasing the kaoline reinforcement from 0% to 20%. Adding reinforcement from 0% to 20%, the compression strength was found to be increased by 54.8%, and tensile strength was enhanced by 55.1% when compared to monolithic pure Aluminum. And, it suggests the suitability of Al-Kaoline composite material where lighter weight and higher strength were required for instance in the manufacturing of automobile pistons and automobile bodies.

Sun *et al.* (2021) examined the microstructure and mechanical properties of fine-grained AZ31 magnesium alloy reinforced with an average particle size of 40 µm sub-micron vanadium fabricated via powder metallurgy. The mixed initial materials in a 500 ml chrome steel vessel were mechanically milled for various levels of milling time (10, 30, 50, 70, and 90 hrs.) at 200 rpm milling speed and the ratio of the ball (Φ5, Φ8, Φ10 mm) to the powder was 60:1 under argon control atmosphere during materials handling also. The results showed that the average crystallite size of AZ31-2.5 wt. % V_P composite powders were refined to 25 nm after milling for 90 hrs., which was much lower than that (130 nm) of AZ31 powders without the reinforcement. After the densification process, the AZ31-2.5 wt. % V_P composite exhibited fine-grained structure and high mechanical properties. The ultimate average grain size of the composite was 3.08 µm. Moreover, compared to the as-cast AZ31 Mg alloy, the micro hardness, YS, UTS, and EL of AZ31-2.5 wt. % V_P composite enhanced by 102%, 128%, 59% and 10%, respectively. Moreover, due to the above advantages, the AZ31-V_P composite had fitted to utilize in the fields of aerospace, and vehicle industries.

Mazaheri *et al.* (2020) focused on improving the wear resistance of AZ31 Mg alloy by reinforcing 38 wt.% ZrO_2 (estimated) nanoparticles and increasing pass number. It was fabricated using friction stir processing (FSP) in two different pass numbers i.e. one and four passes. As a result of the addition of reinforcement and pass number, the average grain size of AZ31 base metal was decreased from 11 µm to 2 µm during four passes of FSP applied on AZ31/ZrO_2 Nano composite surface. The grain size of the AZ31/ZrO_2 nano composites decreased to about 40% and 80% after one and four passes respectively. The micro hardness value also improved around 65% and 90% after one and four passes respectively. In addition, the processed nanocomposite after four passes obtained a wear rate of about half of the AZ31 base metal, and an average friction coefficient was decreased from 0.5 to 0.22. Therefore, most of the composite properties were based on the ZrO_2 reinforcement and processing techniques of FSP.

Padmanaban *et al.* (2020) investigated A356 Al-Si alloy with 7.5 wt % Si and 0.3 wt %Mg and Al-Si MMCs with 5 to 20 vol. % of SiCp were produced using a house-made Rheo-Die Cast (RDC) machine. In the case of RDC composites, the grain size of the matrix was markedly decreased with the increasing percentage of SiCp reinforcement. In addition, the wear resistance was found to be nearly three times higher than that of RDC alloy. Therefore, fine-grained with non-dendritic microstructure, spherical shaped Si particles, good wettability, and uniform distribution of SiCp with matrix played a major role in the improvement of wear behavior of both alloy and composite materials.

Esen *et al.* (2020) studied the effect of coupling of unalloyed Mg and Mg-alloys (AZ91 and WE43) with Ti6Al4V alloy on corrosion and degradation behaviors of composites that were produced via liquid infiltration into porous Ti-alloy samples. It showed that Ti6Al4V-Mg composites fractured and lost their mechanical stabilities even after 1 day. A relatively less amount of fractures was observed in Ti6Al4V-WE43 composites and they could partly preserve their mechanical integrities. Among the composites, Ti6Al4V-AZ91 composites were the only ones able to preserve their mechanical integrities. Comparatively, Ti6Al4V-AZ91 composites can be considered to be a candidate composite for bone implants.

Sahu *et al.* (2020) investigated the tribological behavior and effect in mechanical properties of AZ31 Mg alloy with 3%, 6% and 9% Al composition manufactured via friction stir alloying process. The results showed as the friction coefficient, average COF, wear rate, and wear volume loss in the case of 6% Al alloying were less as compared to other compositions. In addition, The proper amount of alloying (6% Al) into the AZ31 Mg matrix depicted the finest grain (8 µm, 87% finer than base metal) with uniform distribution, an increment in hardness, and superior wear resistance that reduced plow, plastic flow, and adhesion wear. Therefore, the mechanical properties were improved due to the alloying process and it shows the best results were obtained in the case of 6% Al alloying.

Zang *et al.* (2020) fabricated nano-ZrO_2-reinforced AZ31 alloy composites by friction stir processing with three multi-passes and high rotation speeds. The compositions were taken

AZ31/2.14 vol% ZrO_2, AZ31/4.29 vol% ZrO_2, and AZ31/6.43 vol% ZrO_2 in the developed composite samples. In this study, the average grain sizes of the stir zone center in the AZ31/2.14 vol% ZrO_2, AZ31/4.29 vol% ZrO_2, and AZ31/6.43 vol% ZrO_2 composites were 8.46, 8.23, and 8.39 µm, respectively. After three cumulative FSP passes, the best tensile properties were observed in the AZ31/6.43 vol% ZrO_2 composites. During increasing the friction stir processing passes, uniformly distributed ZrO_2 particles with fine microstructure (i.e. less agglomeration) and strong interfacial bonding between the Mg matrix and ZrO_2 particles were obtained. In addition, the hardness and tensile properties of the MMCs had been enhanced in the composites.

Kumar *et al.* (2019) studied on microstructure and mechanical properties of AZ31Mg alloy reinforced with 5, 10, and 15 vol.% of ZrO_2 particle composites produced via the stir casting process. As a result, the finest grain size around 20 µm was obtained for AZ31 with 15vol.% ZrO_2 composition since AZ31 alloy has a grain size of about 70 µm. In addition, AZ31 alloy reinforced with 15 vol.% of ZrO2 composite showed a high hardness value of 102 HV, proof stress of (120MPa), and tensile strength of (198 MPa) compared to the base metal. Relatively, the developed composites significantly improved by 65, 33, and 41% in hardness, proof stress, and tensile strength respectively compared to the matrix alloy. Therefore, the addition of ZrO_2 reinforcement had provided refinement of grain size i.e. decreasing grain size and enhancing the hardness, proof strength, and tensile strength even though ductility decreases.

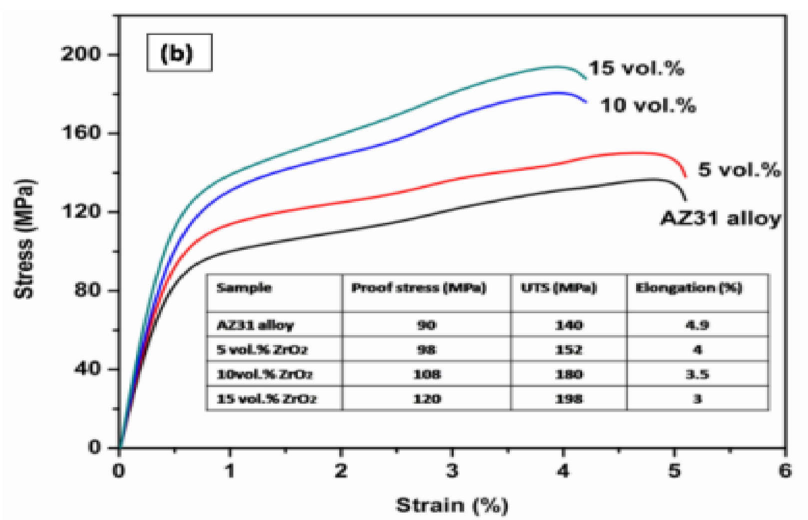

Figure 2.3 Tensile properties vs. ZrO_2 reinforcement percentage (Kumar *et al.*, 2019).

Kavimani *et al.* (2019) fabricated using homogeneously reinforced AZ31 alloy with 0.2, 0.3, 0.4, and 0.5 wt.% of graphene oxide (r-GO) nano sheets via solvent-based powder metallurgy. It was carried out by following a series of methodologies involving solvent processing, mechanical alloying, cold pressing, and finally sintering under an argon atmosphere at 560◦C. Microstructure characterization studies revealed that GO nano sheets were uniformly distributed with better bond strength since no cracks were observed in the micrograph and a few micro-voids due to density reduction. r-GO (0.4 wt%) reinforced AZ31 Mg alloy improved the hardness, wear, and corrosion resistance efficiency up to 84% but the further increment in the r-GO content reduced the wear rate. The manufactured composites had been recommended to be applicable in engineering applications where high wear and corrosion resistance are mostly desired for instance brake shoes. Madeshwaran *et al.* (2018) studied the effects of molybdenum disulfide (0.05wt%, 0.1wt%, 0.25wt%, and 0.5wt %) on thermal expansion and mechanical properties of epoxy composites which were fabricated using both ultra-sonication and mechanical stirring for 4 hrs. at 700 rpm. The results indicated that the incorporation of ultralow content (0.1% by weight) of ex-MoS_2 in the epoxy matrix had significantly increased the flexural (9.0%) and tensile strength (39.2%) properties of composites. Moreover, The Coefficient of thermal expansion of composites was significantly reduced with the addition of ex-MoS_2 in the composites. And, it assures that interfacial interaction between epoxy and MoS_2 had a significant role besides the improvement in mechanical properties of epoxy nano-composites.

Narayanasamy & Selvakumar (2017) investigated the tribological and mechanical behavior of Magnesium matrix hybrid composites reinforced with a wt. % composition of TiC (0, 5, 10, 15, and 20) and a fixed 7.5 wt. % of MoS_2 produced via Powder Metallurgy. The hardness of the hybrid composite samples was increased with an increase in the weight percentage of TiC up to 15% due to the uniform distribution of TiC particles in the matrix. And, the optimal wt. % of TiC reinforcement content was about 15% for any value of the applied load, distance, and speed since it tended to increase wear rate and coefficient friction beyond this wt. %. But, Mg-7.5MoS_2 composite had a minimum friction coefficient than other composites with larger wear debris which could be smaller while TiC wt. % increases. Therefore, the improved tribological behavior towards wear resistance was obtained from the combination of TiC with MoS_2 particles in the manufactured composites.

Emee *et al.* (2016) studied the effect of milling time using 1, 2, 5, 10, and 15 hours and 250 rpm milling speed using a planetary mill in mechanical properties and corrosion resistance of Mg-10wt%. Zn alloy. It was synthesized by mechanical alloying followed by compaction under

400MPa and sintering in a tube furnace at 350 °C in argon flow. As a result, the micro-hardness of Mg-10wt%Zn alloy was increased from 66.73 HV to 88.72 HV. And, the sintered density reached the highest value of 1.813 g/cm^3 when milling time was increased from 1 hour to 10 hours. However, the prolonged milling time above 10 hrs. resulted in the reduction of density due to the excessive heat generation at higher milling time and the existence of cold welding during mechanical alloying. Therefore, it caused to reduce its densification effect and minimizes the compressibility of the milled alloy which affects the properties.

2.1.2 Processing technologies of magnesium metal matrix composite

The metal matrix composite manufacturing techniques can be categorized into the following three broad categories as Solid-state processing, liquid state processing, and In-situ processing techniques. For Mg metal matrix, some methods were used to manufacture particulate reinforced magnesium metal matrix composites (MMCs) including powder metallurgy, squeeze casting, gas pressure infiltration, stir casting, and disintegrated melt deposition (Ren *et al.*, 2010).

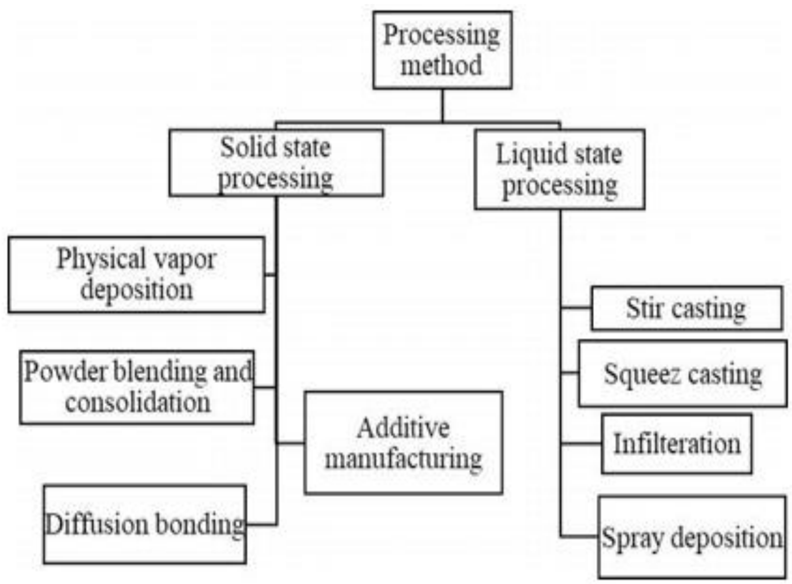

Figure 2.4 Manufacturing methods for MMCs materials (Abbas *et al.*, 2021).

2.1.2.1 Solid-state methods

Solid-state fabrication of MMCs is the process that forms a bond between matrix and reinforcement in solid states due to mutual diffusion occurring between them at elevated temperatures and pressure. Comparatively to Liquid state fabrication of MMCs, Low temperature assisted solid-state fabrication process reduces the probability of forming unpleasant reactions on the boundary between the matrix and reinforcing phases. Kopeliovich (2012) defined sintering as it was the method in PM that involves the consolidation of powder grains by heating the "green" compact part to a high temperature below the melting point. The particles were expanded (diffused) into the neighboring particles in the composite. And, powder metallurgy has offered an advantage over reducing machining operation due to forming parts with minimum tolerances. Moreover, It allowed the fabrication of material even if it is difficult to produce in other ways, namely refractory or hard materials, permanent magnets, Porous metals, wear-resistant materials, a mixture of materials that had a dissimilar Mpt or insoluble in the liquid state as well as the combination of nonmetal with metals. In contrast to the liquid state fabrication of Metal Matrix Composites, the PM method allowed to obtain the dispersed phase up to 50% in the materials. From other methods, diffusion bonding was one of the solid-state methods that were usually used to manufacture a part having an uncomplicated shape like a plate, tube, etc.

Abbas *et al*. (2021) stated that during the physical vapor deposition method, the fibers were continuously passed over the substrate of the metal with high partial pressure. And then, the surface was coated using the produced vapor to condense on it. The deposition rate was 5-10 μm per minute. The hot isostatic pressing was used to consolidate the coating fibers. For instance, Sputtering was a physical vapor deposition method in which argon ions are used for bombarding catholically connected targets to deposit the coating.

2.1.2.2 Liquid metallurgy methods

Liquid state fabrication of MMCs involves the process at the liquid state of matrix metal with the incorporation of the reinforcement phase and it is followed by the Solidification process. In this method, the interfacial bonding, i.e. the molten matrix and dispersed phase, plays a great role in the mechanical properties of the composites. For that reason, enhancing the wetting feature using a proper coating of the dispersed phase led to minimizing interfacial energy and inhibiting chemical interaction between matrix and reinforcement (Kopeliovich, 2012). Some ways of liquid state fabrication for MMCs are Stir Casting, Infiltration, Gas Pressure Infiltration, Squeeze Casting Infiltration, Pressure Die Infiltration, and others.

Kopeliovich (2012) assures that Stir Casting was characterized by features such as limited content of dispersed phase, not more than 30 vol. %. In addition, its lack of homogeneity in the distribution of the dispersed phase over matrix material was caused by local clouds (clusters) of the dispersed particles (fibers) and gravity segregation of the reinforcements due to a difference in the densities of the reinforcement and matrix phase. Semi-solid condition of the matrix affected the uniform distribution of reinforcements in the composite. Thus, the high viscosity of the semi-solid matrix material enabled better mixing of the dispersed phase. Alternatively, the spray co-deposition method allowed for the fabrication of near-net-shape of Metal Matrix Composites. Examples of spray co-deposition can be Aluminum matrix material reinforced by silicon carbide (SiC) was produced by spray co-deposition followed by Rolling. In the chemical vapor deposition process, the vapors were decomposed and formed a coating on another substrate that was carried out at elevated temperatures. And it also stated that the Squeeze Casting Infiltration method was similar to the Squeeze casting technique used for metal alloys casting which is suitable for manufacturing simple small parts like automotive engine pistons made from an aluminum alloy as matrix and alumina short fibers as the dispersed phase.

Abbas *et al.* (2021) investigated that during utilization of spray co-deposition, the droplet/powder velocities were typically 20-40 m/s, and the thin layer of semisolid reinforcement was presented on the surface of the ingot. Indeed, the MMCs produced by spray deposition often exhibited inhomogeneous distribution, and the ceramic layer was normal to growth direction which leads to hydrodynamic instabilities in powder injection. The porosity in the as-sprayed state was typically 5–10% leading the process to be adopted for bulk production in MMCs. Another method of liquid state method is Squeeze Casting Infiltration which is a forced infiltration method used in the fabrication of Metal Matrix Composites. As a result, it revealed grain refinement, very little porosity in castings along with the high pressure of dies that lead to an increase in the strength in composites.

2.1.2.3 In-situ process

The in-situ processing involves a chemical reaction in which a dispersed (reinforcing) phase is formed in the matrix as a result of precipitation from the melt during its cooling and Solidification. Abbas *et al.* (2021) studied the capability of the method which provides the thermal compatibility between matrix and dispersed phase, and surfaces that are free from contaminations. And, Kopeliovich (2012) also stated that dispersed phases of in situ fabricated Metal Matrix Composites may consist of intermetallic compounds, carbides, borides, oxides, one of the eutectic ingredients from the products.

2.1.3 Significance and limitations of powder metallurgy

As some literature stated that the powder metallurgy process provides good results in having better mechanical, metallurgical, and other properties in the MMCs. For instance, it accomplishes a more uniform distribution of particles in the metal matrix with or without the reaction along with the matrix and dispersed phase.

Rodríguez *et al.* (2020) stated that PM had a role in Cu-based MMCs material such as appropriate material utilization, neat net shape product i.e. less scrapping and complex geometrical shape by using isostatic pressing, etc. As Huan *et al.* (2018) stated that good mechanical, electrical, and metallurgical properties were obtained. Besides, it had a significant advantage over the reduction of material removal processes that supports the cost-minimizing and also the capability of producing novel material that could be hard to make in other melting or forming processes. As Song *et al.* (2016) also reviewed that the PM process was capable of providing simplicity, flexibility, and also net shape products in the manufacturing of Nano-MMCs. Kopeliovich (2012) also validated that the Powder metallurgy process reduced machining operation due to forming parts with minimum tolerances and also alleviate and simplify the production process during producing complex geometry. In addition, Powder metallurgy permitted the manufacture of materials, which cannot be able to manufacture with any other technologies: refractory materials, hard materials, wear-resistant materials, permanent magnets, porous metals, and mixtures of dissimilar metals possessing different melting points or insoluble in the liquid state, various combinations of mixtures of metals with non-metals.

Some investigations also showed that it was suitable during the production of material difficult to form alloys as well as MMCs (Paul and Georges, 2011). As Z. Ren et al. (2010) revealed that the mechanical property of Carbon Nano tubes reinforced MMCs recommended and concluded the powder metallurgy process was the most preferable in future production. And, Suryanarayana (2001) suggested that PM was the most preferable method to manufacture bulk ultra-fined grained Mg alloys compared to other processes.

Comparatively, the Powder metallurgy process is a method preferably used rather than other processes like casting, stamping, or machining. Reasonably, it becomes more suitable when the materials own the property of high wear resistance or strength with a high operating temperature that exceeds the temperature resistance of die casting alloys.

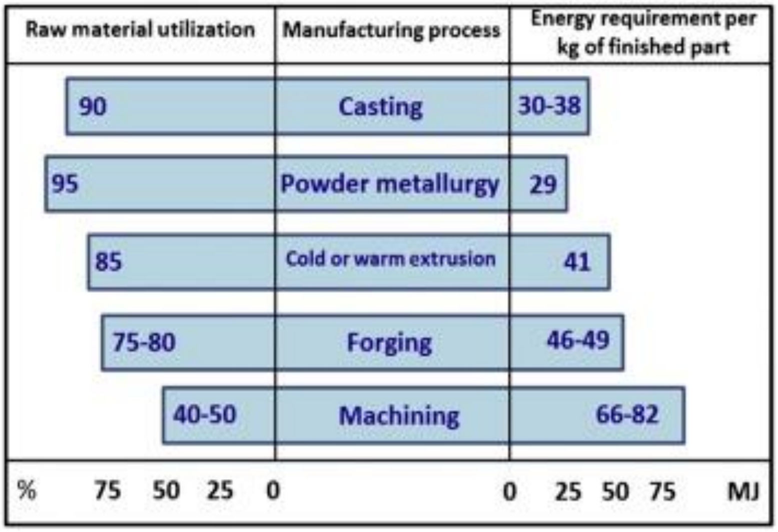

Figure 2.5 Energy and raw material utilization for different manufacturing processes (Torralba, 2014).

In addition, it eliminates the finishing during machining operation cause of offering a great precision and evades the casting defects namely blow holes, shrinkage, and inclusions (Upadhyaya, 1998). Unfortunately, the PM method is suitable for Mg MMCs materials even though several techniques can be utilized during the fabrication of metal matrix composite materials based on some works of literature justification. Likewise, it has some drawbacks that have little influence on its demand in the manufacturing industry. It was the cost of fine powder of the raw materials and the die materials (Tjong, 2013).

From the above manufacturing techniques of MMCs, it is justified that powder metallurgy is suitable for Mg-based MMCs. Comparatively, it can provide a way of manufacturing the composites with:

- Providing uniformly dispersed composites
- Capability of manufacturing materials like refractory materials through following easy steps
- Better mechanical, metallurgical properties
- Less manufacturing time and cost with low temperature assisted
- Less requirement of the skilled person

2.1.4 Influence of process parameters in powder metallurgy process

As the world is shifting towards renewable sources of energy, the demand for Magnesium is increasing due to its excellent strength to weight ratio and corrosion resistance properties. Although, because of its low strength and wear resistance, the use of pure magnesium is quite limited. Various reinforcing materials are added to the Mg matrix to fabricate high-strength and wear-resistant Mg matrix composites. Meanwhile, the manufacturing methods have an influence on desired properties of the product according to the application areas. From various manufacturing methods, Powder metallurgy has been the most commonly used fabrication method for Mg-based materials metal matrix composite. It has different stages for manufacturing the products with their perspective parameters. Properties of a powder metallurgy product depend on the process parameters such as Compaction pressure, sintering temperature, sintering time, Rate of reinforcement, size of the matrix and reinforcing elements, etc. Some of the literatures showed some parameters that highly influence the manufactured product properties like mechanical, physical and others.

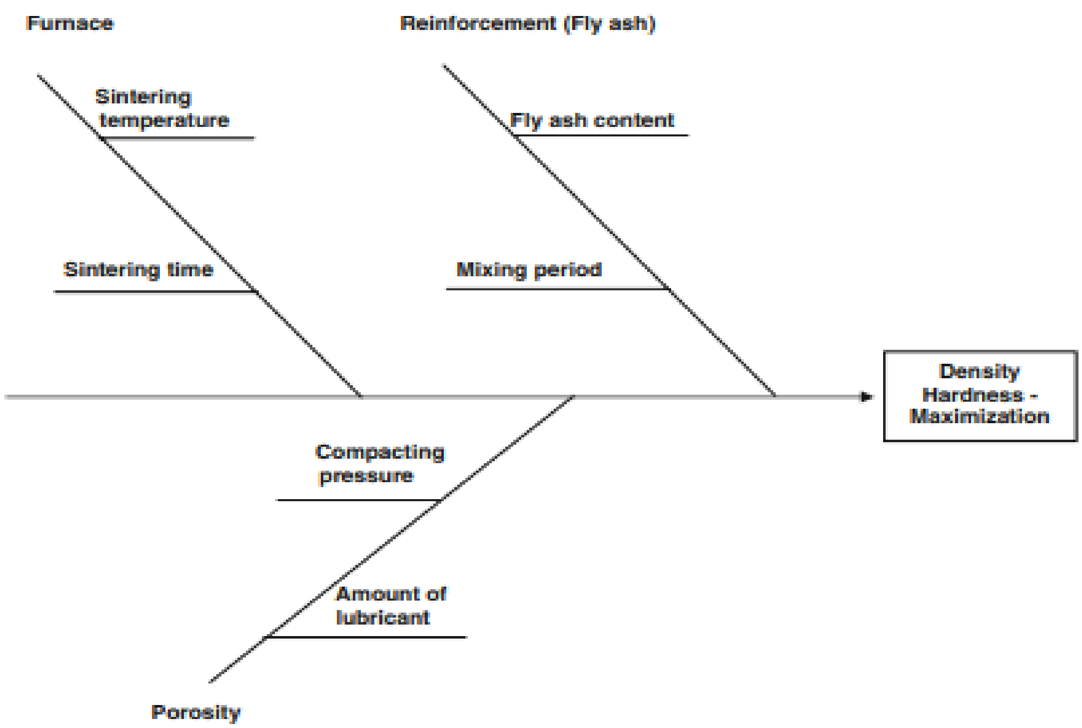

Figure 2.6 Cause and effect diagram of Al-Si alloy/fly ash composite (Jailani *et al.*, 2009).

The literature survey revealed that SiC, graphite (Gr), TiC, and graphene (Gn) are the most commonly used reinforcement additives in the metal matrix for improvement of the strength and wear resistance of metal-based materials. Kumar *et al.* (2020) showed the impact of compaction pressure on the electrical conductivity and hardness properties at different levels of pressure. Mechanical and electrical properties were improved when a small particle size of 3–5 µm of Cu-matrix material was used. The size of Nano-reinforcements, such as CNTs, should be sufficiently larger (30–50 nm) to avoid agglomeration. Besides, the optimum range of compaction pressure of 550–650 MPa, the sintering temperature of 800–900°C, and sintering time of 60–90 min were the factors that contribute to obtain better properties.

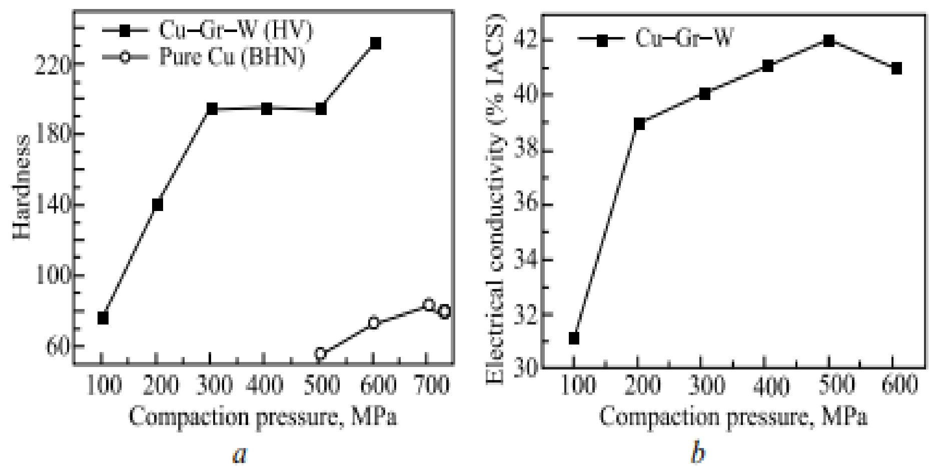

Figure 2.7 Effect of compaction pressure on hardness (a) and electrical conductivity (b) of copper-based materials (Kumar *et al.*, 2020).

According to their investigation provides better mechanical and electrical properties had been obtained when small particle size of 3–5 µm of matrix material (Cu) was used. Compaction pressure of 550-650 MPa was considered optimum for enhanced mechanical and electrical properties in Cu-based composites. And, Sintering temperature within the range of 800–900°C and 60–90 min sintering time had provided better mechanical and electrical properties of Cu-based composites. When the sintering time increased further, electrical conductivity was reduced which was related to the formation of oxides or thermal expansion in the material.

Zago *et al.* (2020) investigated the influence of high sintering temperature, up to 1350 °C, on the dimensional and geometrical precision of low alloyed steel parts. The parts were prepared by compacting commercial water atomized iron powder with mixing of 3%wt Cr and 1.5%wt Mo, to which 0.8%wt lubricant and 0.55%wt C (graphite) alloys. And, it was compacted up to 7.0 g/cm3 and sintered in a vacuum furnace at four different sintering temperatures values as 1200 °C, 1250 °C, 1300 °C, and 1350 °C (i.e. higher than the standard ones). Then, the results showed the significant dimensional change of diameters (i.e. increasing in diameter) with increasing sintering temperature, while a dimensional change of height increases on increasing sintering temperature and size but the effect was more evident for small sizes. Unfortunately, the influence of high sintering temperature on geometrical characteristics was surprisingly low. And also, high sintering temperature can be a significant cause of providing good improvement in mechanical properties of the sintered part without influencing dimensional and geometrical precisions.

According to Zamani *et al.* (2019) studied a process parameter of wt. % of reinforcement processed via powder metallurgy that can also affect the final property of a composite material. Generally, researchers found that the addition of Gr reinforcement reduced the mechanical properties such as tensile strength and hardness of the composite relative to the base material, but the wear behavior was improved. Yu *et al.* (2018) examined the effects of heat treatment on the microstructure and wear properties of Al–Zn–Mg–Cu/in-situ Al– 9Si–SiCp/pure Al composites fabricated by powder metallurgy process. Even though using pure Al powder enhanced the densification, it resulted in heterogeneous precipitation as well as differences in hardness among the grains in the composites. Heat treatment was conducted to solve this problem which consists of solution treatment, quenching, and aging treatment stages. They found that the hardness of the sample aged at 100–160 °C was higher than that aged at 200–240 °C. In addition, when the wear test was conducted under a load of 100 N with various linear speeds. As a result, the wear behavior changed from abrasive to adhesive wear when the linear speed was increased to 1.0 m/s and also lower wear rate obtained from the aged one than as-sintered composite during all conditions.

Linong *et al.* (2013) studied the impact of reinforcement type on the final property of a composite material. The experimental results revealed that the tensile strength of the composite with the addition of 5wt% β-SiC nanoparticles could be increased to 215 MPa, increasing by 110% compared with pure Al matrix. Comparative experiments reflected that the β-SiC nanoparticles showed a significant reinforcement effect than traditional α-SiC micro-sized particles. In order to fabricate nano-SiCp/Al composite, the preparation process and sintering procedure were investigated to develop a cost-effective production.

2.1.5 Properties of composite materials processed via powder metallurgy

Properties of composite materials depend on the factors such as the property of the reinforcement, the property of the matrix materials, and the interface between them. However, different researchers examined different properties under different conditions. For instance, Farhadinia *et al*. (2017) investigated the mechanical properties and microstructure of a hybrid reinforced composite under hot pressing of powder metallurgy methods. It was carried out using aluminum as a matrix with different amounts of TiB_2, ZrB_2, and Al_2O_3 powders as the dispersed phase. The mechanical properties of the composites were investigated based on micro hardness and compression tests. The results showed well-distributed particles in the matrix that leads to a uniform microstructure of the composites.

Zhu *et al.* (2020) studied the friction and wear behavior of Mg powder reinforced with 5 wt.% WS_2 and 15-20 wt.% SiC particles fabricated via powder metallurgy processing. Tribological behaviors of MMMC samples were examined using a Bruker Universal Mechanical Tester (UMT) platform under room temperature and 110 °C. as a result of a normal load of 4 N (~ 0.5 GPa), room temperature and 110 °C, the friction coefficients of Mg MMCs were found to be reduced by 37.5% and 54.5% respectively, along with narrower, shallower and smoother wear tracks, in comparing with unreinforced Mg, and WS_2 particles. And, wear debris showed in trapped in the microscopic reservoirs due to SiC protrusions embedding on the Mg MMC surface. The findings demonstrated the agreement between the superior anti-wear behaviors of the WS_2 reinforced Mg composites and studies of lubricating mechanisms of WS_2 additives. Therefore, Mg reinforced with WS_2 and SiC provided outstanding anti-wear and frictional properties in addition to enhancing the mechanical strength. The manufactured composite can be qualified to be used in the tribological application based on the obtained results.

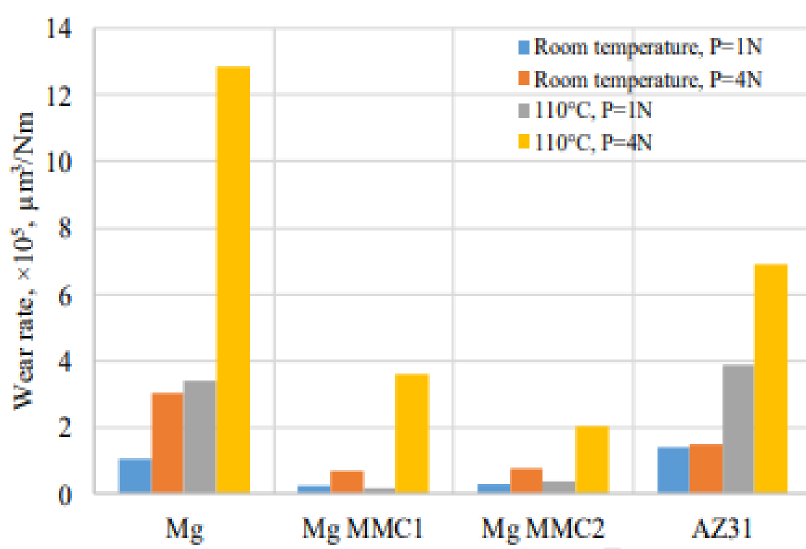

Figure 2.8 Various testing conditions of wear rate sliding against Al_2O_3 balls (Zhu *et al.*, 2020).

According to Zamani *et al.* (2019), the optimum combination of the reinforcement content was determined based on the responses of mechanical and tribological behavior of aluminum–graphite (Al–Gr) composites. Graphite was used as reinforcement at 3, 5, and 7 wt. %. in pure Al. Results showed that the increase in graphite content reduced the density of the material and the hardness of the composite material.

Kaviyarasan *et al*. (2019) also investigated the hardness and wear resistance properties of the magnesium reinforced with 0.5%, 1%, 1.5% and 2% wt.% of SiC manufactured via the powder metallurgy technique. As a result, the average values for all the hardness tests of pure Mg, 99.5%Mg0.5%SiC, 99%Mg-1%SiC, 98.5%Mg-1.5%SiC, and 98% Mg-2%SiC was obtained as 13 HV, 16 HV, 27 HV, 35 HV, and 65 HV respectively. From the average values of all the hardness tests, 2% SiC reinforced samples obtained a high value. The tribological behavior of the composite sample (i.e. pin) carried out under pin on disc wear test apparatus at three different velocities of 0.4, 0.6, and 0.8 ms^{-1} as well as two loads of 5 and 10N for a constant sliding distance of 500m. Meanwhile, the reinforcement of SiC particles made the friction force to be higher with the same sliding velocity. Composite pin with 98%Mg-2%SiC ratio showed a higher friction force at all the sliding conditions due to the SiC reinforcement.

2.1.6 Techniques of data analysis

As works of the literature showed that grey relational analysis is the best candidate for finding optimum value during the analysis of interrelationships between multiple responses. For instance, Jain & Kumar (2021) investigated the multi-response optimization of process parameters of the friction stir welded 6061-T6 aluminum (Al) alloy using Taguchi L_{16} orthogonal array-based grey relational analysis. The analysis of variance (ANOVA) method was used to analyze the effect of input parameters on output responses. From the confirmation test, the optimum FSW process parameters predicted by the Taguchi method improved the grey relational grade by 13.52%. The experimental result also assured that the Taguchi-based GRA method was feasible in finding solutions to multi-response optimization problems in the FSW process.

Unnikrishnan *et al.* (2020) showed that grey relational analysis combined with L_9 consists of 3 factors and 3 levels of the Taguchi method were taken to experimentally evaluate the weld ability of AZ31B magnesium alloy by FSW process. As a result of the confirmation test, better results in the optimization of welding parameters in FSW of AZ31B magnesium alloy were obtained through grey relational analysis along with the Taguchi-based method.

2.2 Literature summery

Generally, summarizing surveyed literature, researchers identified and investigated the effects of process parameters and the degree of the effects on the manufacturing process namely the powder metallurgy process. Additionally, the types and composition of reinforcement materials used in the developed composites to obtain optimum results according to the application areas of the sector. Property and composition of base metal i.e. AZ31 magnesium alloy were also well presented in various literature. Moreover, Application areas of metal matrix composite especially magnesium-based metal matrix composites are mentioned in different sections of automotive and aerospace industries because of tending to provide better tribological and mechanical properties. For instance, property of high specific strength leads to improving the fuel economy that establishes environmentally friend material. The compatibility and wettability properties of Mg alloy are also important properties to obtain the improved property of Mg alloy reinforced composites during production via the powder metallurgy process. Regarding the required property of lightweight or high strength to weight ratio, the reinforcements like SiC, $MoS_{2,}$ and ZrO_2 reinforcements can be the reinforcements to magnesium alloy MMCs because SiC made an interfacial bond without making inter-metallic phases and enhance strength this makes it a proper candidate for magnesium-based MMCs. Also, the appropriate composition of MoS_2 and ZrO_2 provided good interfacial bonding, minimum coefficient of friction, and improved wear resistance with other ceramic reinforcement distribution as well as corrosion resistance of Mg alloy MMCs. Moreover, the optimization method of Grey relational analysis can provide an optimal value over the multi-response experiments with the cooperation of the Taguchi method.

2.3 Research gaps

In the current market, lightweight materials with good strength are the desired property in the automotive and aerospace manufacturing industries. Due to this, it mainly focuses on the materials (i.e. base metal and reinforcements) and manufacturing technologies to provide MMCs materials with better characteristics of the properties namely high strength to weight ratio, hardness and compression, friction resistance, corrosion resistance, and tribological property. According to surveyed literature, these behaviors have not been investigated under the powder metallurgy process parameters with a different weight percentage of reinforcements, milling time, compaction pressure, and sintering temperature to obtain the optimum values of properties of the developed material. Even though, the sectors require the advancement to obtain novel and improved MMCs. Therefore, in this research, the above-mentioned properties have been experimentally investigated and studied to obtain an improvement in the property and optimum value through optimizing the process parameters of Mg alloy-based MMCs.

CHAPTER THREE: METHODS AND MATERIALS

3.1 Introduction

In this research, several materials and facilities were utilized under the proposed methods with the corresponding phase to conduct an experiment. This chapter consists of a details explanation of the matrix and reinforcement materials used to fabricate Mg MMCs, methods of preparation, sample preparation for various tests of the properties, optimization techniques, and generally instruments and machines sequentially.

3.1.1 General method of the research

The research was planned to achieve the specific tasks effectively and sequentially. The tasks started with identifying the problem or gaps in works of literature (and/or application areas). And, it was followed by selecting the appropriate materials and processing methods for the MMCs. After that, the corresponding factors and their levels were designed through Taguchi orthogonal array for the experiment. Based on DoE, The MMMCs have been manufactured with the appropriate manufacturing technique i.e. PM. It also then proceeded to further mechanical properties tests to optimize the process parameters using the GRA tool. In short, it is described further to accomplish the objectives of this thesis work using the methodology flow chart as shown in figure 3.1.

3.1.2 Materials and equipment

The main objective for manufacturing the MMMCs was mainly to have a property of high strength to weight ratio. For that matter, the material selection was taken as the basic footstep to obtain the desired product for the specified application area. The materials selected based on their properties were AZ31 Mg alloy as matrix and SiC, ZrO_2 and MoS_2 as reinforcement which had a mesh size of around 200 microns. The AZ31 magnesium alloy compositions are depicted in table 3.1 with their weight percentage in the magnesium alloy. In this study, the composite materials i.e. matrix and reinforcement materials, which were used for manufacturing the magnesium metal matrix composites, are tabulated with their various properties in table 3.2.

Table 3.1 Chemical composition of AZ31 magnesium alloy (Kavimani *et al.*, 2019).

Elements	Al	Zn	Mn	Fe	Cu	Si	Ni	Mg
Wt. %	3.5	1.4	0.3	0.003	0.008	1.2	0.001	bal.

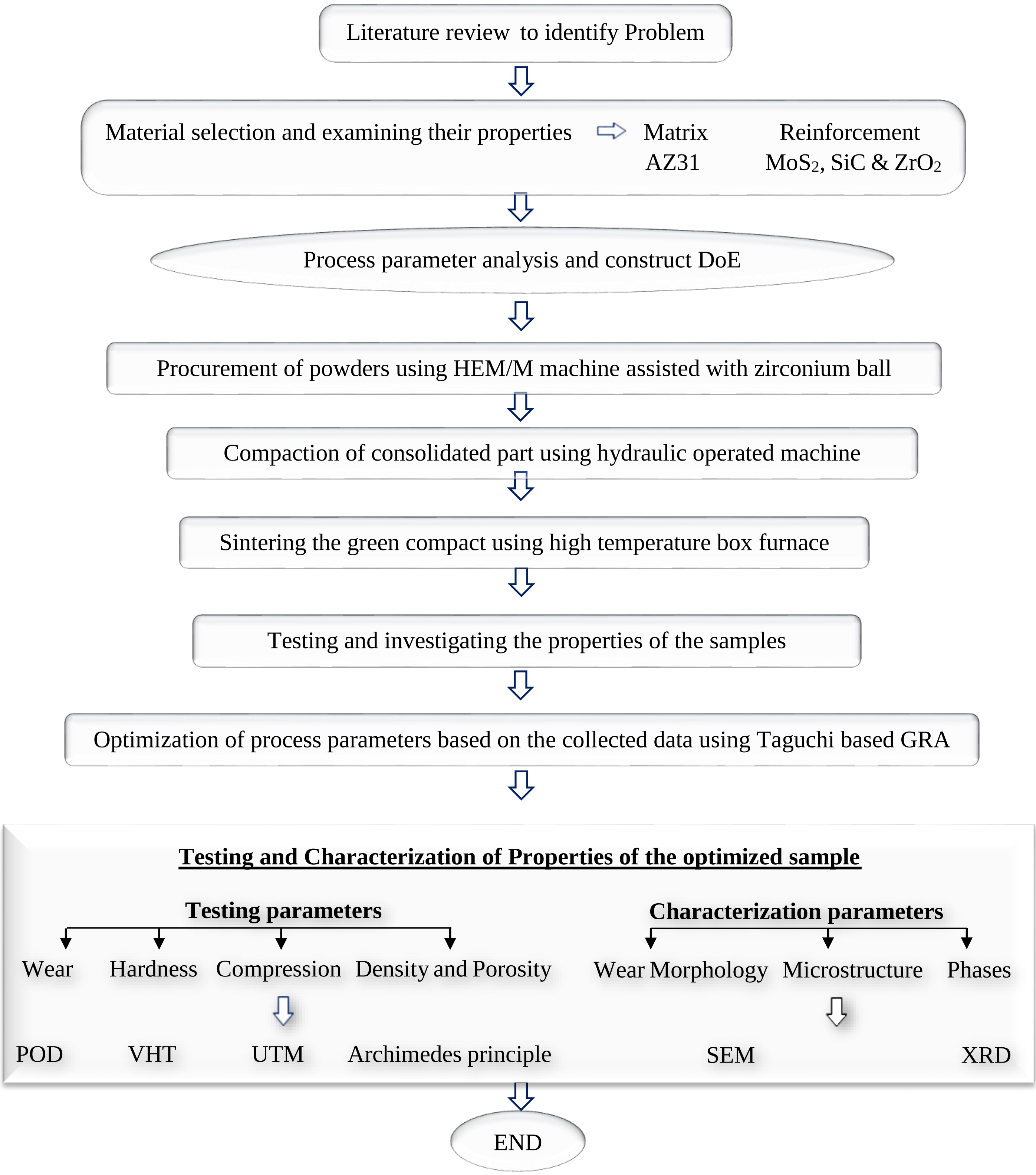

Figure 3.1 Flow chart of the research methods.

Table 3.2 AZ31 Mg alloy and reinforcement material properties.

Elements	Mg	AZ31 Mg alloy	SiC	ZrO_2	MoS_2
Color	White silvery	Shiny grey	Colorless	White	Black
Density (g/cm^3)	1.738	1.8	3.21	5.68	5.06
Yield strength (σ_y)	20MPa (cast)	189.6(extruded)	21GPa	230MPa	1017 ± 239
Melting pt. (°C)	650	605-630	2730	2715	1185

The MMMCs were then fabricated via powder metallurgy process with calculated mass for individual materials as shown in table 3.3. During composite fabrication via powder metallurgy process, the estimated weight (or mass) of the materials was calculated based on the volume percentage of the base metal and reinforcements. it was estimated around 50g for the total mass of the matrix material (around 0.05 Kg) and 35g (0.035 Kg), 30g (0.03 Kg), and 11g (0.011 Kg) for the reinforcements of SiC, ZrO_2, and MoS_2 respectively.

Table 3.3 The mass of base metal and reinforcing materials.

Trial no.	Reinforcement Wt.%					
	SiC		ZrO_2		MoS_2 (Vol. 4%)	BM (Vol. 81%)
	Vol %	Wt. (g)	Vol %	Wt. (g)		
1	5%	0.403	10%	1.427	0.508	3.662
	10%	0.806	5%	0.713		
	15%	1.209	0%	0		
Tot. mass		35g	30g		11g	50g

In table 3.3, the mass of the reinforcements is shown for the different composition of the reinforcements. That is used for one experimental run based on the design of the experiment. For this thesis work, some of the tools were used for various testing and characterizing process under sample preparation besides the machines utilized for different purposes as shown in table 3.4.

Table 3.4 The tools for sample preparation.

No.	Tools and chemicals	Tasks
1	File/rasp	To file the samples roughly during adjusting the dimensions.
2	Caliper	To measure sample dimensions accurately
3	Sandpaper (220, 800, 1200, and 2000 grits)	To get rid of the damages for obtain a flat surface

Moreover, different testing and manufacturing equipment were also utilized throughout the experiments during measuring and testing the specimen. It is listed in table 3.5 below with their specific tasks during the manufacturing of MMMC samples.

Table 3.5 The equipment used in Testing and Manufacturing processes.

No.	Equipment’s	Functions
1	Electronic weighing machine	To measure the weight percentage of matrix and reinforcement and weight loss during the wear test
2	High energy mill/ mixer	For blending and reducing the matrix and reinforcements
3	Hydraulic pressing machine	Used to compact the composite materials powders
4	High-temperature box Furnace	For sintering the green compact at various temperatures with a specific heat rate.
5	Grinding and polishing	To make a scratch-free, flat surface of the specimen by removing the damages
6	Scanning Electron Microscope (SEM)	To investigate the surfaces of wear morphology and fractography
7	Vickers hardness machine	To examine the hardness property of the samples
8	Universal testing machine (UTM)	To test the resistance of the compressive load applied to the specimens
9	Pin-on-disc	To test the wear and friction behavior of the optimal specimen.

3.1.3 Methods of powder metallurgy process

The MMMC specimens were prepared under the powder metallurgy manufacturing process to obtain better material properties. Several processing stages were there during the manufacturing of the samples using PM. At first, the estimated amount of powder for the experiment was calculated based on the vol. % of the powders (i.e. Rt. and BM) and expected green compact dimensions. Precisely, the calculated amount of powder was measured for each experiment run using an analytical precision balance with a weighing capacity of 252g/0.1mg as shown in figure 3.2.

Figure 3.2 Analytical precision balance used during measuring powders.

Precisely, the calculated amount of powder was measured for each experiment run using an analytical precision balance with a weighing capacity of 252g/0.1mg as shown in figure 3.2. The manufacturing process was achieved sequentially by following the procedures expressed in the flow chart as stated in figure 3.4. And, it was conducted based on the DoE using different machines for different tasks. The machine facilities used in different stages during the PM manufacturing processes were the ball milling machine, hydraulic pressing machine, and sintering apparatus. Ball milling is a physical method used to synthesize particles assisted with various balls inside the vials. In this study, a high energy mixer/mill machine was operated to obtain fine and uniformly mixed powders (i.e. matrix and reinforcement mixture) using zirconium balls.

Figure 3.3 Zirconium balls in vials for ball milling operation.

Its operation was carried out as per DoE using uniform size zirconium balls with a 2:1 ball to powder ratio. And, it was operated under uniform rotational speed for intervals of 40 min with a 15 min gap to reduce overheating of the powders in the vial.

Measuring amount of powders precisely

⇩

Mixing the matrix and reinforcement materials using HEM/M machine

⇩

Compacting the mixtures using hydraulically operated mounting press

⇩

Ejecting the green compact from mold using appropriate press equipment’s

⇩

Sintering the green compact using sintering apparatus

Figure 3.4 Flow chart for composite fabrication using PM processes.

Cold pressing was then carried out under a hydraulically operated mounting press machine using a mold. It was used to compact uniformly mixed powders at room temperature in order to form a solid part called a green compact. In this study, the pressing mold assisted with vertical oriented hydraulic fluid, was taken to produce the sample as shown in figure 3.6 (b). It was geometrically designed with 20mm and 80 mm internal and outer dia. respectively and 30 mm height. The experiment was operated under 20 min holding time after applying the uniaxial load in to the samples at different levels of compaction pressure adhering to the DoE.

Figure 3.5 The green compact with a given pressure.

In order to enhance the material properties of the samples, sintering furnace apparatus was used to apply heat into the green compact i.e. compacted powder. The process was operated under considering the atmosphere to increase the product's mechanical strength, density, and translucency as well as reduce oxidation of the samples. During the sintering process using a high temperature box furnace, the heat was applied with a 15^{0}c/min heating rate under various levels of sintering temperature at 40 min constant sintering time. Since the process does not require liquefying the material, the levels of the sintering temperature were taken below the melting temperature of the base metal.

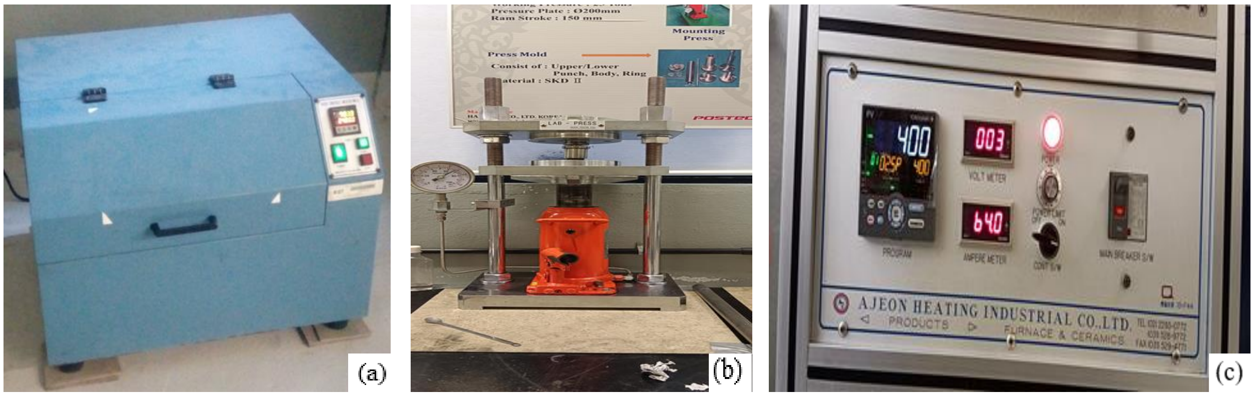

Figure 3.6 Ball milling, hydraulic press, and sintering equipment used during manufacturing.

3.1.4 Method of data analysis

Based on the data found from the experiment, the optimum combination of process parameters for a good quality product can be selected and analyzed through Taguchi-based GRA optimization technique. In this study, the response data were analyzed using multi-objective optimization technique i.e. GRA to obtain the optimal level combination of the process parameter for the factor. Since GRA based Taguchi method is suitable for data analysis to provide an optimum sample during the analysis of interrelationships between multiple responses using the response graph method. In order to implement, several equations of GRA were utilized under each step to obtain optimal parameter combinations. At first, the response data were transformed to S/N ratios (η or Y_{ij}) based on Taguchi Quality Loss Function (QLF) to minimize the sensitivity of quality characteristics to noise factors. Type of quality characteristics are smaller the better, nominal the best, and larger the better. Those types were used to rely on the desired property of the product (Sahu & Pal, 2015; Rajyalakshmi & Venkata, 2013).

For smaller the better,

$$\eta = -10 \log \left[\frac{1}{n} \sum_{i=1}^{n} {Y_i}^2\right] \quad (3.1)$$

For larger the better,

$$\eta = -10 \log \left[\frac{1}{n} \sum_{i=1}^{n} \frac{1}{{Y_i}^2}\right] \quad (3.2)$$

And, variability along with the units was avoided through normalizing the Y_{ij} (η) to the Z_{ij} ($0 \leq Z_{ij} \leq 1$) using respective equations 3.3 and 3.4. and., scale it.

Normalization, which has a value between 0 and 1, is a method of transforming a single input into evenly distributed data and then scaling it for extra analysis. Since the objective of this study is to minimize the density and increase strength and hardness, the smaller the better and larger the better were taken for the characterizing the quality respectively. For both hardness and compressive strength during normalizing, the equation of larger the better was used as stated below (Kuo *et al.*, 2008; Sahu & Pal, 2015).

$$z_i^*(x) = \frac{z_i(x) - \min z_i(x)}{\max z_i(x) - \min z_i(x)} \quad (3.3)$$

And, the formula of the smaller the better for density and porosity normalization method is,

$$z_i^*(x) = \frac{\max z_i(x) - z_i(x)}{\max z_i(x) - \min z_i(x)} \quad (3.4)$$

After that, each normalized S/N ratio value were taken to find the grey relational coefficients (GRC) using Eq. “3.5” (Kuo *et al.*, 2008; Rajyalakshmi & Venkata, 2013),

$$GRC_i(x) = \frac{\Delta_{min} + \beta\Delta_{max}}{\Delta_{oi}(x) + \beta\Delta_{max}} \quad (3.5)$$

Where, Δ_{oi} is deviation sequence of reference value x_o and x_i normalized value of the responses. Δ_{max} & Δ_{min} denotes the maximum and minimum values of “Δ” respectively. β is the coefficient of distinguishing in the range of $0 \leq \beta \leq 1$. When all parameters are equally weighted, then the coefficient of distinguishing (β) is equal to 0.5.

At the last, the grey relational grades (G_i) were calculated using Eq. “3.6” for selecting optimal levels for the process parameter (Rajyalakshmi & Venkata, 2013; Sahu & Pal, 2015). Optimal levels for factors as well as influential process parameter was analyzed further using the response graph method.

$$G_i = \frac{1}{m}\sum GRC_i \quad (3.6)$$

3.1.5 Designs for composite fabrication

The composite was manufactured using a material AZ31 as base metal and SiC, ZrO_2, and MoS_2 as reinforcement. The experiment was designed under four input parameters i.e. the milling time, compaction pressure, sintering temperature, and reinforcement percentage (compositions). Hence, the composition of the composite was one of the process parameters used to design the experiment, the experiment was decided to carry out by taking the volume percentage of SiC reinforcement as one of the input parameters to represent the percentage of ZrO_2 simultaneously. And, MoS_2 as well as base metals were taken as a constant volume percentages throughout the manufacturing process as tabulated in table 3.6.

Table 3.6 Compositions of matrix and reinforcing materials.

S.No.	Reinforcement (Mesh) size (μm)	Reinforcements (vol. %)			BM (vol. %)
		SiC	ZrO_2	MoS_2	
1	200	5	10	4	81
2		10	5	4	
3		15	0	4	

The experiment was carried out based on the principle of design of experiment (DoE) to randomly construct designs for factors and their levels. As Dr. Genichi Taguchi proposed the orthogonal array (OA) method for a minimum experimental run with random combinations, the experiment proceeded with the L_9 orthogonal array design of experiment for this study (Taguchi & Rajesh, 2000). The experiment was designed using three levels for each selected factor i.e. input parameters. The selected factors for the experiment were volume percentage of reinforcement, milling time, compaction pressure, and sintering temperature. And, their corresponding levels for the factors are stated below in table 3.7.

Table 3.7 levels and Process parameters.

Level. No.	Reinforcement (Vol. %)	Milling time (Hrs.)	Compaction pressure (MPa)	Sintering temp. (^{0}C)
	SiC			
1	5	2	50	400
2	10	4	60	425
3	15	6	70	450
Remaining 81 wt.% is AZ31 Mg alloy				

The Taguchi-based L_9 orthogonal array design was used to design the factors with their level randomly to obtain the response of experiments. It was designed using Minitab 17 statistical software. The MMMC samples were then manufactured using PM processing techniques following to design of the experiment.

Table 3.8 Design of Experiment based on L_9 orthogonal array.

Exp't run no.	Process Parameters			
	Reinforcement (Wt. %)	Milling time (Hrs.)	Compaction pressure (Mpa)	Sintering temp. (^{o}c)
1	5	2	50	400
2	5	4	60	425
3	5	6	70	450
4	10	2	60	450
5	10	4	70	400
6	10	6	50	425
7	15	2	70	425
8	15	4	50	450
9	15	6	60	400

Moreover, the experimental results of response variables adhering to DoE were taken to optimize the process parameters using density, hardness, and compression. The design used for conducting the experiment is stated in table 3.8.

3.1.6 Sample preparation methods

The sample preparation has a role to prepare the specimen for different testing methods after the successful production of different samples. Due to this, it supports to obtain result values accurately during testing and characterizing the samples. The samples are usually prepared using the sectioning process and grinding the surface for testing the mechanical properties. In this thesis work, the sample surface was sectioned using an abrasive cutter following ASTM standards for a specific type of test dimensions.

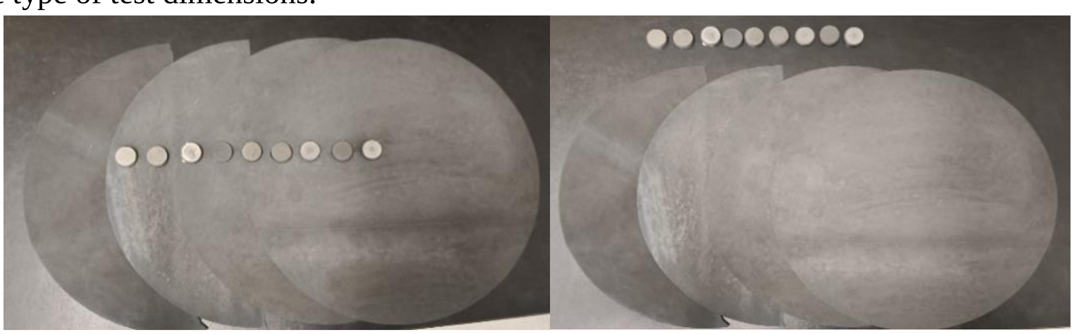

Figure 3.7 Sample preparation for mechanical testing and characterizing the samples.

Characterization of the material is essential to investigate the different behaviors and properties of the products. In this study, characterization of the optimal samples was followed in order to analyze the behavior of the samples before and after mechanical testing along with their objectives. During sample preparation, the samples were taken for rough grinding operation for dimensions using files. It was then exposed to grinding using sand papers from coarse to fine grades with the orientation of 90^0 from the previous direction of grinding. Sequentially, the sandpapers of 220, 800, 1200, and 2200 grades were used and assisted with an air blower after each grinding operation in order to remove debris as shown in figure 3.7. The specimen was then polished to prepare a flat, scratch-free, and mirror-like surface at the end. SEM characterizing tools, JCM/6000PLUS BENCH TOP SEM model, Jeol, Japan, were used for the analysis of wear morphology and fractography after wear and compressive tests respectively as well as the microstructure of the optimal samples. And, X-Ray Diffractometer (XRD), with XRD-7000 X-RAY DIFFRACTOMETER MAXIma model of SHIMADZU Corporation (Japan) company, was used to investigate the crystalline phases and elements in the MMMCs samples with their corresponding sample preparation procedures and sample holder devices. It had operated by only cleaning the powders from surfaces without no further preparation.

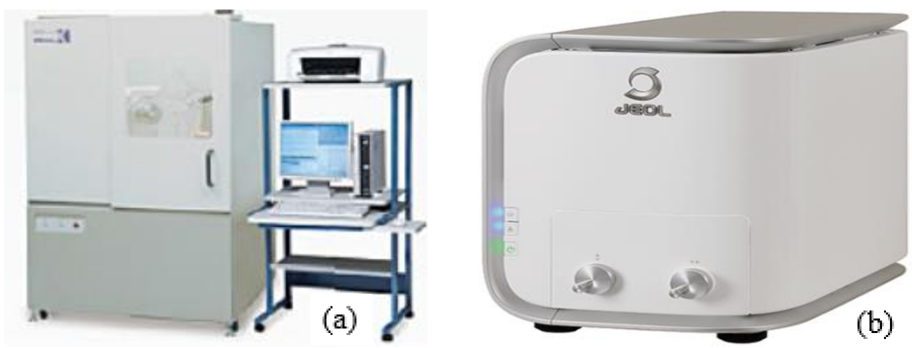

Figure 3.8 Characterizing equipment (a) X-Ray Diffractometer, and (b) SEM.

3.1.7 Physical, mechanical, and tribological testing methods

The testing and characterization of the samples were conducted sequentially after a successful manufacturing of the MMMCs samples. The samples were corresponding to measuring density and porosity, hardness, wear (wear morphology), and compression (fractography is a method in failure analysis for studying the fracture surface of materials) properties. The sample, which was obtained from the optimum process parameters using Taguchi-based GRA techniques, was also prepared for the different tests with corresponding ASTM standards for further verifications of the results. For hardness and compressive tests, the sample preparation method was achieved following the same steps used in the 1st phase of sample preparation. However, the sample preparation for the wear test was prepared based on ASTM standards. Characterization of the samples was also carried out using XRD, SEM, and OM.

3.1.7.1 Density measurement methods

Density can simply take as a concentration of something within a given defined occupied space. The density of mono or hybrid composite materials can be determined using the density of base metal and reinforcements based on Archimedes' principle. The theoretical density of the composite samples was obtained by finding the occupied space of matrix and reinforcement in the composite with their corresponding density based on the rule of mixture. A simple procedure was followed; finding the densities of all the materials (or elements) in the composite and converting each material composition into a number range of 0 -1. Each value was then added after multiplied by the density of its material to determine the theoretical density (Mansor, M. R. *et al.*, 2013). Therefore, it was obtained using Eq. (3.7).

$$\rho_{th} = (\rho_{BM} * V_{BM}) + (\rho_{rein1} * V_{rein1})^n \qquad (3.7)$$

Where V_{BM} and V_{rein1} represent percentile contribution in the composite, ρ_{BM} and ρ_{rein1} is the base metal and reinforcement density respectively. And, n represents no. of reinforcement.

The experimental density for MMMCs was also calculated using the principle of Archimedes. Since the buoyant force existed is equal to the multiplication of mass of the displaced water and gravity (i.e., the weight of the displaced water) when the object is submerged in the water or fluids as stated by Archimedes **(**Nguyen *et al.*, 2016; Abbas *et al.*, 2020). The surfaces of the samples were prepared using 100 grit-grade sandpaper and tested as per ASTM B962-08 standard.

Figure 3.9 Experimental density measurement in distilled water.

The composite samples were first weighed in air and then suspended in distilled water at 25^0c using Oil with a viscosity of 20 to 65 cSt (or 100 to 300 SSU) at 38 °C for further sample preparation. Stirrer machine was utilized to adjust the temperature for the oil to submerge the samples. The apparatuses used for determining the weight in the air and weight in water are shown in figure 3.9.Therefore, the experimental density was calculated according to Eq. 3.8 **(**Nguyen *et al.*, 2016; Abbas *et al.*, 2020).

$$\rho_{ac} = \frac{w_{air}}{w_{air} - w_{water}} * \rho_w \quad (3.8)$$

3.1.7.2 Porosity determination method

From the experimental and theoretical density, Porosity or void fraction was determined by measuring the void spaces entirely in a composite. The porosity (ϕ), which is expressed in a range of 0 to 1 (or in percentile 0% to 100%), was determined using eq. 3.9 as stated below **(**Nguyen *et al.*, 2016; Rahmani & Majzoobi, 2020).

$$\phi = 1 - \frac{\rho_{Ac}}{\rho_{Th}} \quad (3.9)$$

The relative density of the samples was determined using the eq. 3.10 to analyze the experimental density of the sample relative to the theoretical density of the composites (Asl, 2018; Rahmani & Majzoobi, 2020).

$$\rho_r = \frac{\rho_{Ac}}{\rho_{Th}} * 100\% \quad (3.10)$$

Where, ρ_r, ρ_{Ac} and ρ_{Th} represents the relative density in %, experimental and theoretical density in g/cm^3 respectively.

3.1.7.3 Hardness test

The micro hardness test was used for testing the hardness of the samples in the Vickers hardness tester HVS-50 machine which is mostly applicable for micro parts and thin sections. It was conducted using a Vickers indenter, which is a 136° pyramidal diamond indenter that forms a square indent.

Figure 3.10 Samples after Vickers hardness test using VHT machine.

At first, the surfaces of the sample were polished using sand papers of 220, 800, 1200, and 2000 grades to obtain a mirror surface. And, the hardness test for Mg MMCs samples was conducted according to ASTM E384-17 with a cylindrical shape of sample preparation under ASTM E3-95. In this study, 10 Kgf force was applied gradually for 10 seconds at different positions (i.e. three trials) in order to have average result values. The resulting indent mark was then analyzed optically at 10x magnification to find the lengths of the diagonals to determine the hardness value. The VHT machine then automatically analyzed and brought the HV number using Eq. “3.11” as stated in ASTM E384-17.

$$\boldsymbol{HV} = \frac{\text{Constant x test force}}{\text{surface area of indentation}} = \frac{0.102*2F(\sin\frac{136^0}{2})}{(d)^2} \tag{3.11}$$

Where HV is Vickers hardness value (kgf/mm^2), F is the applied force using the indenter (Kgf) and d is the average length of the diagonals (d_1 & d_2) marked by the indenter in millimeters.

3.1.7.4 Methods for compression test

The compression test is used to obtain the compression strength of the material and determine the elastic and compressive fracture material's (fractography) behavior under applied crushing loads. In this study, the samples were tested using uniaxial compressive load on Universal Testing Machine (UTM) with 50KN capacity at room temperature.

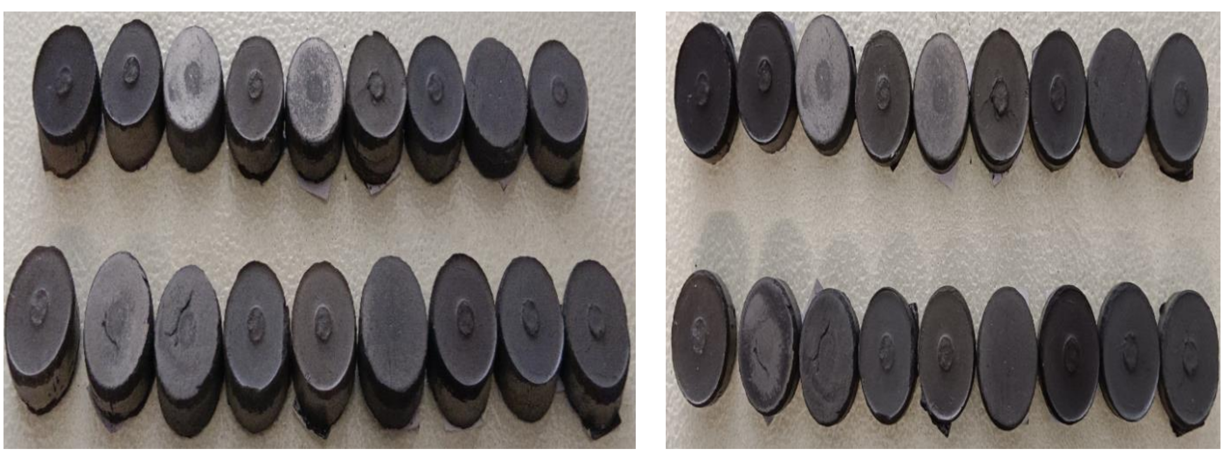

Figure 3.11 Samples used for compression strength tests.

The specimens of Mg MMCs were prepared under the ASTM E9-09 standard of 10 mm in dia. And 8mm of height dimension i.e. 0.8 approximated length to diameter ratio. Compressive strength was determined by applying the loads gradually to the magnesium alloy metal matrix composite samples. It was conducted through applying compressive load (i.e. until the material fails) per cross-sectional area of the samples. And, it can be expressed mathematically as shown in eq. 3.12. However, the test result was analyzed automatically and reported on the screen of the computer-aided UTM.

$$\mathbf{UCS} = \frac{\text{F}}{A_c} \tag{3.12}$$

Where UCS stands for Ultimate compressive strength, F is Ultimate compressive load and A_c is the Cross-sectional area of the samples.

3.1.7.5 Wear test on the samples

Wear is the phenomenon of deformation in the material due to relative motion (like rubbing or impacting) between a surface and contacting substances. In this study, a Dry sliding wear test was conducted on the Mg MMCs samples using the DUCOM TR-20 Micro model (Ducom Instruments Pvt. Ltd. Company in Peenya Industrial Area, Bangalore (India)) of Micro Pin on disk micrometer apparatus.

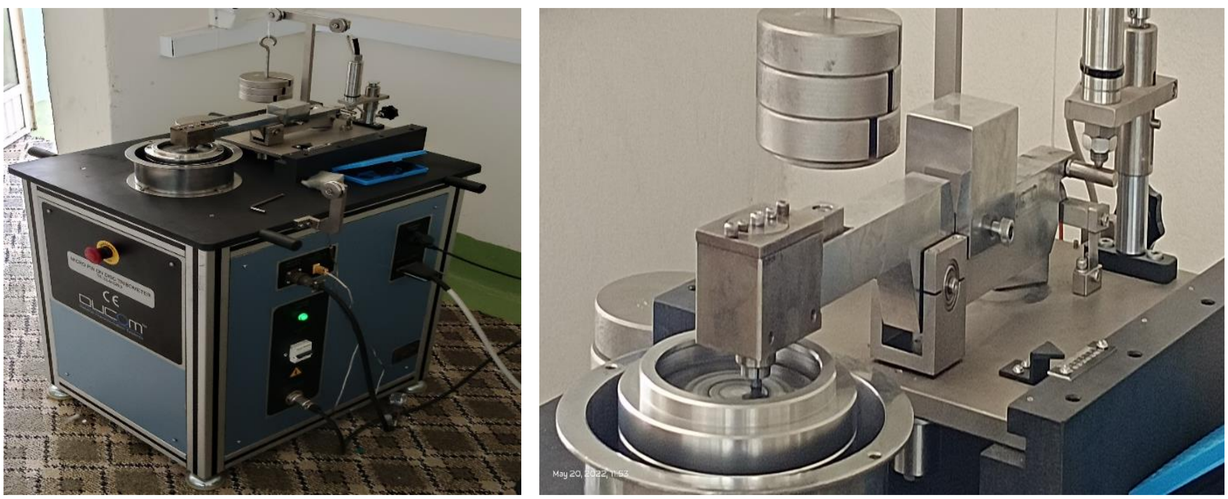

Figure 3.12 Micro Pin on disc micrometer (DUCOM TR-20 Micro model) apparatus.

It was used to analyze the wear rate of samples and investigate the wear mechanisms that occur. In this investigation, the Wear test was conducted under ASTM G99-05 Standard with dimensions of 6mm dia. and 12mm height and then polished using fine sandpaper for sample preparation. The wear property of the samples was determined under the test parameter of 30N applied loads on the 25mm dia. wear truck. And, it was also operated with a sliding speed of 250 rpm at room temperature. Eq. 3.13 was used to obtain the wear rate of the Mg MMCs samples (Prabhu *et al.*, 2019; Kadhim *et al.*, 2018).

$$\mathbf{W.R} = \frac{W_b - W_a}{\pi * d * n * t} \quad (3.13)$$

Where, W_b is the weight of the samples before wear and W_a is the weight of the samples after wear, WL is weight or mass loss ($W_b - W_a$), d is the wear truck diameter of the wear disc, n is the speed in rev/min and t is time.

The wear rate improvement with respect to the mono ceramic reinforced MMMCs (i.e. reinforced with SiC) was obtained using calculated wear rate values based on eq. 3.14 (Jaswin *et al.*, 2011),

$$\mathbf{IWR_{HM}}(\%) = \frac{\mathbf{W_M - W_H}}{\mathbf{W_M}} * \mathbf{100}\% \quad (3.14)$$

Where, $\mathbf{IWR_{HM}}$ denotes the improvement of wear rate of hybrid with respect to mono reinforced MMMCs, $\boldsymbol{W_H}$ & $\mathbf{W}_M$ also denotes the wear rate of hybrid and mono reinforced MMMCs respectively.

CHAPTER FOUR: RESULT AND DISCUSSIONS

4.1 Introduction

This section of the study deals with the analysis of various properties of the manufactured composites and discussions based on the results specifically density, porosity, relative density, hardness, and compressive strength of mechanical properties. The metallurgical and tribological properties are also interpreted using the optimal sample from optimization results.

4.1.1 Analysis and modeling of the response variables

This study mainly focuses on having a high strength-to-weight ratio through reducing the weight besides the fact of desiring high mechanical properties of the materials. Therefore, the smaller the better criteria are taken for density and porosity, and the larger the better for hardness and compressive strength of the material. The analysis for the selected criteria is carried out using equations 3.1 and 3.2 as stated in the previous chapter. But, the variations in the response values are observed due to the contribution effect of levels of the process parameter of the powder metallurgy.

4.1.1.1 Analysis of density

The experimental densities of the samples are obtained through finding the weight of the materials in air and water. In figure 4.7, it shows the correlations of process parameters with the measured values of experimental responses of the materials. The smaller the better criteria are used to analyze the response of the density for each experimental run. And, it is depicted using the main effect plots and response table in figure 4.7(c) and table 4.1. As the main effect plot shows that the density is decreasing when the reinforcement percentage decreases. Meanwhile, it follows the same path for the milling time, compaction pressure, and sintering temperature. The density shows abrupt change at 425^{o}c sintering time, i.e. the higher values relative to other levels as the main effect plot shown in figure 4.7(c).

Table 4.1 The response table for density.

Level	Rt. (A)	MT (B)	CP (C)	S.Temp. (D)
1	-6.446	-6.429	-6.359	-6.499
2	-6.333	-6.249	-6.289	-6.085*
3	-6.090*	-6.191*	-6.220*	-6.284
Delta	0.356	0.238	0.140	0.414
Rank	2	3	4	1

The response table also provides the grades of influential parameters upon the responses as tabulated below in table 4.1. The sintering temperature is the first influential parameter up on the density and followed by reinforcement percentage, milling time, and compaction pressure. And for porosity, the reinforcement percentage takes the first rank and is followed by sintering temperature, milling time, and compaction pressure. In table 4.1, the optimum combinations of process parameters are identified using levels of each process parameter. It is obtained as $A_3B_3C_3D_2$ for experimental density. It has been observed that the density is increased with the addition of ZrO_2 and followed by SiC in the composites as shown in figure 4.1. It is due to increasing the number of reinforcements, which have higher density, used in the manufactured composite. The experimental density varied from 1.98 g/cm^3 that had been reinforced with 15 vol. % SiC and was being processed to 2hrs. milling time, 70 MPa compaction pressure, and 425 ^{o}c sintering temperature to 2.20 g/cm^3 for 5 vol. % SiC and 400 ^{o}c sintering temperature. Indeed, the experimental density of the manufactured composites shows a high value at 400^{o}c sintering temperature and 5% SiC reinforcement composition.

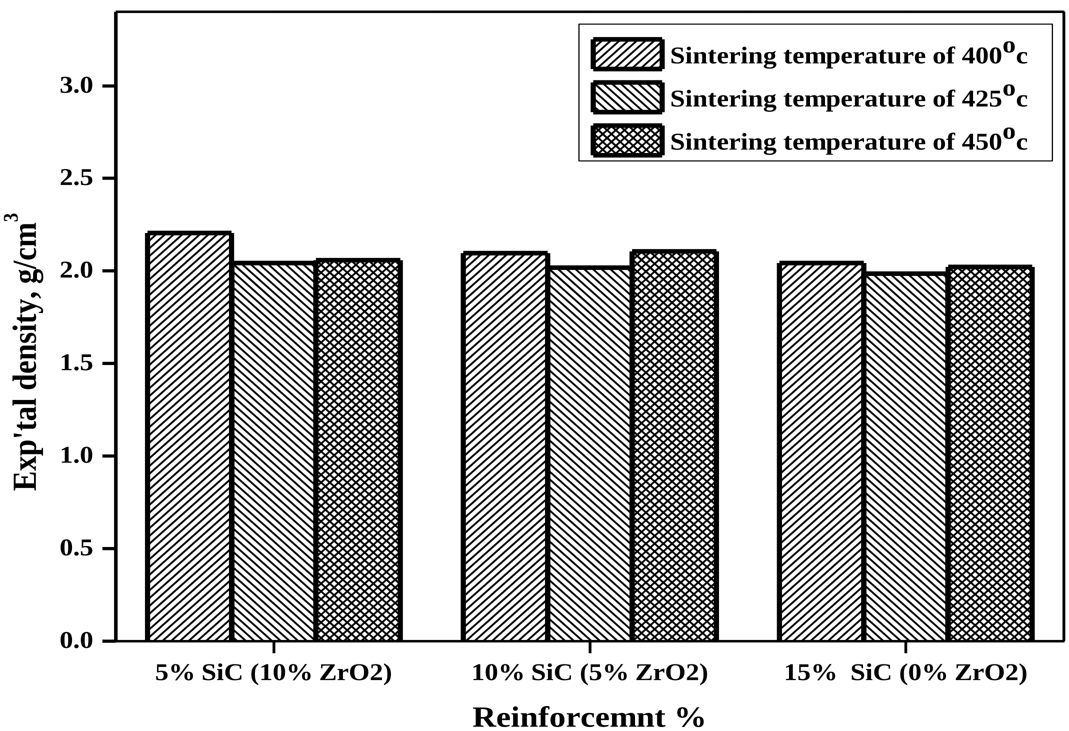

Figure 4.1 Density versus reinforcement content of the manufactured composites.

The regression model is used to predict the independent variables i.e. output values at any input values of dependent variables. The model for experimental density is stated in eq. 4.1 to obtain the predicted values with an interaction effect.

$$\boldsymbol{\delta}_{\mathbf{Exp't}} = 2.94 - 0.014\ \text{Rt.} - 0.163\ \text{MT} - 0.0072\ \text{CP} - 0.00048\ \text{STemp.} + 0.00317\ \text{Rt.*MT} - 0.00006\ \text{Rt.*CP} + 0.00193\ \text{MT*CP} \quad (4.1)$$

Where, $\boldsymbol{\delta}_{\mathbf{Exp't}}$ represents the experimental density of the composites.

The R-Square value for this model is 87.95% as obtained from the model summary. Its value is nearly approached 1. This implies that the model has an efficiency to predict the experimental density at any input values of dependent variables i.e. levels of the process parameters values.

4.1.1.2 Analysis of porosity

The porosity of the samples is expected to have lower values in the manufactured composites. It is determined using the calculated values of theoretical density and the measured values of the experimental density of the materials using eq. 3.9. The theoretical and experimental densities are used to determine the porosities of all samples of the composites. In figure 4.2, it shows the measurement values of the theoretical and experimental density of the materials.

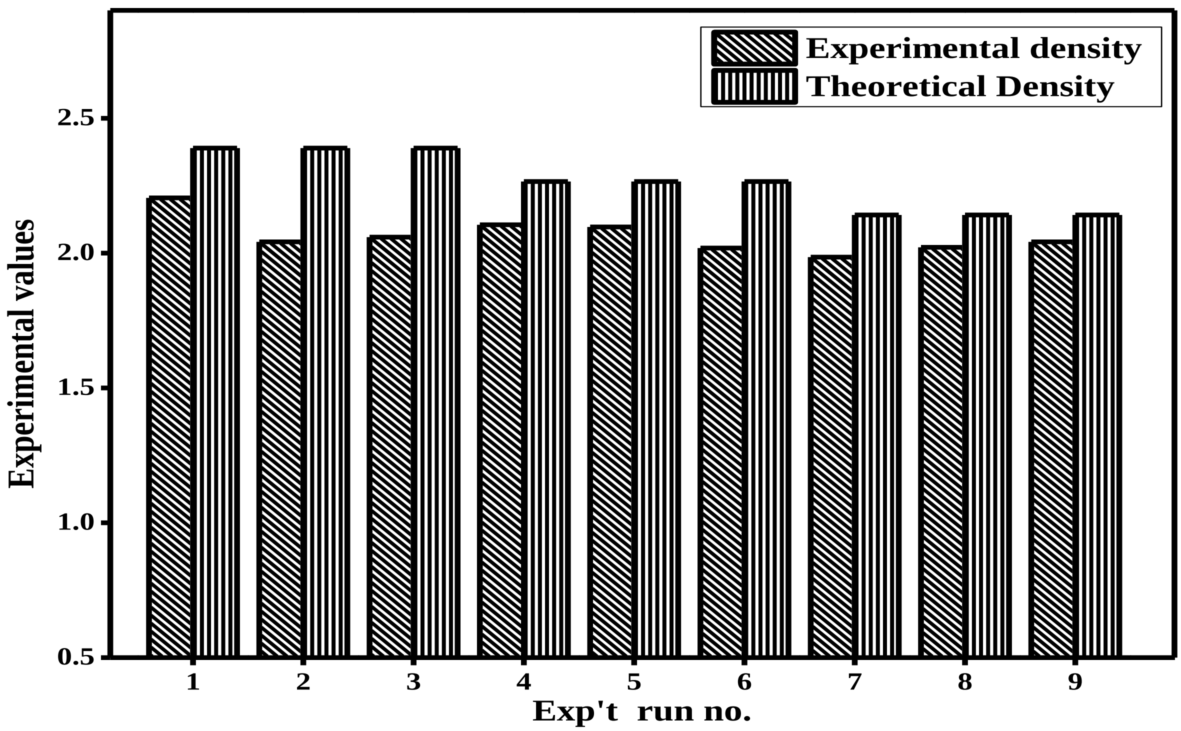

Figure 4.2 The theoretical and experimental density of the samples.

The relative density of the material is also determined using the experimental and theoretical density. It is observed that it is in the range of 0.84 – 0.96 values as shown in figure 4.3. Since the MMMCs are targeted to have less porosity, the smaller the better criteria are used to optimize the response of the porosity for the manufactured samples. In figure 4.7(d), the main effect plot is shown that the porosity is reduced when the reinforcement percentage decreases. This implies that the addition of micro-sized reinforcements had a great impact to increase the density and also porosity of the composites as the same result obtained by other works of literature (Arif *et al.*, 2017).

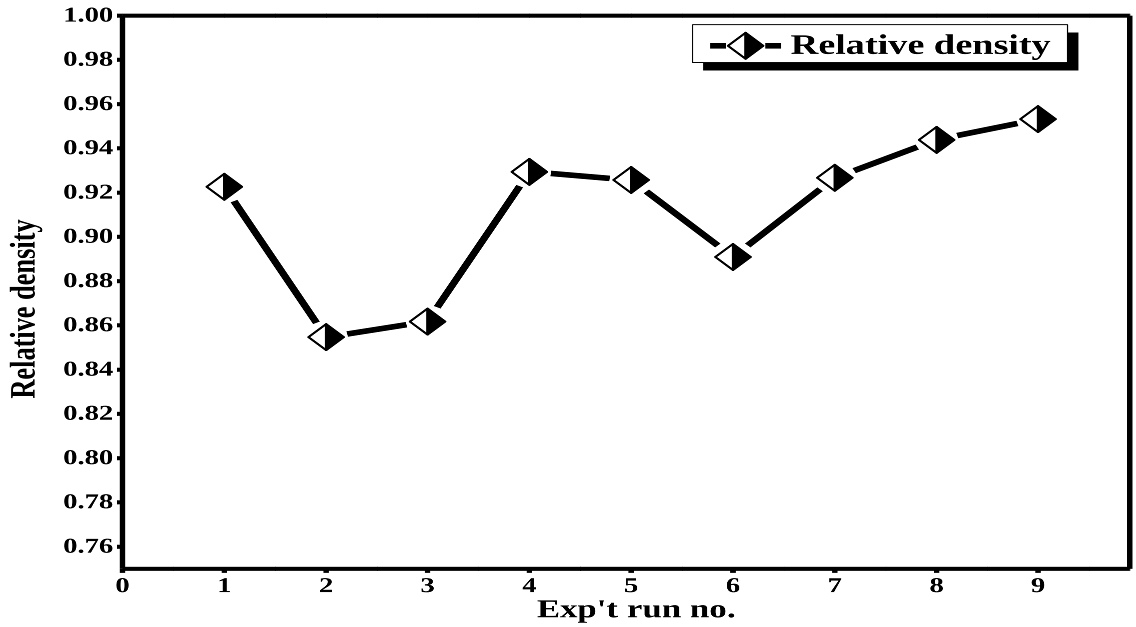

Figure 4.3 Relative density of the samples for each experiment runs.

However, it is increased when the milling time, compaction pressure, and sintering temperature are decreased as depicted in the reverse form of the density. Indeed, the sintering temperature from 425^{o}c – 450^{o}c shows an increment in the porosity. This implies that the porosity is minimum at 425^{o}c sintering temperature according to the main effect plot as illustrated in figure 4.7(d). In table 4.2, the process parameters, which influence the responses, are stated with their grades in the table form. The reinforcement percentage takes the first rank and is followed by sintering temperature, milling time, and compaction pressure.

Table 4.2 The response table for porosity.

Level	Rt. (A)	MT (B)	CP (C)	S.Temp. (D)
1	18.72	22.65*	22.16*	23.81*
2	21.61	21.45	22.13	19.57
3	24.77*	21.01	20.82	21.74
Delta	6.05	1.64	1.34	4.24
Rank	1	3	4	2

In figure 4.4, it illustrates the porosity correlation with the reinforcement composition and sintering temperature with including the effects of other process parameters. It has been varied from 0.04 values i.e. around 4% that had been reinforced with 15 vol.% SiC and 400^{o}c sintering temperature to 0.15 values around 15% which was obtained from 5% SiC reinforcement composition and 425^{o}c sintering temperature. In 5% SiC reinforcement composition, the porosity shows high values during sintering at 425^{o}c and 450^{o}c respectively. Meanwhile, low porosity is detected at 400^{o}c sintering temperatures. The same pattern is shown for the 15% SiC reinforcement composition. However, for 10% SiC reinforcement content, the higher value of porosity is detected at 425^{o}c sintering temperature and a lower rate of porosity is shown at 400 and 450^{o}c. Therefore, the particles were highly diffused in the composite during sintering from 400 – 450 ^{0}c in order to arrange themselves. And, the porosity is increased when different compositions and types of reinforcement are used during manufacturing the composites.

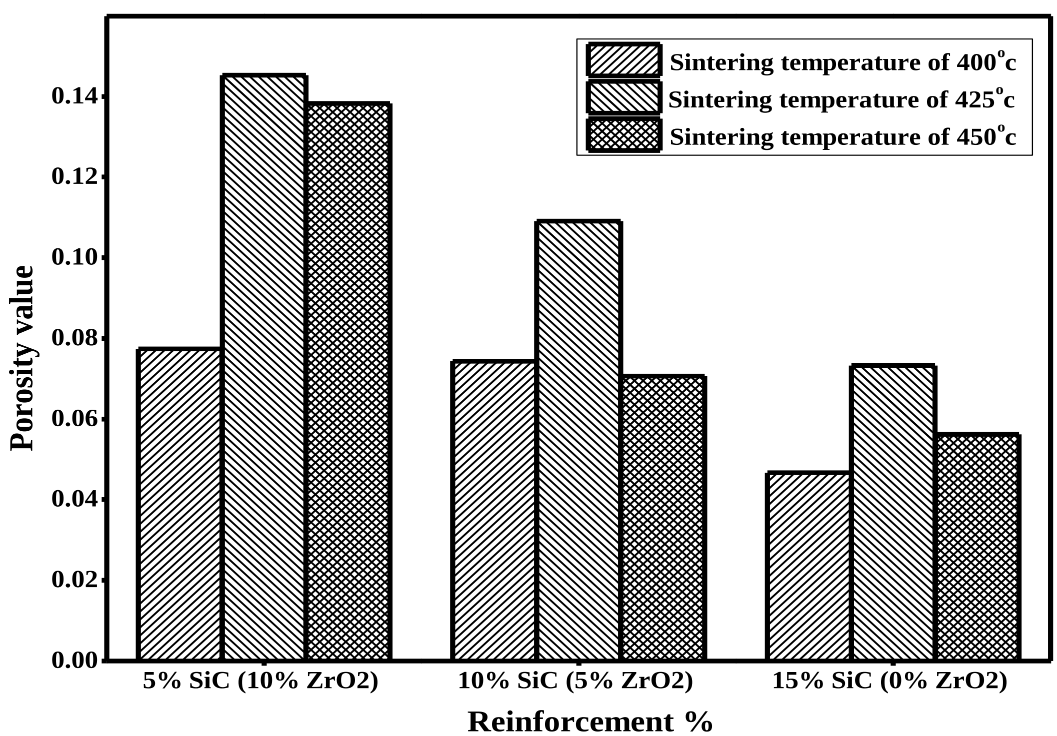

Figure 4.4 The porosity values relative to reinforcement and sintering temperature.

The optimum combinations of process parameters are identified using the main effect plot for individual process parameters. Therefore, it is obtained as $A_3B_1C_1D_1$ in order to have improved properties concerning the porosity. The regression model for porosity is used to obtain the predicted values with an interaction effect as stated in eq. 4.2.

$$\varphi = -0.185 - 0.0038\, Rt. + 0.0728\, MT + 0.0032\, CP + 0.00018\, STemp. - 0.00145\, Rt.*MT + 0.000028\, Rt.*CP - 0.00087\, MT*CP \quad (4.2)$$

Where φ represents porosity

As the model summary showed that the R-Square value for this model is 93.51% which lies between 90 -100%. Therefore, the model has the efficiency to predict the porosity at various levels of parameters.

4.1.1.3 Analysis of hardness

The influence of process parameters on the hardness is clarified using the main effect plot for S/N ratios in figure 4.7(b). It is depicted as the hardness property of the composites has a strong correlation with different process parameters. The hardness property of the material is reduced when the sintering temperature and milling time increase as shown in the main effect plot for hardness. On the other hand, it shows a direct relationship with the compaction pressure and reinforcement percentage in the range of 10-15 vol. %. Moreover, the response table in table 4.3 assures that the compaction pressure has a great impact on the hardness property as the compression strength and followed by reinforcement percentage, sintering temperature, and milling time.

Table 4.3 Response table for S/N ratio of hardness.

Level	Rt. (A)	MT (B)	CP (C)	S.Temp. (D)
1	42.43	42.43*	41.34	42.83*
2	41.32	42.08	42.20	42.09
3	42.69*	41.94	42.91*	41.54
Delta	1.37	0.49	1.58	1.29
Rank	2	4	1	3

The optimum combination of process parameters is identified using response table 4.3 from their levels of process parameters. It is obtained as $A_3B_1C_3D_1$ for optimum hardness value of composites. In figure 4.5, the bar graph shows the correlation of the influential parameters i.e. influences of the compaction pressure and reinforcement composition with experimental responses of hardness value of magnesium alloy hybrid composites. However, the other process parameters effects were also included in the bar graph. In 15 vol.% of SiC reinforced MMMCs, it has recorded an increment hardness value with the highest level of the compaction pressure. The hardness values of the samples have been varied from 102.78 HV that had been reinforced with 10 vol.% SiC and had been processed with 50 MPa compaction pressure to 152.72 HV for 15 vol.% of SiC and 70 MPa compaction pressure. When the compaction pressure increases from 50 – 70 MPa sequentially, the hardness value shows an increment (i.e. with huge differences between them) for 10 and 15% SiC reinforcement composition. But, for 5% SiC reinforcement composition, it shows a nonuniform increment pattern. This implies that the hardness is highly influenced by the number of reinforcements and compositions due to the tendency of having high porosity relative to mono-reinforced composites. In addition, the hardness is also increased when the compaction pressure increase from low to high levels. Therefore, compaction pressure is one of the parameters that influence the hardness value next to the reinforcement composition. The regression model for hardness is used to obtain the predicted values with interaction effect as stated in eq. 4.3.

$$\boldsymbol{\vartheta} = 498 - 11.8\ Rt. - 38.6\ MT - 5.36\ CP - 0.254\ STemp. - 0.81\ Rt.*MT + 0.286\ Rt.*CP + 0.808\ MT*CP \quad (4.3)$$

Where $\boldsymbol{\vartheta}$ represents the hardness value of the composites

The R-Square value of the model is 84.69 %, which is approached to 1 value, as obtained in the model summary so this indicates the model's efficiency to predict the responses at any input values of parameters.

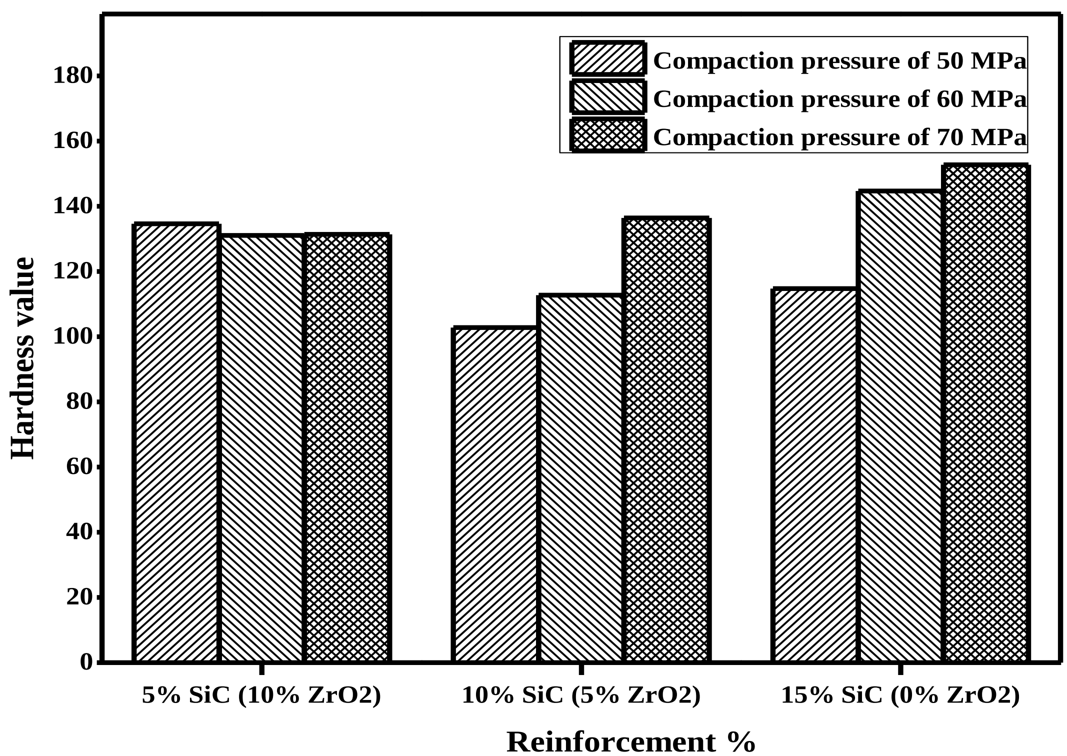

Figure 4.5 Hardness values versus reinforcement composition and compaction pressure.

4.1.1.4 Analysis of compression strength

Process parameters that influence the compressive strength were determined using the main effect plot for S/N ratios in figure 4.7(a). It is depicted as the compressive strength properties are dependent on different parameters. The compression strength of the composite is reduced due to the increment in reinforcement percentage of SiC and decrement in sintering temperature. It is possibly due to reducing the reinforcement percentage of ZrO_2 causing to decrease in the compressive strength. The milling time from 2 – 4 hours decreases compressive strength and increases with a range of 4 – 6 milling hours. This indicates that the size reduction and uniform distribution of powders have an impact on the properties of the composite. In addition, it is also obtained the influential process parameter for compressive strength property using the main response table. The main response table shows the main factor affecting the compression strength as shown in table 4.4. The compaction pressure has taken the first grade for influencing the property of compression strength and followed by reinforcement percentage, milling time, and sintering temperature.

Table 4.4 Response table for S/N ratio of compression strength.

Level	Rt. (A)	MT (B)	CP (C)	S.Temp. (D)
1	39.71*	39.11*	36.28	37.87
2	37.83	37.37	38.86	38.25
3	36.91	37.97	39.31*	38.33*
Delta	2.81	1.74	3.03	0.46
Rank	2	3	1	4

The optimum combination of process parameters is identified using a response table for individual process parameters. It is obtained as $A_1B_1C_3D_3$ for the optimum value of the compressive strength. The regression model is constructed using the given experimental values for predicting the response value of compression strength as mentioned in eq. 4.4.

$$\sigma_{Comp.} = 26.1 - 4.132\ Rt. - 2.62\ MT - 0.358\ CP + 0.0985\ STemp. + 0.1843\ Rt.*MT + 0.0525\ Rt.*CP + 0.0191\ MT*CP \quad (4.4)$$

Where, $\sigma_{Comp.}$ represents compression strength of the material.

In figure 4.6, the bar graph shows the correlation of the influential parameters with experimental responses of compressive strength of magnesium alloy hybrid composites. Indeed, the other process parameters effects were also included in the bar graph. In 5 vol.% of SiC reinforced MMMCs, it has recorded the highest value of compressive strength as illustrated in figure 4.6. The compression strength of the samples has varied from 110.48 MPa which had been reinforced with 5 vol.% SiC and had been processed on 70 MPa compaction pressure to 52.71 MPa for 15 vol.% SiC and had been compacted using 50 MPa pressure. The reason for the high compression strength value might be the highest level of compaction pressure since it is approved in the table of responses. And, different reinforcement composition i.e. the ZrO_2 in nature provides high fracture toughness that enhances compression strength as shown in figure 4.6.

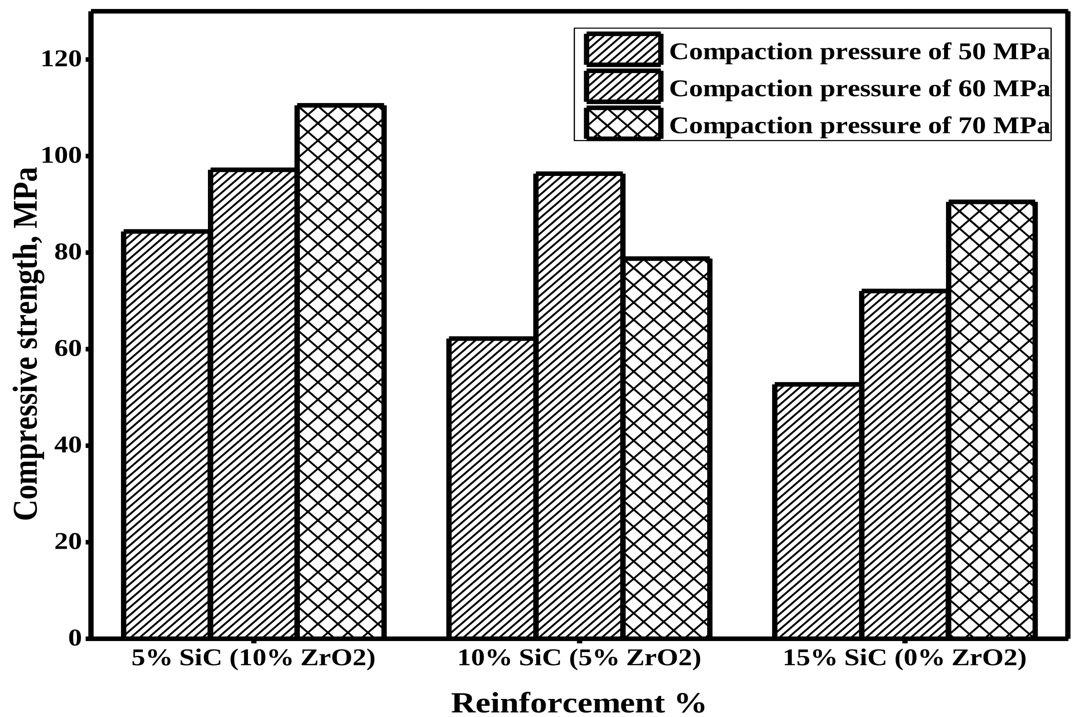

Figure 4.6 Compression strength versus reinforcement composition and compaction pressure.

As the model summary showed that the R-Square value of the model is 99.11%. It is nearly approached 1 value making the model capable of predicting the compression strength of the materials. As a result, the mechanical properties are enhanced based on the fact that the SiC and ZrO_2 are working as a barrier to the motion of dislocation due to the nature of uniform distribution on the magnesium alloy matrix (Arif *et al.*, 2017).

The main effect plot is depicted to show the effects of the process parameters in the given responses. In this study, the effects of process parameters i.e. reinforcement composition, milling time, compaction pressure, and sintering temperature on the density, porosity, hardness, and compression strength responses were studied. And, It is illustrated by correlating each process parameter with the test result of the response variables individually as shown below in figure 4.7

(a-d). This implies that the reinforcement percentage and sintering temperature have a great impact on the density and porosity than the compaction pressure. However, it is also commonly observed from the main effect plot, compaction pressure has a higher impact on hardness and compressive strength. It was also reported in other studies that the mechanical property has merely influenced by compaction pressure (Kumar & Bharti, 2021).

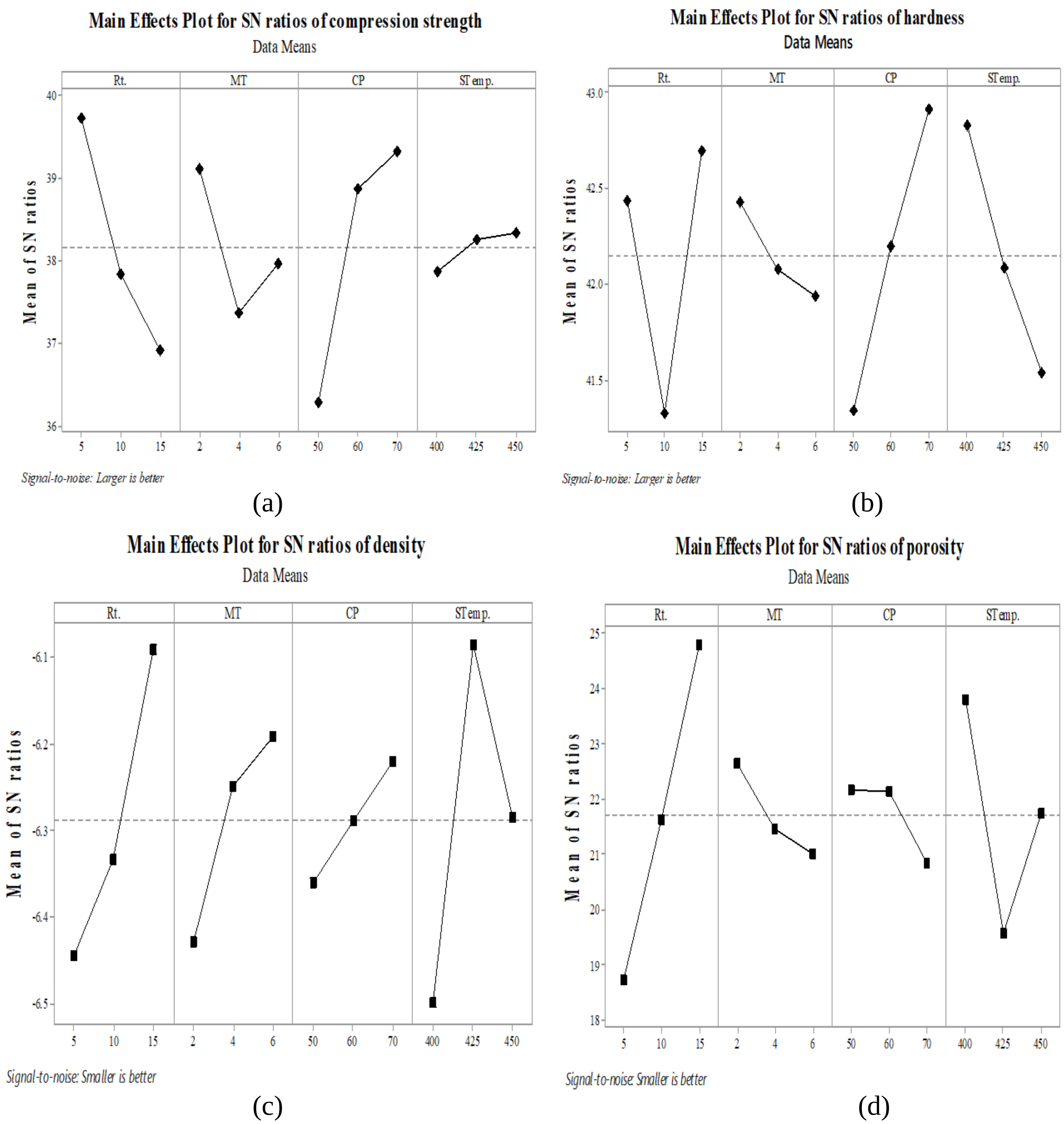

Figure 4.7 Main effect plot for (a) compression strength, (b) hardness, (c) density, and (d) porosity.

4.1.2 The Optimization using Taguchi based Grey Relational Analysis

In multi-response optimization, the Taguchi-based GRA tools are mostly used to determine the optimum response values (Prakash *et al.,* 2020; Hussain *et al.,* 2020). In this study, the optimization of multi-objective response was analyzed using GRA coupled with the Taguchi method to determine the optimal level combination of PM process parameters used for composite manufacturing. For optimization, three levels for four process parameters are used as a measuring index to analyze the four responses to obtain the optimum level and combination of parameters. The optimal level is the highest value obtained from the values of grey relational grade. The optimal parameter combinations are obtained through mean GRG analysis at each level. This analysis was carried out under the following steps mentioned in the previous chapter using Minitab-17 software.

4.1.2.1 Signal to noise ratio of the experiment values

The qualities of measurements are essential for enhancing the signals with considering the uncontrolled variables i.e. to reduce noises in the response results. That responds with optimum properties in the expected product of composite. The qualifications are “smaller the better”, “nominal value the better” and “the larger the better”.

Table 4.5 S/N ratio of the experimental values.

Exp’t run no.	Experimental density	Porosity	Hardness	Compression Strength
1	-6.8658	22.2308	42.5817	38.5258
2	-6.2003	16.7549	42.3496	39.7506
3	-6.2717	17.1876	42.3708	40.8659
4	-6.4663	23.0159	41.0403	39.6792
5	-6.4322	22.5785	42.6952	37.9289
6	-6.0997	19.2455	40.2382	35.8792
7	-5.9552	22.7032	43.6777	39.1333
8	-6.1138	25.0107	41.1974	34.4369
9	-6.2004	26.6109	43.2082	37.1563

In this study, the responses i.e. density, hardness, and compressive strength were taken as a response for the L_9 OA design of the experiment. Due to this, the theoretical and experimental density as well as the porosity and relative density were determined using equations 3.7-3.10 as mentioned in the previous chapter. The statistical formula of “the smaller the better” was utilized for porosity and experimental density to determine the performance quality of the composites. Since the experimental density and porosity were in need to provide the property of high strength to weight ratio in a product (Zhu *et al.*, 2018). The S/N ratios for the 'smaller the better' condition were obtained based on the principle of minimizing the noise factors for porosity and experimental density. Meanwhile, the sample's hardness and compressive strength responses were analyzed using the 'larger the better' statistical formula as expected to have higher properties. The S/N ratios for each response were tabulated in table 4.5.

4.1.2.2 Normalizing the experimental values

In this step, the data obtained from the S/N ratio is normalized to scale it for further analysis by eliminating the effects due to variability and different unit.

Table 4.6 Normalized data of the experimental values.

Exp't run no.	Experimental density	Porosity	Hardness	Compression Strength.
1	1.000	0.444	0.681	0.636
2	0.269	1.000	0.614	0.827
3	0.348	0.956	0.620	1.000
4	0.562	0.365	0.233	0.815
5	0.524	0.409	0.714	0.543
6	0.159	0.747	0.000	0.224
7	0.000	0.396	1.000	0.730
8	0.174	0.162	0.279	0.000
9	0.270	0.000	0.863	0.423

Therefore, all experimental runs of S/N ratio values are normalized between 0 and 1 values using eq. 3.3 and 3.4 as mentioned in the previous chapters. The transformed values for the response are tabulated in table 4.6.

4.1.2.3 Grey relational coefficients and Grey relational grades

The grey relational coefficients were determined following the steps which are used to transform the response data as a single response for further analysis. GRCs are calculated by using the normalized S/N ratio data to figure out the relation between actual and experimental data using eq. 3.5. The deviation sequence values for each response are tabulated under table 4.7 including the GRC values. The maximum and minimum values are the values of 0 and 1 and 0.5 is taken for the coefficient of distinguish for each response. The values transformed into a single response using eq. (3.6) is called Grey relational grade (GRG.). From those, the highest value of GRG is taken as the 1st rank for 9 experimental runs and the lowest value is considered as the last rank. In figure 4.8, the GRG values, obtained using eq. 3.6, with their corresponding ranks is illustrated for the MMMCs. Therefore, the 1st rank from 9 experiment runs is experiment run number 3 due to having the highest value of GRG as stated in figure 4.8. For this experiment, the optimum level of process parameter is $A_1B_3C_3D_3$ among the levels of the process parameters. Meanwhile, the mean value of GRG is used to obtain influential factor and optimum level combination from each process parameter using the main effect table 4.8 as shown below.

Table 4.7 Deviation sequence of the normalized S/N ratio.

Exp't run no.	Deviation sequence				GRC			
	Exp'tal density	Porosity	Hardness	Comp. St.	Exp'tal density	Porosity	Hardness	Compression Strength
1	0.000	0.556	0.319	0.364	1.000	0.474	0.611	0.579
2	0.731	0.000	0.386	0.173	0.406	1.000	0.564	0.742
3	0.652	0.044	0.380	0.000	0.434	0.919	0.568	1.000
4	0.438	0.635	0.767	0.185	0.533	0.440	0.395	0.730
5	0.476	0.591	0.286	0.457	0.512	0.458	0.636	0.523
6	0.841	0.253	1.000	0.776	0.373	0.664	0.333	0.392
7	1.000	0.604	0.000	0.270	0.333	0.453	1.000	0.650
8	0.826	0.838	0.721	1.000	0.377	0.374	0.409	0.333
9	0.730	1.000	0.137	0.577	0.406	0.333	0.786	0.464
Mean GRC					0.486	0.568	0.589	0.601

The optimum level combination of parameters based on responses has been found from the main effect table is factor A at level 1 i.e. Reinforcement Percentage at 5% SiC and 10% ZrO_2; factor B at level 1 i.e. milling time at 2 hrs.; factor C at level 3 i.e. compaction pressure at 70 Mpa and factor D at level 2 i.e. sintering temperature at 425^0c. As a result, the optimal levels combination of PM process parameters has been found as $A_1B_1C_3D_2$. In addition, the influential process parameter has been obtained from the main effect table of GRG values. It is computed as Rt. compositions have taken the first rank and followed by compaction pressure depending on the contribution of the response value. The mean GRC for compression strength is 0.601 which is the highest among all the responses. This implies that the compression strength has a strong interaction with all process parameters relative to the density, hardness, and porosity. Therefore, the factors can easily influence the compression strength more than other responses.

Table 4.8 Response table of mean GRG.

Level	Rt. (A)	MT (B)	CP (C)	S.Temp. (D)
1	0.6915*	0.5998*	0.4933	0.5652
2	0.4992	0.5280	0.5667	0.5760*
3	0.4933	0.5561	0.6240*	0.5428
Delta	0.1982	0.0718	0.1307	0.0332
Rank	1	3	2	4

The reinforcement composition is the strongest among controlled process parameters from the value of mean GRG difference between low and high levels. It has been obtained as high as 0.1982 followed by compaction pressure, milling time, and sintering temperature respectively as shown below in table 4.8. It can be interpreted as the reinforcement composition has a strong correlation with the responses i.e. density, porosity, hardness, and compression strength of MMMCs. And, it is followed by compaction pressure as the second process parameter that influences the responses.

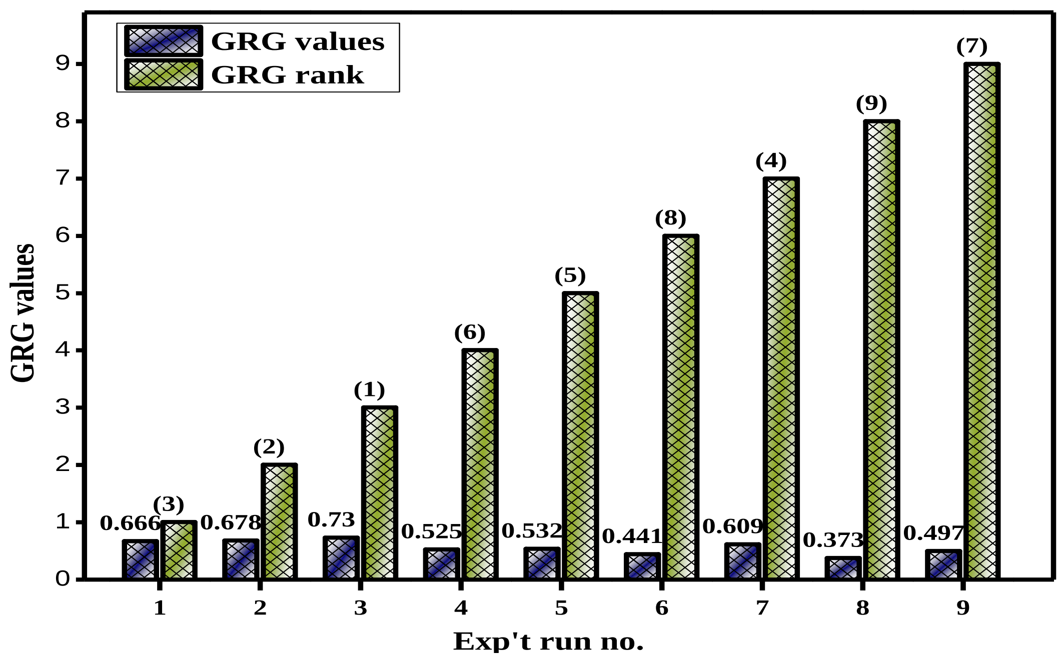

Figure 4.8 Ranks and values of GRG.

4.1.3 Interactions effects of the process parameter

In this study, the responses of the process parameters are analyzed and evaluated further using different techniques to develop a regression model. Due to this, different illustrations and diagrams are used for implementing the interaction effects between process parameters using a 3D surface plot and contour plot for the response. The desired response values, which are correlated with the two predicted parameters, can be investigated using a 3D surface plot. Figure 4.10 show the 3D surface plots for GRG using two of the influential process parameters of PM. The 3D surface plot for GRG variation wrt Rt. composition and milling time are shown below in figure 4.10(a). The plot indicates that the GRG value increases with increasing the milling time and reducing the composition of reinforcements. It is also nearly observed the same interpretation as the above in figure 4.10(b & c). The increment of the reinforcement composition proportionally to compaction pressure (and indirectly to sintering temperature) makes the GRG value to reduce. The time used for milling the powder from 2 hrs. – 6 hrs. leads to an increment in the value of GRG as illustrated in figure 4.10(d & c). And also, increasing the compaction pressure proportion to the sintering temperature provides a better response for GRG as shown in figure 4.10(f). The 3D surface plots of GRG responses show nonuniform changes in the slope of the curve that predicts the possibility of occurring the interaction effect among the process parameter.

The 2D topographical map of a 3D surface i.e. contour plot is provided using two influential parameters on the y axis and the desired response value as contours on Z-axis. It is used in order to analyze the interaction effect among the parameters on a given response and obtain the range for optimal responses. The contour plots for response GRG using two predicted process parameters are shown in figure 4.9 below. The contour plot of the response for GRG wrt the milling time and reinforcement percentage is indicated in figure 4.9(a). The maximum GRG value is in the range of 0.7 and above with the high level of milling time and a low level of Rt. %. And, it also shows the possible interaction effect between the process parameters. Figure 4.9(b) also shows a contour plot for GRG by varying Rt. % and compaction pressure parameters. By varying these two parameters, the maximum GRG value is in the range of 0.7 and above. The process parameters of sintering temperature wrt the Rt. % to obtain the GRG value that is in the range of 0.7 and above as shown in figure 4.9(c). The contour plot indicates the compaction pressure, milling time, and also sintering temperature has a high influence on the response of GRG than the reinforcement composition. And, it shows the possible interaction effect between parameters on GRG values due to the existence of curvature formation in figure 4.9(a-c). The compaction pressure with respect to the milling time provides a higher value of GRG in the range of 0.7 and above as shown in figure

4.9(d). It indicates that the compaction pressure and milling time show a higher effect on the response of Grey relational grade.

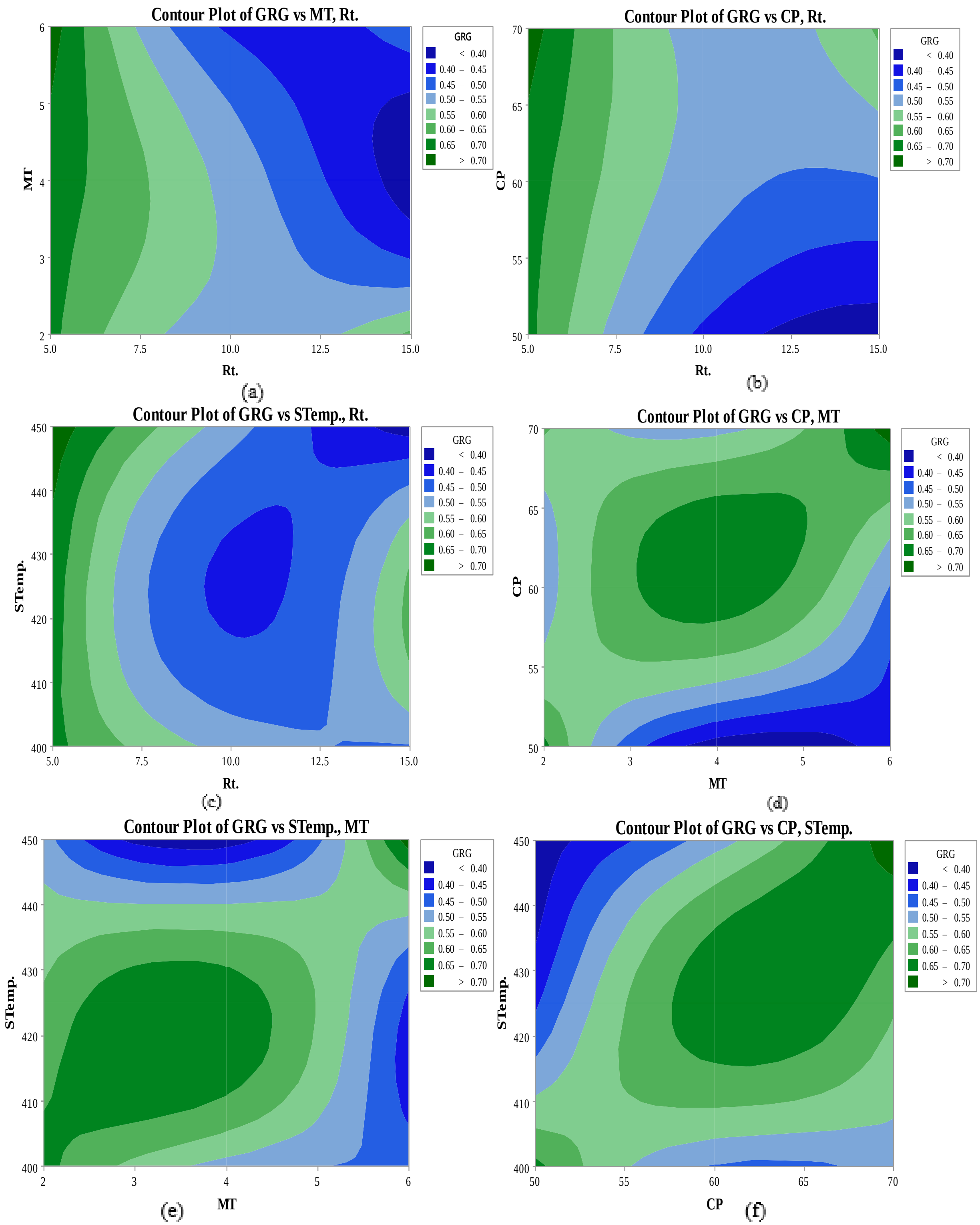

Figure 4.9 The contour plot of predicted process parameters on the GRG response.

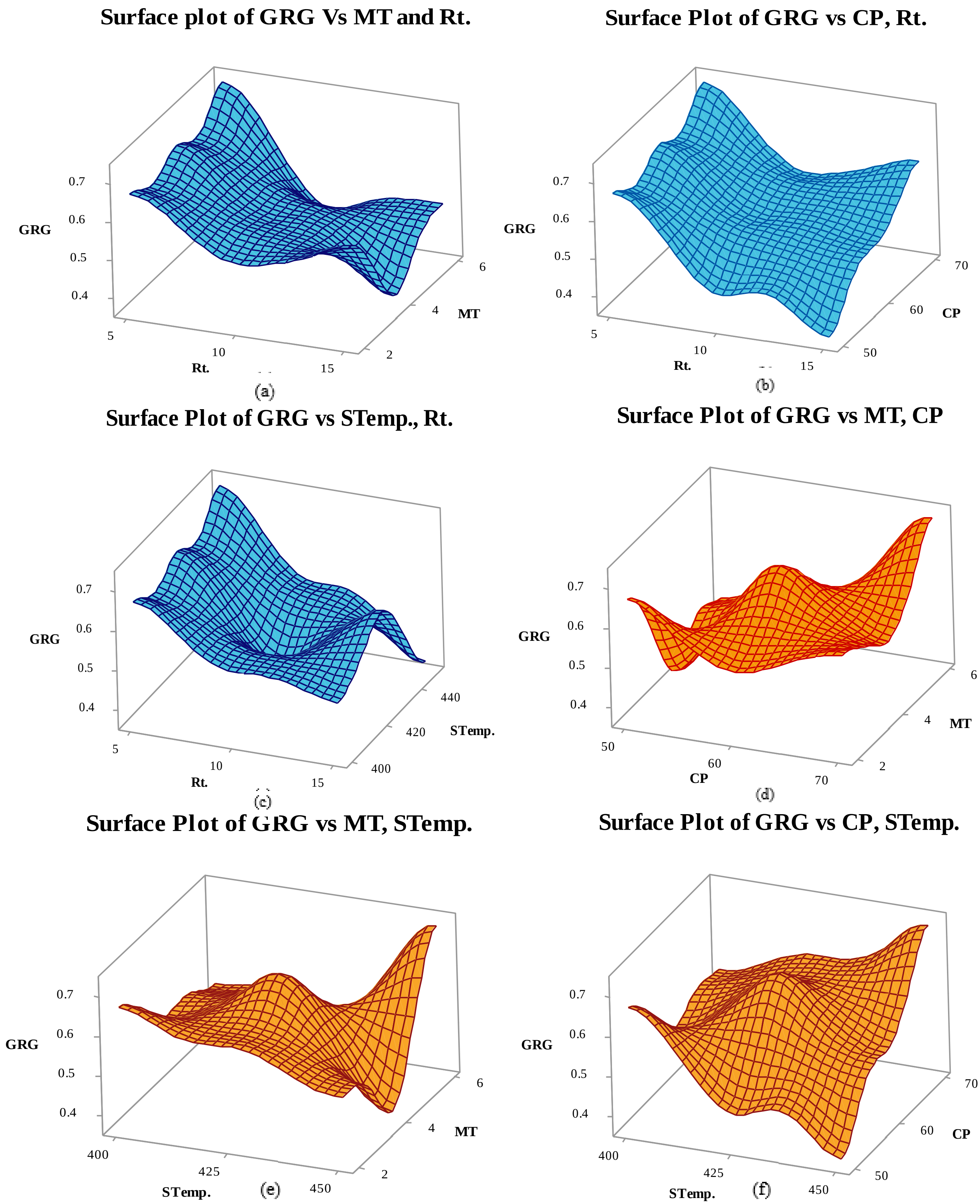

Figure 4.10 The 3D surface plot of predicted process parameters on the GRG response.

The milling time with respect to the sintering temperature has been shown in figure 4.9(e). The response of grey relational grade is studied with the process parameters of milling time and sintering temperature. This study reveals that the interaction effect of the process parameter is observed in the contour plot of the grey relational grade response. In figure 4.9(f), it shows that the process parameters of compaction pressure and sintering temperature have influenced the response values of grey relational grade. The highest GRG value is in the range of 0.7 and above for both contour plots. As the contour plot indicated that the compaction pressure has a high influence on GRG response relative to milling time.

4.1.4 Confirmation test for optimum levels

The confirmation test was carried out on the manufactured sample based on the optimal process parameter combinations. Some literatures investigation were used to comparatively study the improvement of physical and mechanical properties of the hybrid composite to confirm the results weather it is better or not relative to the present hybrid composites and base metal i.e. AZ31 Mg alloy. As instance, Khan *et al.* (2020) was taken different composition as Al-5SiC-9ZrO_2 and others to investigate various properties. It was obtained the mechanical properties such as micro hardness, compression strength around 67± 4 Hv and 103± 5 MPa respectively. Its properties of micro hardness and compressive strength were better relative to base metal (i.e. 36± 3 Hv and 47± 4 MPa) and Al-5SiC i.e. 54± 5 Hv and 66± 3 MPa respectively. The optimal level of process parameters combination i.e. $A_1B_1C_3D_2$ is taken for confirmation test of various properties since it is essential to confirm with the experimental tests. The results of the confirmation experiment are tabulated below in table 4.9 with the optimal process parameters. The combination of process parameters at optimal level i.e. experimental density, porosity, compressive strength, and hardness value are tabulated below.

Table 4.9 Results of Confirmation test.

Response	The optimum level $A_1B_3C_3D_3$	the optimum level of process parameter $A_1B_1C_3D_2$
Exp’tal density	2.06 g/cm^3	2.04 g/cm^3
Porosity	0.14	0.13
Hardness	131.43 HV	131.89 HV
Compression strength	110.17 MPa	110.35 MPa

Hence, the properties i.e. experimental density, porosity, compressive strength, and hardness value of MMMCs are improved by using GRA integrated with the Taguchi method. And, others literatures results are tabulated in table 4.10 for investigating different properties comparatively with the current work.

Table 4.10 Properties of the optimum and its comparison with other composites.

Composition	Physical properties		Mechanical properties		References
	Exp'tal density	porosity	Micro hardness (VHV)	Compressive yield strength (MPa)	
AZ31 Mg alloy-4MoS_2- 5ZrO_2- 10SiC	2.11	0.07	112.73	96.37	Present work
AZ31 Mg alloy-4MoS_2- 10ZrO_2- 5SiC	2.04	0.13	131.89	110.35	Present work
Al-5SiC	_	_	54± 5	66± 3	Khan *et al.* (2020)
Al-5SiC- 3ZrO_2			58± 4	87± 3	
Al-5SiC- 6ZrO_2			62± 3	98± 3	
Al-5SiC- 9ZrO_2			67± 4	103± 5	
Pure Mg	1.69	_	32.5		Kumar *et al.* (2020)
Mg-4SiC	1.72		41		
Mg-8 SiC	1.76		57		
Mg-12 SiC	1.80		71		
Al- 6B4C- 1ZrC	2.79	1.3	-	-	Manohar *et al.* (2021)
Al- 6B4C- 2ZrC	2.82	1.6	-	-	
Al- 6B4C- 3ZrC	2.86	1.6	125	-	
Al- 6B4C- 4ZrC	2.89	1.8	-	-	
Al- 6B4C- 5ZrC	2.93	2.1	-	-	
Al-8Gr-1SiC		-	95	-	Manohar *et al.* (2021)
Al-8Gr-2SiC		3.46	99	-	
Al-8Gr-3SiC		-	102	-	
Al-8Gr-4SiC		-	111	-	
Al-8Gr-5SiC		-	115	-	
Al-8Gr-6SiC		-	121	-	

As a comparison, the hybrid composites demonstrated improved mechanical properties and physical properties when compared with other latest studies of hybrid composites. Moreover, as shown in Table 4.10, the optimum AZ31 Mg alloy-4MoS_2- 10ZrO_2- 5SiC sample exhibited the maximum compressive strength with a yield strength of 110.35 MPa and hardness value of 131.89 HV.

4.1.5 Regression model for grey relational grade

The model for the GRG responses is constructed with considering the main and interaction of the process parameters to predict the response values. The regression equation developed for the GRG considering the interaction effect among the process parameters is stated below in eq. 4.5.

$$\boldsymbol{\omega} = 2.21 - 0.175\ Rt. - 0.216\ MT - 0.0427\ CP + 0.00187\ S.Temp. - 0.0031\ Rt.*MT + 0.00295\ Rt.*CP + 0.00456\ MT*CP \quad (4.5)$$

Where $\boldsymbol{\omega}$ represents the output value of grey relational analysis

As the model summary showed that the R-Square value of the model is 92% so it is significant since it lies between 90 -100% i.e. it is nearly approached to 1 value. This implies that the model has an efficiency to predict the response values at any parameter value. The predicted GRG values are calculated using the above model eq. 4.5 for each experimental run. And, it is used to analyze the predicted value of GRG with the experimental values of GRG. In figure 4.11, the experimental and predicted GRG is expressed in graph form. And, the graph shows that both values of experimental and predicted GRG plots are nearly the same. Due to this, the influence of interaction effects of process parameters has detected a significant influence on grey relational analysis responses.

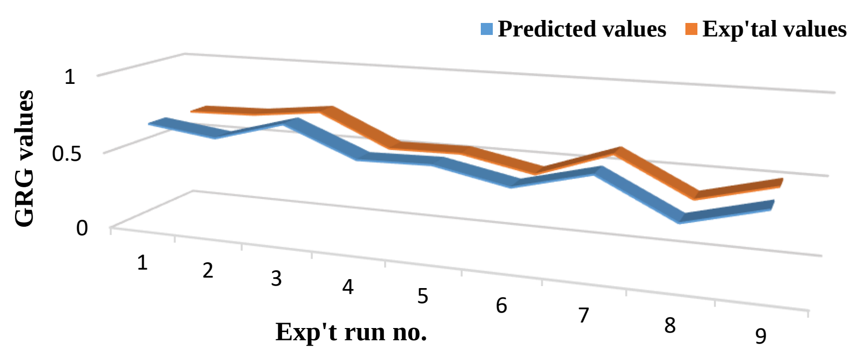

Figure 4.11 The predicted and experimental GRG versus experiment run numbers.

In figure 4.12, the distribution of the normal probability plot shows the values are not far from a theoretical normal distribution i.e. it tends to form normal distribution when relative to residuals values.

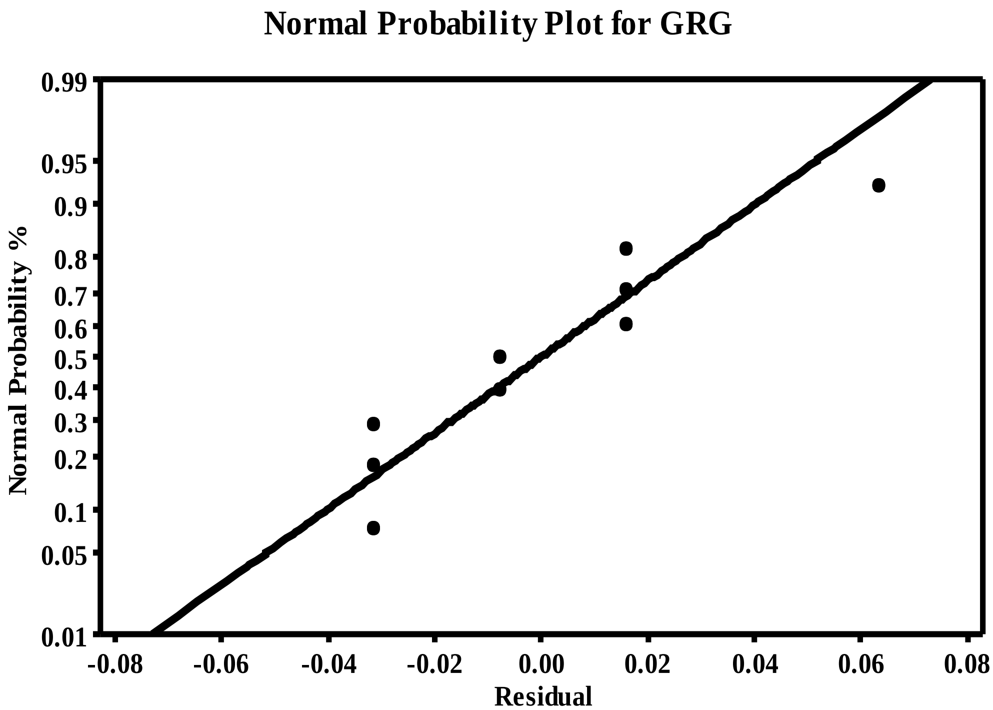

Figure 4.12 Normal distribution of the GRG values.

4.1.6 Wear test

The wear resistance of the MMMCs is examined through the wear loss and wear rate determination of the materials. In this study, the wear test is conducted in the optimum, hybrid and mono reinforced MMMCs samples on pin-on-disc equipment of the DUCOM TR-20 MICRO model. The wear behavior is investigated under the load of 30N and sliding speed of 250 rpm on a 25mm diameter wear truck under 300 sec. time. The mass (weight) loss is obtained using the weight difference of the samples i.e. before and after conducting the wear test. It is measured using an analytical precision balance with a weighing capacity of 252g/0.1mg. And, the wear rate of the samples is determined using eq. 3.13 as mentioned in the previous chapter. The results of the weight loss and wear rate of hybrid and mono reinforced samples are tabulated below in table 4.11.

Table 4.11 Mass loss and wear rate of the samples at a specified load.

Material type	Rt. %	Mass loss (g)	Wear rate (x 10^{-8} Kg.m^{-1})
Hybrid MMMCs	5%	$2.3*10^{-3}$	2.3428
	10%	$2.7*10^{-3}$	2.7502
Mono hybrid MMMCs	15%	$3.1*10^{-3}$	3.1676

The reinforcements of MMMCs made the matrix to be stronger and resist the wear during the dry sliding wear test. From table 4.11, mass loss is decreased according to the reduction of the volume percentage of silicon carbide relatively to the vol. % of zirconium dioxide in the composite. Similarly, it also showed the same ideas in figure 4.13. The wear rate is also high due to taking an average load value i.e. the higher load with high sliding speed makes the wear rate higher due to the frictional heat at the contact surface of the pin and disc. Similar results of the study are obtained by other researchers (Arif *et al.*, 2017; Dessalegn, 2021).

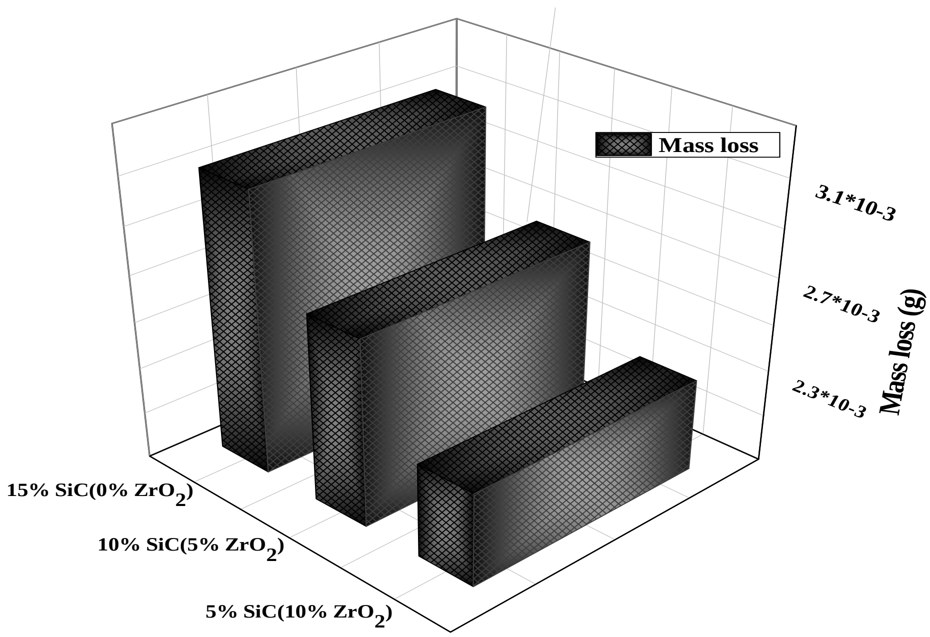

Figure 4.13 Mass loss of optimal sample at different reinforcement compositions.

The variation of wear rate is observed for different volume percentages of SiC as shown in figure 4.14. The wear rate of hybrid MMMCs is lower than the mono hybrid MMMCs at constant process parameters of 30N load and 250 rev/min sliding speed for 300 seconds at room temperature. As stated in table 4.11, The 5vol. % of SiC has a low wear rate than both 10vol.% and 15vol.% of SiC reinforced MMMCs at a 30N constant applied load. The wear rate is gradually reduced when the composites have a high volume percentage of ZrO_2 based on the bar graphs as shown in figure 4.14. The wear rate of the composite has exhibited a good improvement with the addition of ZrO_2 reinforcement which has provided the same result for other researchers (Aydin & Sun, 2019). Indeed, the hybridization of the particles enhances mechanical properties as well wear resistance of the composites. However, it also causes a significant change in the friction coefficient of the composite during hybridizing the reinforcements with ZrO_2 particles (Jalilvand & Mazaheri, 2020).

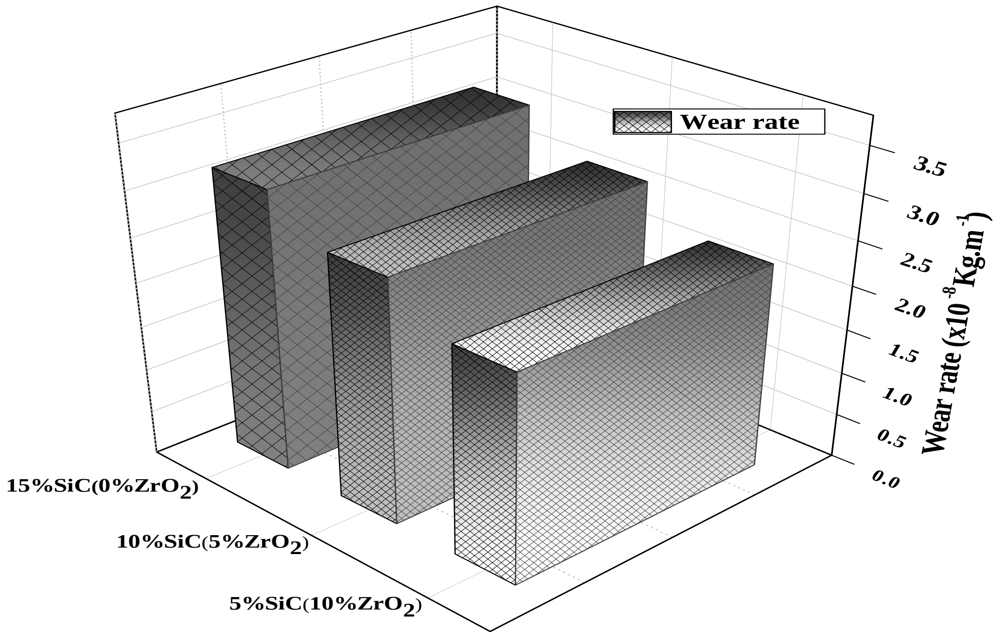

Figure 4.14 Wear rate of the optimal sample at different reinforcement compositions.

The enhancement of the wear resistance is expected due to silicon carbide and zirconia reinforcements. Naturally, both are harder and strong that makes the base metal resist the wear. When the composition of zirconia is increased and uniformly distributed all over the matrix, the wear rate of the composites also tends to decrease. Improvement on the performance of the wear resistance in percentile for 10vol. % SiC and 5vol. % is obtained at around 12.9% and 25.8% respectively compared to mono reinforced MMMCs. The wear loss and wear rate are decreased with increasing the composition of ZrO_2 and SiC, which is attributed to the hardness and wear resistivity of the reinforcements. In general, the property of composite materials enhances besides increasing the type and contents of the reinforcement. This is due to the fact that the hardness and strength of the composite are enhanced based on the contents and vol. % of the reinforcements. Some works of the literature revealed the same results (Abbas *et al.*, 2020; Purohit *et al.*, 2018).

4.1.7 Microstructure analysis

The scanning electron microscope is suitable to study and characterize the surface of solid objects. The topography of the composite samples is observed using SEM at different magnifications as depicted in figure 4.15. And, the SEM observation of MMMC samples revealed the distribution of particles and the average particle size using Image j software. In figure 4.15, the reinforcement particles are uniformly distributed in the magnesium alloy matrix on the manufactured composites. This is due to the effect of milling time more than the other factors.

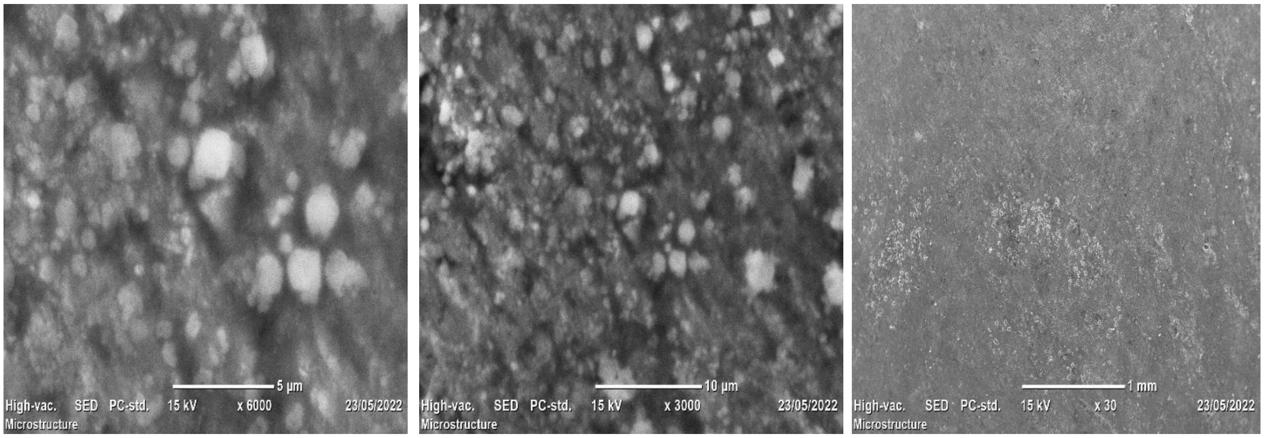

Figure 4.15 Microstructure of the optimal samples.

The average grain sizes of the manufactured composite are obtained using a micrograph of SEM. It is around 809.14 nm based on the redundant measurements taken from a number of particles. And, the nature of distribution and particle size in the composite is determined and analyzed using OriginPro 8.5 software as depicted in figure 4.16.

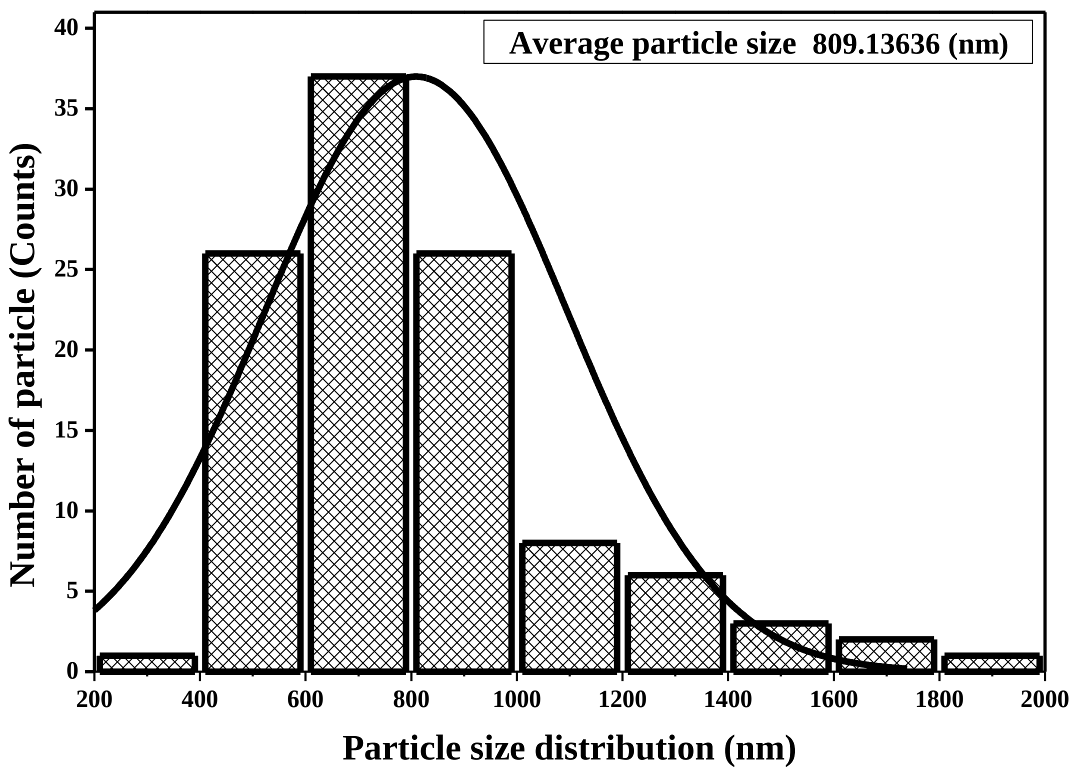

Figure 4.16 The particle size distribution using Image j SW.

4.1.8 X-Ray diffraction analysis

The XRD pattern of the AZ31 powders and AZ31 with 5, 10, and 15 vol.% SiC composites provides the elements in the composites as illustrated in figure 4.17. The elements of the composite was identified using XRD results. The silicon carbide and Magnesium oxide peaks are detected among the identified compound phases based on the XRD pattern of composite samples. It is observed that the composite sample contain low volume percentage of reinforcements peaks. Meanwhile, there is no $Mg_{17}Al_{12}$ phase or peak detected in the XRD pattern which is similarly obtained in vanadium reinforced AZ31 Mg-alloy composites (Sun *et al.*, 2021). This might be due to the decomposition of the $Mg_{17}Al_{12}$ phase during the high-energy milling process. This implies that the aluminum is dissolved into the Mg alloy matrix during the process. The presence of the magnesium oxide phase may be due to heat generated in the process of milling. And, it is due the temperature-assisted sintering process during the manufacturing of the samples.

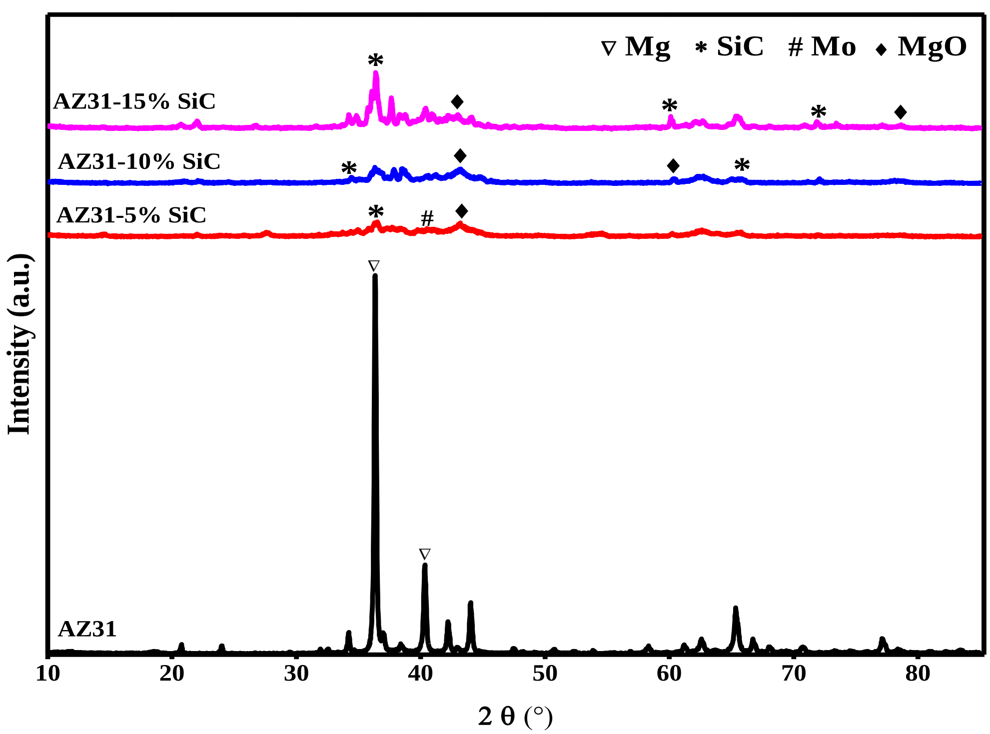

Figure 4.17 XRD spectrum of samples at different reinforcement compositions.

4.1.9 Analysis of fractography

The surface morphology i.e. fractography of the samples at different magnifications is illustrated in Figure 4.18. It is used to analyze the fracture mechanism of the composite after applying a load until it fails. The fracture mechanisms of the composites were observed using the SEM at different magnifications to analyze the fractography of the micrographs. It is clearly observed that cleavage cracks and facets are depicted in figures 4.18 (a) and (b) i.e. it implies the existence of brittle fracture in the MMMCs. That might have an impact on the properties of the composites. Meanwhile, the micro pores and dimples are observed in the micrographs. Therefore, it exhibits a modern fracture mechanism i.e. it shows both brittle and ductile fractures as the same phenomenon was observed in AZ31 alloys reinforced with vanadium MMCs (Sun *et al.*, 2021).

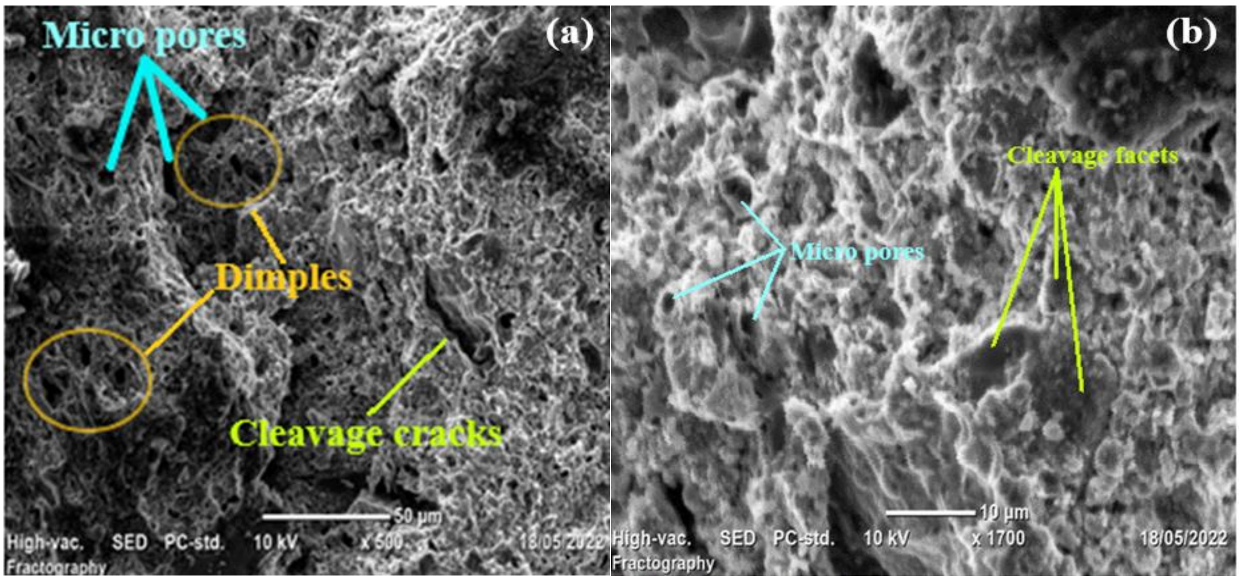

Figure 4.18 SEM micrograph displaying the Fracture mechanism of the optimal samples.

4.1.10 Analysis of wear morphology

In this study, the wear morphology of MMMCs is also studied after conducting a wear test under 30N applied load using pin on disc apparatus. The worn surface of the samples is investigated using SEM characterizing tool. It is observed that the worn surface shows various wear mechanisms; commonly continuous grooves, wear debris, delamination, and scratches are detected. Most of the wear mechanisms occurred along with the sliding directions. From figure 4.19, the worn surface indicates that abrasive wear, mild wear (i.e. delamination and oxidation), and fatigue wear mechanisms are mainly detected in the samples. Investigations on SEM micrographs of worn surfaces validated the improvement of the wear resistance due to the presence of the ZrO_2 and SiC. And, the addition of molybdenum disulfide reduces wear loss cause of guiding the uniform distribution of the particles over the matrix materials. The composites manufactured with the addition of ZrO_2 and solid lubricants show an improvement in reducing the wear losses as reported in other literature (Arif *et al.*, 2020; Kavimani *et al.*, 2020).

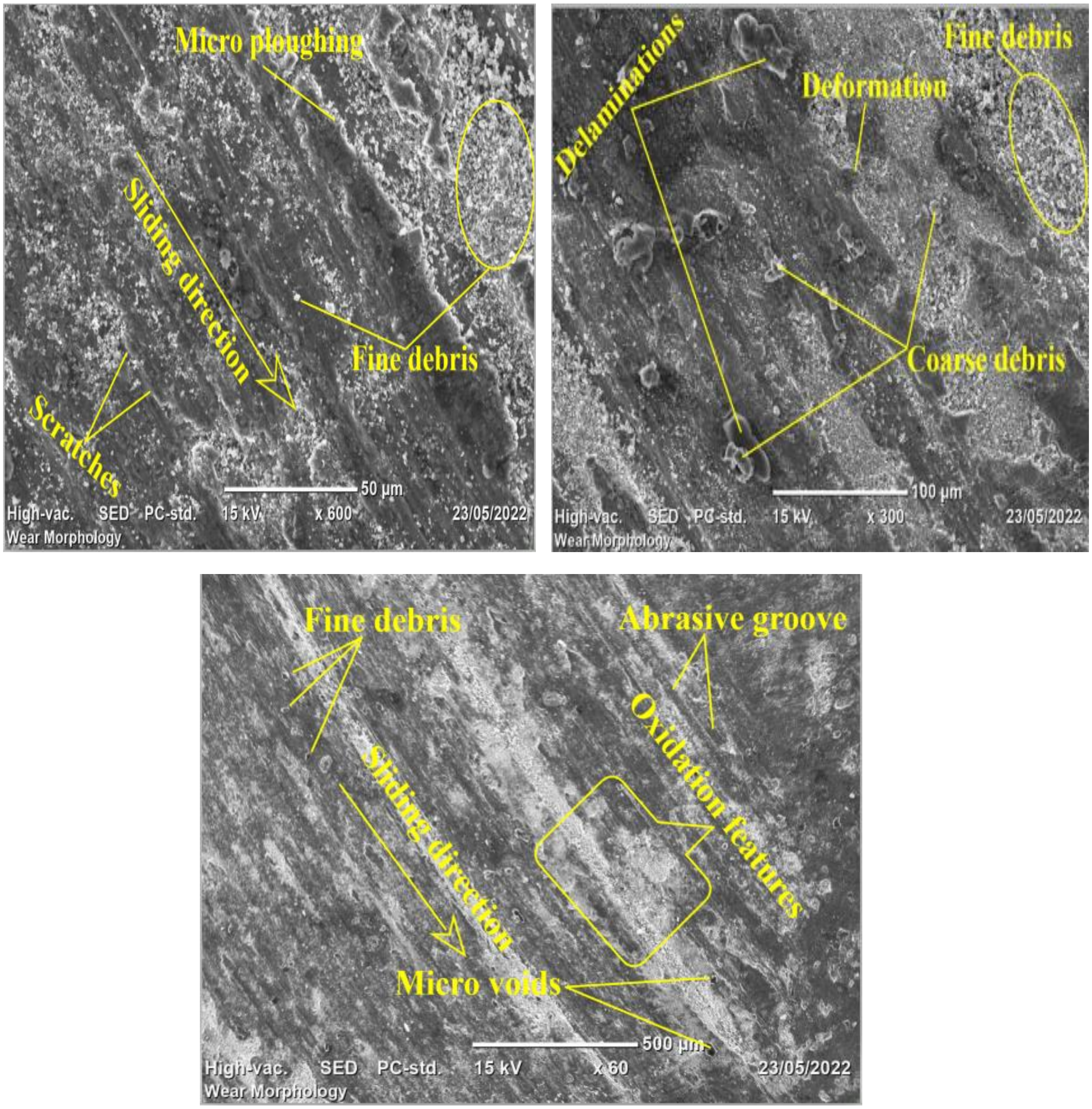

Figure 4.19 SEM micrographs of wear morphology at different magnifications.

CHAPTER FIVE: CONCLUSION AND RECOMMENDATIONS

5.1 Conclusion

In this research work, the hybrid composites were manufactured based on DoE and investigated the effect of powder metallurgy process parameters on multi responses of SiC, ZrO_2 and MoS_2 reinforced AZ31 Mg alloy composite based on the GRA integrated with the Taguchi method. The optimization of the MMMCs had brought the optimum combination of the process parameters to obtain an average properties from the multi responses. Moreover, the characterization is also carried out on the hybrid composite. And, it conclude the following results:

- The magnesium alloy MMCs properties of the density and porosity are mainly influenced by the sintering temperature and reinforcement composition. And, the optimum levels for individual responses of density and porosity were obtained as $A_3B_3C_3D_2$ and $A_3B_1C_1D_1$ respectively.
- The hardness and compression strength of the composite is highly affected by compaction pressure and reinforcement composition. The optimum levels, in order to obtain better properties, were revealed as $A_3B_1C_3D_1$ and $A_1B_1C_3D_3$ for hardness and compressive strength of the composite respectively.
- The 3D surface plots and the contour plot also depicted that the reinforcement percentage and compaction pressure significantly affected the GRG values at 5vol.% and 70Mpa.
- The optimal process parameter combination for responses i.e. density, porosity, hardness, and compression strength was obtained as $A_1B_1C_3D_2$ based on the response table for mean GRG. It was obtained as reinforcement percentage at 5vol.%, milling time at 2 hrs., compaction pressure at 70Mpa, and sintering at 425^0c.
- Reinforcement percentage among the controlled process parameters had shown a strong correlation with the MMMCs response parameters. As response table for GRG revealed that the reinforcement percentage was the most influential process parameter followed by compaction pressure, milling time, and sintering temperature sequentially.
- The compression strength value also revealed a strong relationship with the process parameters due to having the highest mean GRC value i.e. 0.601 compared to the hardness, porosity, and exp'tal density.

- Meanwhile, the confirmation test reveals that the density, porosity, hardness, and compression strength of SiC, ZrO_2, and MoS_2 reinforced AZ31 magnesium alloy composites is about 2.04g/cm^3, 13%, 131.89 HV, and 110.35 MPa. The hybridization of the particles improved the property of the composites. The density, porosity, hardness, and compression strength are about 98.88%, 93.56%, 100.35%, and 100.16% than that of the optimal level values respectively.
- SEM observation of the fractured samples for fractography analysis indicated cleavage cracks, facets, micropores, and dimples on the optimal sample. Both brittle and ductile fracture mechanisms were observed in the optimal sample.
- The surface morphology of SEM micrographs shows the nature of the reinforcement distribution in the Mg alloy matrix was uniform and the XRD pattern also revealed that no existence of the intermetallic compound (as instance $Mg_{17}Al_{12}$) phase.
- And, the dry sliding wear tests indicated that the wear resistance is improved by about 12.9% and 25.8% for 10vol. % SiC and 5vol. % SiC (i.e. optimum) respectively relative to the mono reinforced MMMCs. Therefore, the hybrid magnesium alloy MMCs revealed a significant improvement in tribological properties.
- The SEM micrograph taken from the worn surface indicated that abrasive wear, mild wear (i.e. delamination and oxidation) and fatigue wear mechanisms have mainly detected on the optimal sample.

5.2 Recommendations

In this study, Magnesium alloy metal matrix composite is manufactured as per design of the experiment. It is used to determine the mechanical properties i.e. hardness and compression strength and tribological properties i.e. wear resistance. And, it optimize the process parameter of powder metallurgy through Taguchi-based GRA optimization tools. Nevertheless, it is recommended to perform other tests on the manufactured sample to investigate more about the mechanical and tribological properties of the manufactured MMMCs. As the results implies the material and manufacturing techniques have a great role to obtain the desired properties of the composites. Therefore, high efficient tools are recommended to overcome the difficulties during manufacturing and testing the samples. In addition, it also used to enhance the properties of manufactured MMMCs.

5.2.1 Future work

As the future work, the optimized sample validation experiment can be done through the stir casting process followed by characterization and testing of the samples to compare the performance index of stir casting and powder metallurgy. Moreover, the secondary operations on the manufactured samples are also recommended in order to enhance further the property of the MMMCs.

Research Fund Acknowledgement

This research project is funded by Adama science and Technology University under the grant number ASTU/SM-R/634/22, Adama, Ethiopia.

References

Abbas, A., Huang, S. J., Ballokova, B., & Sülleiová, K. (2020). Tribological effects of carbon nanotubes on magnesium alloy AZ31 and analyzing aging effects on CNTs/AZ31 composites fabricated by stir casting process. Tribology International, 142, 105982.

Abbas, A., Rajagopal, V., & Huang, S. J. (2021). Magnesium Metal Matrix Composites and Their Applications. In *Magnesium Alloys*. IntechOpen.

Arif, S., Alam, M. T., Ansari, A. H., Siddiqui, M. A., & Mohsin, M. (2017). Study of mechanical and tribological behaviour of Al/SiC/ZrO2 hybrid composites fabricated through powder metallurgy technique. Materials Research Express, 4(7), 076511.

Arif, S., Jamil, B., Shaikh, M. B. N., Aziz, T., Ansari, A. H., & Khan, M. (2020). Characterization of surface morphology, wear performance and modelling of graphite reinforced aluminium hybrid composites. Engineering Science and Technology, an International Journal, 23(3), 674-690.

Asl, M. S. (2018). A statistical approach towards processing optimization of ZrB_2–SiC–graphite nanocomposites. Part I: relative density. *Ceramics International*, *44*(6), 6935-6939.

Aydin, F., & Sun, Y. (2019). Microstructure and wear of a sintered composite with a magnesium alloy AZ91 matrix reinforced with ZrO_2 particles. Metal Science and Heat Treatment, 61(5), 325-329.

Burke, P., & Kipouros, G. J. (2011). Development of magnesium powder metallurgy AZ31 alloy using commercially available powders.

Cheng, Y. L., Qin, T. W., Wang, H. M., & Zhang, Z. (2009). Comparison of corrosion behaviors of AZ31, AZ91, AM60 and ZK60 magnesium alloys. *Transactions of Nonferrous Metals Society of China*, *19*(3), 517-524.

Connor, N. (2020, July 31). *What is Density of Magnesium Alloys - Elektron 21 - Definition*. Material Properties. Retrieved March 9, 2022, from https://material-properties.org/what-is-density-of-magnesium-alloys-elektron-21-definition/

Ddodson, B. Stainless magnesium breakthrough bodes well for manufacturing industries. *Gizmag. com, Retrieved*, *29*(08.2013).

Dessalegn, B. (2021). *Synthesis, Mechanical Testing and Characterization of AlMg Matrix SiC Reinforced Composite Via Powder Metallurgy and Optimization of Process Parameters* (Doctoral dissertation, ASTU).

Dziubińska, A., Gontarz, A., Horzelska, K., & Pieśko, P. (2015). The microstructure and mechanical properties of AZ31 magnesium alloy aircraft brackets produced by a new forging technology. *Procedia Manufacturing*, *2*, 337-341.

Esen, Z., Öcal, E. B., Akkaya, A., Gürçay, B., Özcan, C., Özgümüş, B. A., ... & Dericioğlu, A. F. (2020). Corrosion behaviours of Ti6Al4V-Mg/Mg-alloy composites. Corrosion Science, 166, 108470.

Farhadinia, F., Sedghi, A., & Nooghani, M. T. (2017). properties of an Al/(Al_2 O_3+ TiB_2+ ZrB_2) hybrid composite manufactured by powder metallurgy and hot pressing. *Journal of Applied Mechanics and Technical Physics*, *58*(3), 454-460.

HG, P. K., & Xavior, A. (2018). Processing of Graphene/CNT-Metal Powder. *Powder Technology*.

Hussain, M. Z., Khan, S., & Sarmah, P. (2020). Optimization of powder metallurgy processing parameters of Al2O3/Cu composite through Taguchi method with Grey relational analysis. Journal of King Saud University-Engineering Sciences, 32(4), 274-286.

Jailani, H. S., Rajadurai, A., Mohan, B., Kumar, A. S., & Sornakumar, T. (2009). Multi-response optimization of sintering parameters of Al–Si alloy/fly ash composite using Taguchi method and grey relational analysis. The International Journal of Advanced Manufacturing Technology, 45(3), 362-369.

Jain, N., & Kumar, R. (2021). Multi-response optimization of process parameters in friction stir welded aluminum 6061-T6 alloy using Taguchi grey relational analysis. *World Journal of Engineering*.

Jalilvand, M. M., & Mazaheri, Y. (2020). Effect of mono and hybrid ceramic reinforcement particles on the tribological behavior of the AZ31 matrix surface composites developed by friction stir processing. *Ceramics International*, *46*(12), 20345-20356.

Jaswin, M. A., Lal, D. M., & Rajadurai, A. (2011). Effect of cryogenic treatment on the microstructure and wear resistance of X45Cr9Si3 and X53Cr22Mn9Ni4N valve steels. *Tribology Transactions*, *54*(3), 341-350.

JCM-6000Plus Versatile Benchtop SEM. (n.d.). [Photograph]. JEOL. https://www.jeol.co.jp/en/products/detail/JCM-6000Plus.html

Joost, W. J., & Krajewski, P. E. (2017). Towards magnesium alloys for high-volume automotive applications. *Scripta Materialia*, *128*, 107-112.

Kadhim, A., Kadhim, S. M., & Jalil, H. A. A. (2018, December). A study of LSP technique effect on the wear resistance for aluminum and copper alloys. In *AIP Conference Proceedings* (Vol. 2045, No. 1, p. 020008). AIP Publishing LLC.

Karuppusamy, P., Lingadurai, K., Sivananth, V., & Arulkumar, S. (2021). A study on mechanical properties of tungsten carbide reinforced magnesium metal matrix composites for the application of piston. *International Journal of Lightweight Materials and Manufacture*, *4*(4), 449-459.

Kavimani, V., Prakash, K. S., & Thankachan, T. (2019). Experimental investigations on wear and friction behaviour of SiC@ r-GO reinforced Mg matrix composites produced through solvent-based powder metallurgy. *Composites Part B: Engineering*, *162*, 508-521.

Kavimani, V., Prakash, K. S., Starvin, M. S., Kalidas, B., Viswamithran, V., & Arun, S. R. (2020). Tribo-surface characteristics and wear behaviour of SiC@ r-GO/Mg composite worn under varying control factor. Silicon, 12(1), 29-39.

Kaviyarasan, K., Soundararajan, R., Seenuvasaperumal, P., & Sathishkumar, A. (2019). Experimental investigation of dry sliding wear behaviour on ceramic reinforced magnesium composite by powder metallurgy technique. *Materials Today: Proceedings*, *18*, 4082-4091.

Khan, A., Abdelrazeq, M. W., Mattli, M. R., Yusuf, M. M., Alashraf, A., Matli, P. R., & Shakoor, R. A. (2020). Structural and mechanical properties of Al-SiC-ZrO_2 Nano composites fabricated by microwave sintering technique. *Crystals*, *10*(10), 904.

Kopeliovich, D. D. (2012, May 31). *Powder metallurgy - introduction [SubsTech]*. Substance and Technology. Retrieved November 1, 2021, from https://www.substech.com/dokuwiki/doku.php?id=powder_metallurgy-introduction.

Kumar, K. C. K., Kumar, B. R., & Rao, N. M. (2021). Microstructural, Mechanical Characterization, and Fractography of AZ31/SiC Reinforced Composites by Stir Casting Method. *Silicon*, 1-11.

Kumar, N., & Bharti, A. (2021). Optimization of powder metallurgy process parameters to recycle AZ91 magnesium alloy. Materials Physics and Mechanics, 47(6), 968-977.

Kumar, N., Bharti, A., Dixit, M., & Nigam, A. (2020). Effect of powder metallurgy process and its parameters on the mechanical and electrical properties of copper-based materials: literature review. *Powder Metallurgy and Metal Ceramics*, 1-10.

Kumar, S. D., Ravichandran, M., Sakthivelu, S., Meignanamoorthy, M., Chanakyan, C., & Alagarsamy, S. V. (2020). Mechanical properties of magnesium-silicon carbide composite fabricated through powder metallurgy route. *Materials Today: Proceedings*, *27*, 1137-1141.

Kumar, T. S., Shalini, S., Ramu, M., & Govindaraju, M. (2019). Characterisation of AZ31/ZrO_2 composites produced via stir casting. *Materials Research Express*, *6*(11), 1165d1.

Kuo, Y., Yang, T., & Huang, G. W. (2008). The use of grey relational analysis in solving multiple attribute decision-making problems. Computers & industrial engineering, 55(1), 80-93.

Linong, W. A. N. G., Hao, W. U., Xingping, W. U., Minghai, C. H. E. N., & Ning, L. I. U. (2013). Preparation and Mechanical Properties of-SiC Nanoparticle Reinforced Aluminum Matrix Composite by a Multi-step Powder Metallurgy Process. *Journal of Wuhan University of Technology (Materials Science Edition)*, *6*.

Luo, A. A. (2013). Magnesium casting technology for structural applications. *journal of Magnesium and Alloys*, *1*(1), 2-22.

Madeshwaran, S. R., Jayaganthan, R., Velmurugan, R., Gupta, N. K., & Manzhirov, A. V. (2018, April). Mechanical and thermal properties of MoS_2 reinforced epoxy nanocomposites. In Journal of Physics: Conference Series (Vol. 991, No. 1, p. 012054). IOP Publishing.

Makar, G. L., & Kruger, J. L. (1993). Corrosion of magnesium. *International materials reviews*, *38*(3), 138-153.

Malaki, M., Xu, W., Kasar, A. K., Menezes, P. L., Dieringa, H., Varma, R. S., & Gupta, M. (2019). Advanced metal matrix nanocomposites. *Metals*, *9*(3), 330.

Mallick, P. K. (Ed.). (2020). *Materials, design and manufacturing for lightweight vehicles*. Woodhead publishing.

Manohar, G., Maity, S. R., & Pandey, K. M. (2021). Microstructural and mechanical properties of microwave sintered AA7075/graphite/SiC hybrid composite fabricated by powder metallurgy techniques. *Silicon*, 1-11.

Manohar, G., Pandey, K. M., & Maity, S. R. (2021). Effect of microwave sintering on the microstructure and mechanical properties of AA7075/B_4C/ZrC hybrid nano composite fabricated by powder metallurgy techniques. *Ceramics International*, *47*(23), 32610-32618.

Mansor, M. R., Sapuan, S. M., Zainudin, E. S., Nuraini, A. A., & Hambali, A. (2013). Stiffness prediction of hybrid kenaf/glass fiber reinforced polypropylene composites using rule of mixtures (ROM) and rule of hybrid mixtures (RoHM). *Journal of Polymer Materials*, *30*(3), 321-334.

Mazaheri, Y., Jalilvand, M. M., Heidarpour, A., & Jahani, A. R. (2020). Tribological behavior of AZ31/ZrO_2 surface nanocomposites developed by friction stir processing. *Tribology International*, *143*, 106062.

Narayanasamy, P., & Selvakumar, N. (2017). Effect of hybridizing and optimization of TiC on the tribological behavior of Mg–MoS2 composites. *Journal of Tribology*, *139*(5).

Nguyen, Q. B., Sharon Nai, M. L., Nguyen, A. S., Seetharaman, S., Wai Leong, E. W., & Gupta, M. (2016). Synthesis and properties of light weight magnesium–cenosphere composite. Materials Science and Technology, 32(9), 923-929.

Padmanaban, S., Subramanian, R., Anburaj, J., & Thillairajan, K. (2020). Rheo-die-casting of Al-Si-Mg alloy and Al-Si-Mg/SiCp composites: microstructure and wear behavior. Materials Research, 23.

Prabhu, M. S., Perumal, A. E., Arulvel, S., & Issac, R. F. (2019). Friction and wear measurements of friction stir processed aluminium alloy 6082/CaCO3 composite. *Measurement*, *142*, 10-20.

Prakash, K. S., Gopal, P. M., & Karthik, S. (2020). Multi-objective optimization using Taguchi based grey relational analysis in turning of Rock dust reinforced Aluminum MMC. Measurement, 157, 107664.

Purohit, R., Dewang, Y., Rana, R. S., Koli, D., & Dwivedi, S. (2018). Fabrication of magnesium matrix composites using powder metallurgy process and testing of properties. Materials Today: Proceedings, 5(2), 6009-6017.

Qiao, K., Zhang, T., Wang, K., Yuan, S., Zhang, S., Wang, L., ... & Wang, W. (2021). Mg/ZrO_2 metal matrix nanocomposites fabricated by friction stir processing: microstructure, mechanical properties, and corrosion behavior. *Frontiers in Bioengineering and Biotechnology*, *9*, 197.

Rahmani, K., & Majzoobi, G. H. (2020). The effect of particle size on microstructure, relative density and indentation load of Mg-B_4C composites fabricated at different loading rates. *Journal of Composite Materials*, *54*(17), 2297-2311.

Rajyalakshmi, G., & Venkata Ramaiah, P. (2013). Multiple process parameter optimization of wire electrical discharge machining on Inconel 825 using Taguchi grey relational analysis. The International Journal of Advanced Manufacturing Technology, 69(5), 1249-1262.

Ren, Z., Zhang, X. G., Sui, L., Zhang, T., Pang, L., & Jin, J. Z. (2010). Fabrication of ZrB_2 particles reinforced AZ31 magnesium matrix composite by powder metallurgy and subsequent hot extrusion. Materials Research Innovations, 14(3), 206-209.

Rodríguez-Cabriales, G., Lometo-Sánchez, A. M., Guía-Tello, J. C., Medrano-Prieto, H. M., Gutiérrez-Castañeda, E. J., Estrada-Guel, I., ... & Martínez-Sánchez, R. (2020). Synthesis and characterization of Al-Cu-Mg system reinforced with tungsten carbide through powder metallurgy. *Materials Today Communications*, *22*, 100758

Sahu, P. K., & Pal, S. (2015). Multi-response optimization of process parameters in friction stir welded AM20 magnesium alloy by Taguchi grey relational analysis. Journal of Magnesium and Alloys, 3(1), 36-46.

Sahu, P. K., Singh, S., Chen, G., Yijun, L., Zhang, S., & Shi, Q. (2020). Wear behavior of the friction stir alloyed AZ31 Mg at different volume fractions of Al particles reinforcement and its enhanced quality attributes. Tribology International, 146, 106268.

Salleh, E. M., Ramakrishnan, S., & Hussain, Z. (2016). Synthesis of biodegradable Mg-Zn alloy by mechanical alloying: effect of milling time. *Procedia Chemistry*, *19*, 525-530.

Shimadzu. (n.d.). XRD-7000 X-RAY DIFFRACTOMETER MAXIma model [Photograph]. Bara Scientific. http://www.barascientific.com/product/scientific-equipments/elemental-analzer/x-ray-diffractometer/xrd-7000-provide-solution-to-xrd-analysis-by-ease-of-use-and-versatility

Sun, S., Deng, N., Zhang, H., He, L., Zhou, H., Han, B., ... & Wang, X. (2021). Microstructure and mechanical properties of AZ31 magnesium alloy reinforced with novel sub-micron vanadium particles by powder metallurgy. *Journal of Materials Research and Technology*, *15*, 1789-1800.

Suryanarayana, C. (2001). Mechanical alloying and milling. *Progress in materials science*, *46*(1-2), 1-184.

Taguchi, G., & Rajesh, J. (2000). New trends in multivariate diagnosis. Sankhyā: The Indian Journal of Statistics, Series B, 233-248.

Tjong, S. C. (2013). Recent progress in the development and properties of novel metal matrix nanocomposites reinforced with carbon nanotubes and graphene nanosheets. *Materials Science and Engineering: R: Reports*, *74*(10), 281-350.

Torralba, J. M. (2014). Improvement of mechanical and physical properties in powder metallurgy.

Trang, T. T. T., Zhang, J. H., Kim, J. H., Zargaran, A., Hwang, J. H., Suh, B. C., & Kim, N. J. (2018). Designing a magnesium alloy with high strength and high formability. *Nature communications*, *9*(1), 1-6.

Unnikrishnan, M. A., Dhas, J., & Shanavas, S. (2020). Development of Taguchi based Grey Relational Analysis Optimization for FSW of AZ31B Magnesium Alloy. *International Journal of Vehicle Structures & Systems (IJVSS)*, *19*(3).

Upadhyaya, G. S. (1998). *Powder Metallurgy Technology*. Cambridge International Science Publishing Ltd.

Venkatesh, V. S. S., & Deoghare, A. B. (2021). Fabrication and mechanical behaviour of Al-Kaoline metal matrix composite fabricated through powder metallurgy technique. Materials Today: Proceedings, 38, 3291-3296.

Yadav, S., Gangwar, S., Yadav, P. C., Pathak, V. K., & Sahu, S. (2021). Mechanical and corrosion behavior of SiC/Graphite/ZrO_2 hybrid reinforced aluminum-based composites for marine environment. *Surface Topography: Metrology and Properties*, *9*(4), 045022.

Yu, B. C., Bae, K. C., Jung, J. K., Kim, Y. H., & Park, Y. H. (2018). Effect of Heat Treatment on the Microstructure and Wear Properties of Al–Zn–Mg–Cu/In-Situ Al–9Si–SiCp/Pure Al Composite by Powder Metallurgy. *Metals and Materials International*, *24*(3), 576-585.

Yu, H., Zhou, H., Sun, Y., Ren, L., Wan, Z., & Hu, L. (2018). Microstructures and mechanical properties of ultrafine-grained Ti/AZ31 magnesium matrix composite prepared by powder metallurgy. Advanced Powder Technology, 29(12), 3241-3249.

Zago, M., Cristofolini, I., & Amirabdollahian, S. (2020, June). Designing Powder Metallurgy Process-The Influence of High Sintering Temperature on Dimensional and Geometrical Precision. In International Joint Conference on Mechanics, Design Engineering & Advanced Manufacturing (pp. 3-8). Springer, Cham.

Zamani, N. A. B. N., Iqbal, A. A., & Nuruzzaman, D. M. (2019). Mechanical and tribological behavior of powder metallurgy processed aluminum–graphite composite. *Russian Journal of Non-Ferrous Metals*, *60*(3), 274-281.

Zang, Q., Li, X., Chen, H., Zhang, J., Wang, L., Chen, S., ... & Lu, S. (2020). Microstructure and mechanical properties of AZ31/ZrO_2 composites prepared by friction stir processing with high rotation speed. Frontiers in Materials, 7, 278.

Zhu, J., Qi, J., Guan, D., Ma, L., & Dwyer-Joyce, R. (2020). Tribological behaviour of self-lubricating Mg matrix composites reinforced with silicon carbide and tungsten disulfide. *Tribology International*, *146*, 106253.

Zhu, L., Li, N., & Childs, P. R. N. (2018). Light-weighting in aerospace component and system design. Propulsion and Power Research, 7(2), 103-119.

APPENDIX

APPENDIX - A

A-1. Vickers hardness value (HV) with three trials for each sample and mean values of the trials for each replication.

Exp't run No.	Hardness (VHT) trials						Hardness (VHT) Response	
	T1			T2			HV_{avg} -1	HV_{avg} -2
1	150.8	128.4	122.8	152.1	129.1	124.5	134	135.23
2	139.6	130.8	124.3	135.7	126.9	129.1	131.57	130.57
3	136.1	125.8	132.4	134.8	128.3	130.9	131.43	131.33
4	124.6	109.6	101.4	126.2	111.5	103.1	111.87	113.60
5	136.6	134.1	138.3	133.2	139.8	136.3	136.33	136.43
6	107.1	99.2	103.3	106.1	102.4	98.6	103.20	102.37
7	138.3	154.8	165.1	141.5	152.8	163.8	152.73	152.70
8	118.6	112.6	114.2	113.4	110.8	119.1	115.13	114.43
9	146.9	130.0	155.4	148.4	131.3	156.1	144.10	145.27

A-2. Overall measurements of the responses and their corresponding trials

Exp't run no.	Experimental density (g/cm^3)		Porosity (%)		Hardness (HV)		Compressive strength (MPa)	
	T-1	T-2	T-1	T-2	T-1	T-2	T-1	T-2
1	2.20414	2.20417	0.0774	0.0773	134.00	135.23	84.26	84.52
2	2.04181	2.04179	0.14529	0.1453	131.57	130.57	97.22	97.12
3	2.05866	2.05867	0.13823	0.13824	131.43	131.33	110.17	110.80
4	2.10530	2.10531	0.07067	0.07066	111.87	113.6	96.13	96.62
5	2.09705	2.09704	0.07431	0.07432	136.33	136.43	78.78	78.79
6	2.01830	2.01829	0.10907	0.10908	103.20	102.37	62.10	62.35
7	1.98498	1.98500	0.07326	0.07325	152.73	152.70	90.81	90.20
8	2.02159	2.02158	0.05616	0.05617	115.13	114.43	52.60	52.81
9	2.04183	2.04184	0.04672	0.04671	144.10	145.27	72.10	72.06

A-3. Overall measurements of the responses and their corresponding means values.

Exp’t run no.	Experimental density (g/cm^3)	Porosity (%)	Hardness (HV)	Compressive strength (MPa)
1	2.20416	0.077	134.617	84.390
2	2.04180	0.145	131.067	97.170
3	2.05867	0.138	131.383	110.485
4	2.10531	0.071	112.733	96.375
5	2.09704	0.074	136.383	78.785
6	2.01830	0.109	102.783	62.225
7	1.98499	0.073	152.717	90.505
8	2.02159	0.056	114.783	52.705
9	2.04183	0.047	144.683	72.080

APPENDIX - B

B-1 the procedure to calculate the required powder of matrix and reinforcement for the manufacturing operation.

The steps were followed to calculate the required powder for AZ31 Mg alloy matrix and reinforcements i.e. SiC, ZrO_2, and MoS_2. The steps is proceeded as:

The first step – the volume of the cylindrical sample was calculated using the eq. 1,

$$V_{tot.} = \frac{\pi * D^2 * H}{4} = \pi * r^2 * H \quad (1)$$

Where $V_{tot.}$ represents the calculated volume of the samples; H denotes the height of the samples, and D represents the diameter of the samples

B.2 the required parameters and output values for the calculation of the total volume of the samples.

Required sample parameters	Parameter values
Height	8 mm
diameter	20 mm
Volume	2513 mm^3

The required amount of the base metal and reinforcements to manufacture the SiC, ZrO_2, and MoS_2 reinforced AZ31 mg alloy composites.

$$M_x = V_{tot} * \rho_x * \omega \quad (2)$$

Where M_x denotes the required mass of base metal or reinforcements; ρ_x represents the density of base metal or reinforcements, and ω represents the vol.% of the matrix or reinforcement.

B.3 the required total mass of the base metal and reinforcements for the manufacturing operation.

No.	Reinforcement Wt.%					BM (Vol. 81%)	Tot. mass (g)
	SiC		ZrO_2		MoS_2 (Vol. 4%)		
	Vol %	Wt. (g)	Vol %	Wt. (g)			
1	5%	0.403	10%	1.427			6
2	10%	0.806	5%	0.713	0.508	3.662	5.689
3	15%	1.209	0%	0			5.379
Tot. mass required with contingency		35g	30g		11g	50 g	

APPENDIX - C

C-1. The measured amount of the matrix (base metal) and reinforcement's powder.

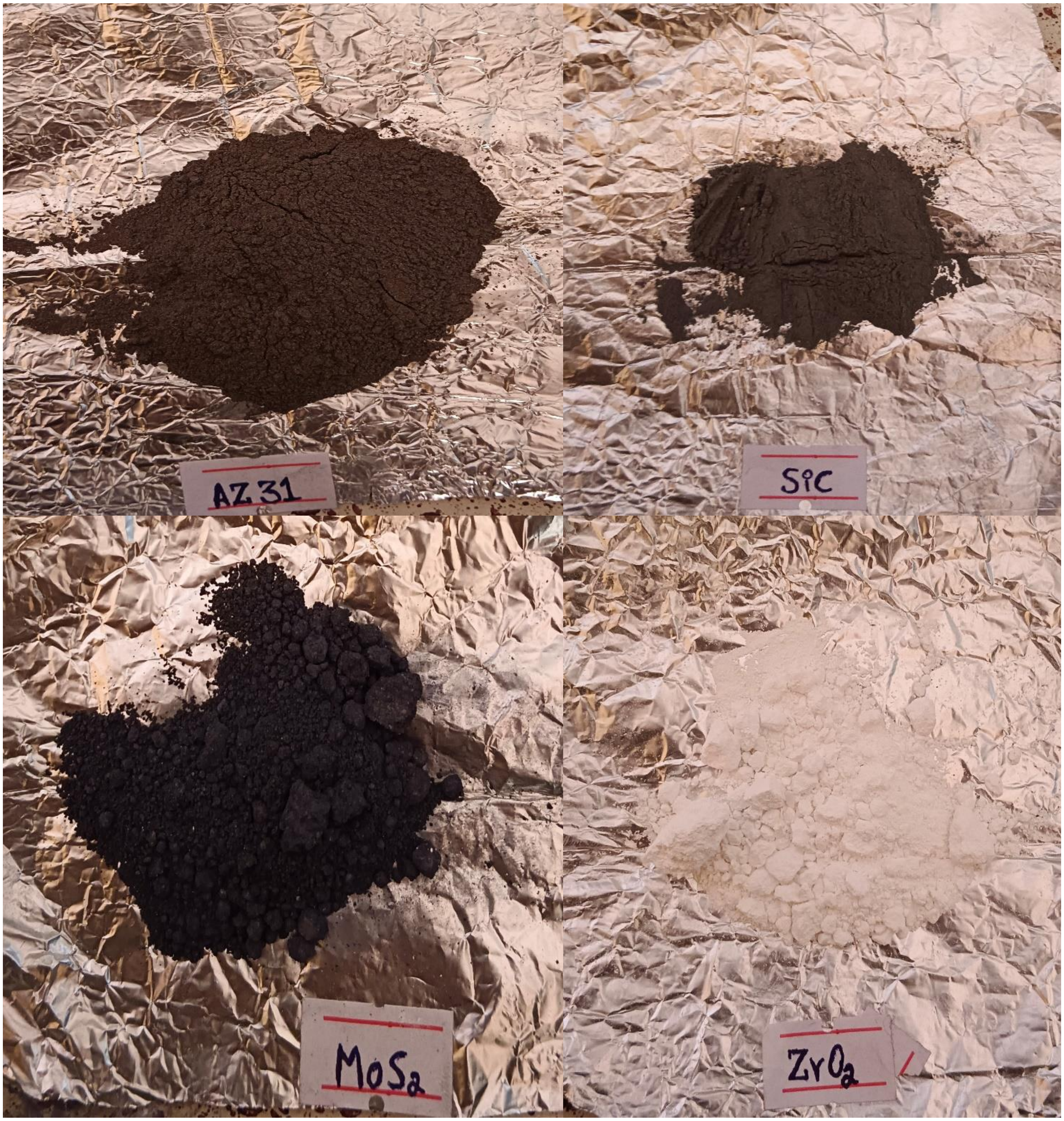

C – 2. Micrographs of some samples after indentation during hardness values determination.